

ABSTRACT

Title of Document: EVALUATION OF THERMAL INTERFACE MATERIALS AND THE LASER FLASH METHOD

Vinh Khuu, Doctor of Philosophy, 2009

Directed By: Chair Professor, Michael Pecht,
Department of Mechanical Engineering

Thermal interface materials (TIMs) are used to reduce the interfacial thermal resistance between the chip and the heat sink, which has become a bottleneck to heat removal in a variety of electronic applications. Degradation in thermal performance of the TIM can contribute to unacceptably high chip temperatures, which can significantly impact device or system performance during operation. While progress has been made in recent years in the development of tools to measure beginning-of-life thermal performance, characterizing the long-term performance of the TIM can be crucial from a life cycle stand point since TIMs may experience harsh operating conditions, including high temperature and high humidity, for extended periods of time in typical applications.

The laser flash method is one approach for measuring thermal conductivity that has an advantage over more commonly used techniques because of the non-contact nature of the measurement. This technique was applied to 3-layer structures to

investigate the effects of thermal cycling and elevated temperature/humidity on the thermal performance of select polymer TIMs in pad form, as well as an adhesive and a gel. While most samples showed little change (less than 10% in thermal resistance) or slight improvement in the thermal performance, one thermal putty material showed degradation due to temperature cycling resulting from bulk material changes near the glass transition temperature. Scanning acoustic microscope images revealed delamination in one group of gap pad samples and cracking in some putty samples due to temperature cycling.

Finite element simulations and laser flash measurements performed to validate the laser flash data indicated that sample holder plate heating, an effect previously unexamined in the literature, can lead to inaccurately high TIM thermal conductivity values due to suppression of the sample temperature rise during the laser flash measurement. This study proposed a semi-empirical methodology to correct for these effects. Simulated laser flash test specimens had bondlines that showed little thickness variation (usually within the measurement error) due to clamping by the sample holder plates. Future work was proposed to refine the laser flash sample holder design and perform additional validation studies using thermal test vehicles based on nonfunctional packages.

EVALUATION OF THERMAL INTERFACE MATERIALS AND THE LASER
FLASH METHOD

By

Vinh P. Khuu

Dissertation submitted to the Faculty of the Graduate School of the
University of Maryland, College Park, in partial fulfillment
of the requirements for the degree of
Doctor of Philosophy
2009

Advisory Committee:
Professor Michael Pecht, Chair
Professor Avram Bar-Cohen
Professor Christopher Davis
Associate Professor Patrick McCluskey
Dr. Michael Osterman
Professor Peter Sandborn

© Copyright by
Vinh Khuu
2009

Dedication

To my parents

Acknowledgements

I would like to thank Professor Pecht for the opportunity to work at CALCE and his support of my work and Dr. Osterman for his support of my research. I am grateful for the help that Professor Bar-Cohen provided on many thermal aspects of my research and in general for broadening my interests and knowledge of thermal packaging. Thanks to Professors McCluskey, Sandborn, and Davis for serving on my dissertation committee and for providing helpful comments on the dissertation.

I wish to express my sincere gratitude to CALCE staff members for assistance in experiments and for providing feedback during morning meetings, notably Ahmed Amin, Dr. Michael Azarian, Dr. Diganta Das, Sony Mathew, Dr. Keith Rogers, Anshul Shrivastava, and Bhanu Sood.

The CALCE and TherPES students and visiting scholars have been an invaluable resource throughout my PhD career. Vidya Challa deserves mention for help with scanning acoustic microscope measurements and ANSYS viscoelastic modeling. I appreciate Mark Zimmerman's assistance in reviewing papers. I gratefully acknowledge the financial support of the CALCE consortium for much of the TIMs research.

Finally, I would like to thank my family, especially my parents, for their constant support of my education. It is a privilege to offer the successful completion of my doctoral studies as a testament to the hopes and dreams they brought to this country nearly three decades ago.

Table of Contents

Dedication	ii
Acknowledgements	iii
Table of Contents	iv
List of Tables	vi
List of Figures	vii
Nomenclature	ix
Chapter 1: Introduction	1
Background and Motivation	1
Problem Statement	5
Research Objectives and Approach	5
Dissertation Overview	8
Chapter 2: Literature Review	9
Thermal Interface Material Reliability and Degradation	13
Thermal Conductivity Measurement Techniques	23
Laser Flash Method	27
Chapter 3: Reliability Tests	31
Theory of the Laser Flash Method	31
Basic Operation	31
Multilayer Analysis	32
Experimental Approach	35
Laser Flash Test Samples	36
Laser Flash Test Sample Holder	38
Sample Preparation	41
Reliability Test Procedure	44
Reliability Test Conditions	45
Results	46
Room Temperature Observations	46
Temperature Cycling Test (-40 to 125 °C)	48
Temperature Cycling Test (-55 to 125 °C)	54
Analysis of Putty B Thermal Performance Degradation	56
Elevated Temperature/Humidity Results	59
Chapter 4: Validation of Laser Flash Results from Reliability Tests	63
Modeling Approach	63
Thermal Simulations	63
Structural Simulations	65
Experimental Results	67
Modeling Results	71
Thermal Simulations	71
Structural Simulations	83
Comparison of Laser Flash Data with Steady-State Data	89
Steady-State Tester Design	89
Time-Dependent Steady-State Measurements of Gel Samples	92

Absolute Steady-State Thermal Conductivity Comparison.....	93
Steady-State Measurement Uncertainty Analysis.....	94
Laser Flash Uncertainty Analysis and Convergence Study.....	94
Chapter 5: Conclusions and Recommendations	99
Conclusions.....	99
TIM Reliability Study.....	99
Laser Flash Method Study	101
Contributions.....	102
Recommendations for Future Work.....	106
Appendix.....	108
Bibliography	113

List of Tables

Table 3.1	TIM test samples.	38
Table 3.2	TIM bondline thicknesses.	43
Table 3.3	TIM layer thermal resistance at room temperature.	47
Table 3.4	TIM layer thermal resistance under temperature cycling (-40 to 125 °C).	48
Table 3.5	Calculated TIM thermal resistance under temperature cycling (-55 to 125 °C).	55
Table 3.6	Calculated Putty B thermal conductivity based on laser flash measurements.	57
Table 3.7	Calculated TIM thermal resistance under 85 °C/85%RH.	60
Table 4.1	Comparison of laser flash measurements with vendor values: a) square test coupons; b) round test coupons.	68
Table 4.2	TIM thermal conductivity based on laser flash measurements with aluminum and Lexan sample holder plates.	71
Table 4.3	Calculated TIM thermal conductivity based on simulation of Gap Filler assuming no contact resistance between the TIM test sample and sample holder plates.	77
Table 4.4	Calculated TIM thermal conductivity based on simulation of Gap Filler using 320 mm ² square samples varying contact resistance between the TIM test sample and sample holder plates.	78
Table 4.5	Steady-state TIM z-displacement.	87
Table 4.6	Steady-state TIM z-displacement of Gap Pad A.	88
Table 4.7	Comparison between experimental TIM thermal conductivity values with datasheet values.	94
Table 4.8	Comparison of Laser Flash Measurements with Vendor Values.	97
Table 4.9	Uncertainty analysis overview of Gap Filler laser flash measurements.	98

List of Figures

Figure 2.1	Schematic illustration of TIM usage in a flip-chip BGA architecture.	10
Figure 2.2	Illustration of TIM thermal resistance.	12
Figure 3.1	Illustration of the laser flash method.	32
Figure 3.2	Configuration used for laser flash measurements of clamped 3-layer test samples.	33
Figure 3.3	TIM thermal resistance measurement and calculation.	35
Figure 3.4	Overview of the experimental procedure.	36
Figure 3.5	Illustration of TIM gap pad bondline.	37
Figure 3.6	Illustration of clamped TIM assembly.	39
Figure 3.7	TIM sample holder plates with coupons.	40
Figure 3.8	Pump-out in the putty A samples: a) Before temperature cycling; b) After 255 temperature cycles.	50
Figure 3.9	a) Non-temperature-cycled Gap Pad A sample b) Temperature-cycled Gap Pad A sample (after 760 cycles).	53
Figure 3.10	a) Non-temperature-cycled Putty A sample b) Temperature-cycled Putty A sample (after 760 cycles).	53
Figure 3.11	Putty B storage modulus as a function of temperature.	58
Figure 4.1	Overview of TIM thermal conductivity calculation procedure.	65
Figure 4.2	Effect of area on TIM thermal conductivity based on the laser flash measurements.	69
Figure 4.3	Effect of area on TIM thermal conductivity based on the laser flash measurements of Gap Filler.	70
Figure 4.4	Thermal finite element mesh.	72
Figure 4.5	Temperature rise profiles from laser flash simulations.	73

Figure 4.6	Local heat flux profile on top clamping plate from laser flash simulations.	74
Figure 4.7	Local temperature rise profiles throughout assembled test structure from laser flash simulations: a) y-axis scale from 0 to 8 K; b) y-axis scale from 0 to 1.2 K.	75
Figure 4.8	Output TIM thermal conductivity based on FEA simulation as a function of input TIM thermal conductivity.	81
Figure 4.9	Structural finite element mesh (5.9 mm opening, 16.4 mm/side square test specimen): a) open; b) solid.	84
Figure 4.10	Z-displacement (m) of Putty B at a 25% TIM compression level: a) open; b) solid.	86
Figure 4.11	Steady-state thermal resistance test vehicle: a) TIM tester schematic; b) assembled TIM tester.	91
Figure 4.12	Measured gel thermal conductivity after high temperature cure.	93
Figure 4.13	Calculated TIM thermal conductivity as a function of thermal diffusion time ratios of 3-layer copper-Gap Pad A-alloy 42 test specimen.	96

Nomenclature

R = thermal resistance

Ha = hardness

m = mean asperity slope

P = contact pressure

k_h = harmonic mean thermal conductivity

σ = root mean squared surface roughness

R_{jc} = junction-to-case thermal resistance

E_a = activation energy

A = acceleration factor

k_b = Boltzmann constant

t = time

T = temperature

k = thermal conductivity

BLT = bond line thickness

α_{CTE} = CTE

τ = shear stress

G = shear modulus

l = length

E = Young's Modulus

A = cross-sectional area

ν = Poisson's ratio

$t_{1/2}$ = half-rise time

L = thickness

α = thermal diffusivity

η_i = square root of the heat diffusion time

H = volumetric specific heat

V = normalized temperature

X = function of H

ω = function of the heat diffusion time ratio

Q = heat pulse function

τ_{time} = shear stress decay time

Chapter 1: Introduction

Background and Motivation

It is generally believed that when two solid surfaces are joined together in mechanical contact, only 1 to 2% of the effective areas are in actual physical contact due to the imperfect contact interface caused by gaps and asperities (Prasher, 2006). In microelectronic applications, this often leads to high resistance heat paths. Due to increasing power dissipation levels occurring in a variety of electronic devices, minimizing the total thermal resistance between the chip and the ambient environment can be crucial in maintaining component operating temperatures at acceptable levels. Current thermal management strategies must address decreasing volumes and more stringent thermal requirements, which have caused interfacial thermal resistance to become a bottleneck to heat removal (Nakayama and Bergles, 2003).

Thermal interface materials (TIMs) play a critical role in the thermal management of electronics by providing a path of low thermal impedance between a heat-generating element, such as a chip, and a heat dissipating element, such as a heat sink. In many microprocessor and discrete RF applications, TIMs, despite aiding heat dissipation, can account for 30 to 50% of the total thermal resistance budget, including the component package up to the ambient environment (Lasance, 2003). A wide array of TIM types, such as greases, phase change materials, pads, films, and adhesives are now commercially available. The selection process can be challenging

since the overall performance of a TIM depends on many factors including process variables, assembly conditions, bulk material properties, and properties of the interface. Characterizing the thermal performance of thermal interface materials in a manner representative of actual applications can be critical since erroneous selection may lead to greater-than-expected thermal resistances in the thermal path.

In many automotive, military, and space applications, TIMs experience harsh operating conditions, including high temperature and high humidity, for extended periods of time. Degradation in the thermal performance of the TIM during its operating life can impair device or system performance, lead to malfunctions, or cause premature failure (Gowda, 2005). For instance, Chiu et al. (2001) showed that thermal grease pump-out (the gradual squeezing out of the grease from the interface gap) after 2000 power cycles can lead to a 50% increase in interfacial thermal resistance while Gektin (2005) showed that 5% voiding in a TIM 1 material (die-to-heat spreader) can lead to over a 70% reduction in overall system thermal performance.

Few models of TIM degradation exist, however. In fact, predicting degradation in thermal conductivity as a function of environmental stress conditions over time is not possible with the current level of understanding. The lack of accurate physics-based models to describe TIM degradation behavior has necessitated improved experimental techniques (Prasher, 2006). In addition, product data on reliability is often not provided by TIM vendors, and if reliability data is made available, which reliability tests are used, how they are conducted, and how thermal conductivity is measured can vary dramatically among manufacturers. Obtaining

accurate reliability data often involves additional design challenges beyond those encountered in beginning-of-life (BOL) thermal performance testing. Having the capability to accurately capture changes in the contact component of the thermal resistance throughout a reliability test is essential for TIM thermal characterization since many degradation and failure mechanisms affect or originate at the contact interface between the TIM and the mating surface.

Evaluating TIM reliability using steady-state material tests, such as those that follow ASTM-D5470 (2006), a test standard commonly used by TIM manufacturers can be challenging. Assessing the impact of environmental exposure with material tests would involve subjecting test specimens to environmental exposure conditions (usually in a test chamber) and then measuring the thermal conductivity using the instrument outside the chamber. In a steady-state material tester, high contact pressures, which are needed to ensure good thermal contact between the test specimen and the hot and cold blocks, can complicate the measurement of low modulus or viscoelastic specimens due to the possibility of disturbing the specimen in the process of loading and unloading it from the tester. Test specimens should remain undisturbed between environmental exposure and thermal conductivity measurements to ensure accurate TIM degradation data.

Thermal test vehicles, which typically consist of heating elements, temperature sensors, and dummy processors designed to replicate TIM application environments, represent another common approach to measuring TIM thermal conductivity and can approximate the stresses and strains in the TIM during environmental exposure more accurately than material test approaches. However,

thermal test vehicles can be costly and time consuming to develop and may not be suitable if high absolute accuracy is required.

The laser flash method is another approach for measuring thermal conductivity that has advantages over other techniques because of the non-contact nature of the measurement. An established technique for bulk material testing of thin solid test specimens, it has also been used to study solders, adhesives, and thermal greases (Gowda et al., 2005; Chiu et al., 2002; Campbell et al., 1999, 2000). However, one common criticism of the technique is that assembled samples don't simulate loading conditions in typical applications (Smith et al., 2008). Some have also noted that the absolute error can be high when measuring multilayer test specimens since other thermal and mechanical properties need to be known (stacked up uncertainties) and the method can be difficult or impossible to use when the coupons/substrates and the TIM have differing thermal diffusivities (Lee, 1977). Practical considerations limiting its wider use by customers are the relatively high cost of a typical laser flash instrument and the fact that the method is not commonly used by TIM vendors and end-users, making comparisons with non-laser flash data difficult. These criticisms have not yet been thoroughly examined in the literature and many questions remain as to how to apply the laser flash method to obtain accurate and realistic thermal resistance data suitable for assessing reliability, particularly of TIMs in pad form. Use of the laser flash method for TIM characterization was examined in this study and the validity of a few criticisms were explored in depth. This research builds on the existing knowledge of TIM characterization techniques and TIM degradation behavior and addresses some perceived deficiencies of the laser

flash method, which may nevertheless offer advantages over more commonly used steady-state thermal conductivity measurement techniques.

Problem Statement

Although studies are available on the thermal performance of solders, adhesives, and thermal greases, little literature exists on the reliability of TIMs in pad form and gels. Temperature cycling and elevated temperature/humidity conditions are commonly encountered in the service life of electronic systems, particularly those used in automotive, space, and military applications, but their effect on thermal performance has not yet been studied for TIMs in pad form and thermal gel. While the laser flash method has been applied to the study of solders and adhesives, a few thermal and mechanical issues that can contribute to error have not yet been addressed in the literature, notably heating of test sample clamping plates during laser flash measurements, clamping of the test specimen, and coupon-TIM thermal diffusivity differences.

Research Objectives and Approach

The first part of this study, which focused on the reliability of polymer TIMs, examined the effects of temperature cycling as well as elevated temperature and humidity on TIM layer thermal resistance using the laser flash method. The thermal performance throughout the reliability tests were determined using thermal resistance values based on laser flash measurements, and the physical changes were examined

using scanning acoustic microscopy and other techniques. Additional measurements were performed to quantify the amount that room temperature effects contributed to changes throughout environmental exposure.

The second part of this study explored the application of the laser flash method to the evaluation of the reliability of TIMs. The effects of sample holder plate heating, which were studied using simulation as well as experimentation, were examined by varying the sample coupon size and varying the contact pressure. With sample holder plate heating effects present, which may lead to inaccurately high TIM thermal conductivity values, this work investigated how to interpret and incorporate the laser flash method to measure changes in thermal resistance. The influence of clamping plates structurally on the TIM layer was also investigated using finite element simulation. Although it is known that TIM thermal conductivity values can be inaccurate or impossible to determine when the thermal diffusivities of the coupon or substrate layers differ significantly from that of the TIM layer, criteria for acceptability assuming a 3-layer resistive case of the Lee method have not yet been established. To address this need, numerical analysis was performed to determine if an acceptable range of thermal diffusion time ratios (coupon to TIM layer thermal diffusion time) could be determined.

The research goals are summarized in the following objectives:

1. Use the laser flash method to measure the thermal performance of TIMs subjected to reliability test conditions.
2. Explain the causes of thermal performance degradation.

3. Assess the effects of sample holder plate heating, clamping, and error due to coupon-TIM thermal diffusivity differences on measured TIM thermal conductivity values.
4. Validate thermal resistance measurements obtained from the laser flash method using a steady-state thermal resistance measurement method.

Objective 1 focuses on measuring the thermal performance changes of select polymer TIMs subjected to three reliability tests (two temperature cycling and one elevated temperature/humidity test). Objective 2 is intended to explain the thermal resistance changes measured using the laser flash method. This involves assessing the effects of environmental exposure on TIM coupon interfaces using scanning acoustic microscopy, visual inspection, as well as other analysis techniques needed to explain the causes of any observed degradation.

Objectives 3 and 4 are intended to validate the laser flash data obtained in objective 1. The third objective addresses three aspects of conducting laser flash measurements that are studied in the context of TIM reliability evaluation using thermal resistance values. These include determining the effects of varying the coupon/substrate areas on calculated TIM thermal resistance values, assessing the impact of clamping TIM samples in laser flash measurements, and determining if thermal diffusion time ratios could be used as criteria to identify TIM-substrate material combinations and thicknesses suitable for the laser flash method.

Objective 4 relates to the accuracy of data obtained using the laser flash method to measure changes in thermal resistance, and how values compare overall to

steady-state techniques, which are generally more accurate and more widely accepted in the industry.

Dissertation Overview

The work is organized as follows. Chapter 2, which focuses on background literature, discusses experimental techniques, previous degradation studies, and theoretical models of TIM degradation, which serve as the foundation for a discussion of the need for improved experimental techniques to measure TIM degradation. Emphasis is placed on the laser flash method, and its advantages over other methods. Chapter 3 describes the fundamentals of the laser flash method and the test fixtures used in this study. Details about the reliability test procedure and measurement conditions are also provided. Experimental data from the reliability tests are presented as well as additional analysis using scanning acoustic microscopy and thermogravimetric analysis to explain observed thermal performance degradation for two groups of TIM samples. Chapter 4 presents the results of the laser flash study, intended to validate data obtained in the TIM reliability study. The analysis addresses factors contributing to error in the thermal diffusivity measurement as well as how well the test structures simulate realistic mechanical loading conditions, primarily in the bondline thickness variation. Finally, Chapter 5 summarizes the important results with recommendations on TIM selection based on the reliability study findings and describes ways to ensure accurate measurements and the effects of characteristics of the samples holder plates and 3-layer laser flash test specimen for measuring TIM specimens.

Chapter 2: Literature Review

Managing thermal contact resistance has been a central issue in the design, assembly, and operation of electronics and electrical equipment since the days of vacuum tubes (Nakayama and Bergles, 2003). Theoretical and experimental research over the past half century has provided insight into the underlying mechanisms governing heat transfer through contacting solid structures, which can occur as conduction through contact spots, conduction through an interstitial medium, or as radiation. Methods to address thermal contact problems from basic principles typically have involved approximating the geometry and using mechanical deformation models combined with thermal models of heat transfer (Madhusudana, 1995; Yovanovich, 2005). This has led to the development of correlations, such as the following expression, describing the solid–solid contact resistance R_{cs} between two nominally flat surfaces assuming plastic deformation of the asperities:

$$R = \frac{0.8\sigma}{mk_h} \left(\frac{Ha}{P} \right)^{0.95} \quad (2.1)$$

where Ha is the hardness, σ is the root mean squared surface roughness, P is the contact pressure, k_h is the harmonic mean thermal conductivity, and m is the mean asperity slope. The use of TIMs to reduce thermal contact resistance has a long history, and early published literature describes their use in spacecraft thermal control applications (Cunnington, 1964). The growth and development of the semiconductor industry since the invention of the transistor, which has placed increasing demands on thermal management, has resulted in a wide array of TIMs available on the market,

which differ in construction, composition, performance, cost and intended application. While solder, metal foil, graphite, and carbon nanotube TIMs have received attention in recent years (Rodgers et al., 2005), polymeric TIMs are the focus of this research due to their widespread availability. Polymer TIMs, which are typically either dispensed or in pad form, consist of a polymer matrix filled with highly conducting particles to enhance their thermal conductivity.

While TIMs can be found in applications ranging from portable electronics to datacenters, their use in flip chip configurations has led users to employ a classification scheme based on their location within the system. Either they are inside the component package at the die-heat spreader interface (Type 1) or outside the package at the heat spreader-heat sink interface (Type 2), as illustrated in Figure 2.1. Die attach material are sometimes classified as Type 0 TIMs (Rodgers et al., 2006).

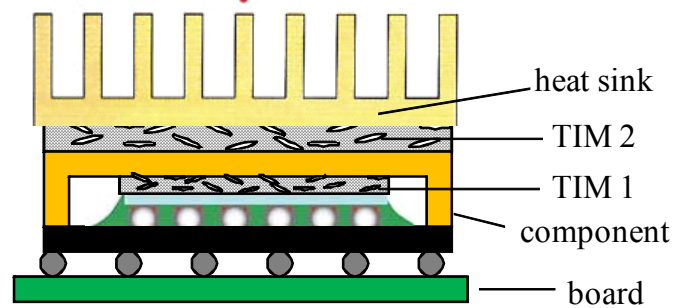


Figure 2.1: Schematic illustration of TIM usage in a flip-chip BGA architecture.

While the primary function of a TIM is to dissipate heat from the chip to allow higher processing speeds, the ability of the TIM to absorb strain resulting from the mismatch of coefficients of thermal expansion (CTEs) of the die, substrate, and

the integrated heat spreader (IHS) during temperature cycling is also important. Furthermore, cooling microprocessors requires not only maintaining the average temperature below a design point, but also reducing the temperature of hotspots. Even though the use of TIMs generally leads to an improvement over bare solid-solid contact, degraded TIM thermal performance remains an important concern due to the potential to affect the total junction-to-ambient thermal resistance, which can impact chip performance, as has been described in several experimental and analytical studies (Jung et al., 2003; Singhal et al., 2004; Somasundaram et al., 2008; Li et al., 2008).

While mechanical, electrical, and cost considerations can influence the selection of the optimal TIM for a given application, thermal performance most directly reflects the primary function. In the past decade, physics-based models have been developed to estimate the thermal performance of TIMs, expressed as a thermal resistance or effective conductivity. The thermal resistance, R , across a TIM layer was used in this study to describe the thermal performance and can be expressed by the sum of the thermal contact resistances, $R_{contact1}$ and $R_{contact2}$, at each interface and the bulk resistance of the TIM:

$$R_{total} = BLT / k_{TIM} + R_{contact1} + R_{contact2} \quad (2.2)$$

where BLT is the bondline thickness and k_{TIM} is the bulk thermal conductivity of the TIM layer. This formulation assumes 1-D heat flow in a direction perpendicular to the interface. These thermal resistances are illustrated in Figure 2.2.

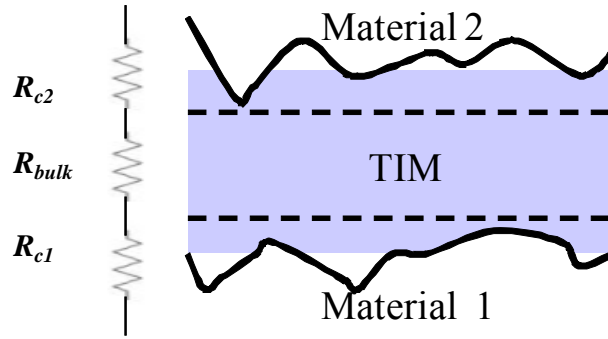


Figure 2.2: Illustration of TIM thermal resistance.

Acoustic mismatch associated with phonon transport, which is also a contributor to $R_{contact}$, is usually important for TIMs with low bondline thicknesses (less than $1\mu\text{m}$) (Smith et al., 2008).

Reliability is the probability that a device, system, or process will perform its prescribed duty without failure for a given time when operated correctly in a specified environment. In the absence of a definition of failure for thermal interface materials, “reliability evaluation” in this study was used to describe changes in thermal performance. This involved thermally characterizing the TIM using the total thermal resistance (bulk plus contact) or effective thermal conductivity and measuring the change over time when subjected to environmental exposure.

Rheology-based models of polymeric TIMs have enabled surface chemistry and wettability of TIMs to be related to the interfacial thermal resistance (Zhou and Goodson, 2001; Prasher et al., 2003; Prasher, 2001). While some theoretical studies have led to improvements in measurement methods (Savija et al., 2003), most have not translated to practical design rules (Prasher, 2006), due in large part to the large number of parameters governing thermal resistance (Bosch and Lasance, 2000).

Several experimental studies have explored the dependence of interfacial thermal resistance on surface characteristics (shape and curvature) (Stern et al., 2006), TIM layer properties (bondline thickness, filler particle size, fraction, and modulus) (Dean and Gettings, 1998; Han, 2003), and contact pressures (Bharatham et al., 2006). Gowda et al. (2003) studied the effects of filler particle size and distribution on the performance of thermal greases. Matayabas and LeBonheur (2005) focused on cured gels in examining how to optimize filler particle size and modulus to achieve reliable performance. Since the accuracy of models in predicting TIM thermal performance is still limited, however, improved experimental techniques are critical for characterizing TIM thermal performance.

Most TIMs research prior to 2000 was experimental in nature, and several literature reviews are available summarizing the historical theoretical and experimental developments related to TIMs as well as those made in recent years (Prasher, 2006; Smith et al., 2008; Goel et al., 2008; Dani et al., 2005; Sarvar et al., 2006; Liu et al., 2006; Linderman et al., 2007). This literature review provides an overview of TIMs research with an emphasis on reliability and degradation and will consider the following topics: reliability and degradation mechanisms of TIMs, thermal conductivity test methods for TIMs, and the laser flash method.

Thermal Interface Material Reliability and Degradation

The proper selection of a TIM often requires considering not only the beginning-of-life thermal performance, but also the reliability, which is often not characterized by TIM manufacturers. Environmental conditions, assembly conditions,

and properties of the TIM and neighboring structures play key roles in determining if and how a TIM experiences thermal performance degradation during its operating life.

The effects of temperature cycling and elevated temperature and humidity, which are addressed in this study, are potential concerns for polymer TIMs. These conditions may be encountered in harsh operating environments, such as those experienced by automotive, space, and avionic applications. Temperature cycling may be problematic for elastomeric TIM pads if there is a large mismatch in coefficients of thermal expansion between the mating surfaces, which can lead to loss of contact at one or more surfaces (Viswanath et al., 2002).

In many instances, degradation in performance due to high temperature can be explained by considering the bulk behavior of polymers. For silicones or siloxanes (a commonly used material for both TIMs in pad form as well as dispensed TIMs), prolonged exposure to heat can cause degradation of the siloxane network, resulting in hardening of the bulk polymer, which over time can leave the polymer dry and brittle and cause it to lose adhesion to metal interfaces (Dal, 2004). Breakage of polymers can be caused by scission of highly linked polymer bonds into free radicals and monomers (Tummala and Rymaszewski, 1997). Elevated temperature produces low-molecular-weight cyclic compounds that can cause bulk polymers to crack (Clarson and Semlyen, 1993). Cracks at the interface or through the bulk of the material can increase thermal resistance at the interface due to the discontinuity of heat flow. For silicone, hardening and cracking occurs at temperatures exceeding 180 °C, which is well above the recommended operating temperature usually specified in

TIM datasheets. In fact, silicone should be relatively resistant to high temperature due to the high dissociation energy of the Si-O bonds (Dal, 2004). Luo et al. (2001) measured only a 2 percent decrease in thermal conductance for a silicone-based paste and up to a 46 percent decrease for non-silicone pastes after isothermal heating at 100°C for 24 hours. The addition of either Al₂O₃ or ZnO fillers into silicone rubber increases both the thermal conductivity and thermal stability but reduces its CTE (Sim et al., 2003). However, it is also important to note that silicones are susceptible to hydrolysis due to the presence of polar Si-O bonds (Dal, 2004).

Past work on the impact of temperature on TIMs reliability has been experimental in nature. In one of the few attempts to model TIM degradation, Samson et al. (2005) proposed an Arrhenius-type equation based on an empirical curve fit to express degradation of thermal performance with time due to elevated temperature for a phase change material:

$$R_{jc}(t) = R_{jc}(t=0) + A\sqrt{t} \exp\left(\frac{-E_a}{k_b T}\right) \quad (2.3)$$

where R_{jc} is the junction-to-case thermal resistance, A is an acceleration factor, E_a is the activation energy for the TIM, k_b is the Boltzmann constant, T is temperature, and t is time.

Moisture in an elevated temperature environment can also cause polymer thermal interface materials to degrade in performance. Silanol formation causes loss of hydrophobicity and adhesion due to migration of hydrophilic Si-OH groups into the exposed surface. This can lead to delamination on metal surfaces. Despite this, moisture can also improve network formation at low temperatures (Dal, 2004). Dal (2004) presented failure and material analysis findings of silicone-based thermal paste

exposed to moisture and high temperature plus moisture. Using a model for moisture diffusion into a thermal interface between the heat spreader and the chip with variables of temperature, humidity and exposure time, Zou et al. (2006) found that shear strength degrades with increasing moisture content, but the shear modulus does not correlate with moisture level in the thermal compound.

Although few studies have addressed the effects of humidity on polymer gap pad pads, fillers, and gels, some studies have examined the effects on polymers used in non-TIM electronic applications. Gomatam and Sancaktar (2004) observed reduced adhesion strength of adhesives exposed to a 90% RH environment. In tests performed by Prabhakumar et al. (2003), the adhesion properties of epoxy-based adhesives did not change significantly due to temperature/humidity testing, although the silicone-based adhesives experienced a drastic drop in adhesion strength.

The change in interfacial contact resistance caused by elevated temperatures was of interest in this study since it was hypothesized that delamination could cause degradation in thermal performance for gap pads, gap fillers, and putties, which are generally regarded as being among the most reliable TIM types. However, increased wetting of the surfaces may also occur, leading to reduced thermal resistance at the interfaces (Gowda et al., 2005). Furthermore, in an elevated moisture environment, reduced adhesion strength and thermal contact of the TIM could result in increased thermal resistance (Gomatam and Sancaktar, 2004). It is important to note that for many silicone-based TIMs, thermal performance may improve over the course of environmental exposure. Material in a softened stage can experience stress relaxation and can better conform to surface irregularities; or silicone extraction may occur,

which causes silicone oil to fill in small gaps and asperities that would otherwise impede conduction across the interface. One goal of this study was to determine whether degradation due to temperature cycling and elevated temperature/humidity occurs in select polymer TIMs and to quantify the change in thermal performance.

Many of the most well known examples of degradation affect dispensed TIMs, such as thermal greases. Because greases do not cure as gels and epoxy adhesives do, they are susceptible to pump out, which is caused by the expansion and contraction of the TIM layer, causing it to squeeze out of the interface gap. One trade-off associated with pump-out is that lower bondline thickness results in lower thermal resistance, but too low of a bondline thickness may result in regions with a lack of TIM coverage, resulting in local temperature rises.

Standoffs have been shown to mitigate the effects of pump out (Sikka et al., 2002). Brunschwiler et al. (2007) developed a method to address the problem of pump out in thermal greases. Their method consists of using nested channels to control the flow of the TIM and prevent pump out. Hierarchically nested channels (HNCs), which are etched onto a mating surface, allow thermal grease to flow easily in predefined paths during thermal cycling, alleviating many of the pressure gradients that can lead to pump-out (Brunschwiler et al, 2007). It is important to note that this solution requires that the die/heat spreader surface include these channels, which may be costly to incorporate from a manufacturing standpoint.

From a material integration standpoint, gels appear to be an attractive option because of their reduced propensity for pump-out. Prasher (2006) showed that gel pump out depends on the ratio G'/G'' (storage/loss modulus). Prasher and Matayabas

(2004) proposed that insufficiently cured gels exhibited grease-like behavior, which leads to the formation of voids. They also noted, however, that lower shear modulus values lead to lower initial thermal resistance, which suggests an optimal range of shear modulus values that can ensure reliable gel thermal performance. Emerson et al. (2005) showed that the flow of the matrix resin in a thermal paste depends on the Peclet number, defined as τ_w/τ_s , (where τ_w is the characteristic time for fluid filtration and τ_s is the characteristic time for deformation of the concentrated suspension). When the Peclet number is greater than one, filtration effects are important. This results in the tendency of filler particles to separate from the rest of the grease.

Nnebe and Feger (2008) examined dry-out in thermal greases using optical microscopy and IR thermography. Local variations in the grease microstructure caused by inhomogeneities in the distribution of the filler particles as well as matrix-filler compatibility can affect the susceptibility of a thermal grease to degradation, particularly at low bondline thicknesses (where the thickness is less than 10 times the largest filler particle size). In aged greases, Nnebe and Feger (2008) applied theories describing fluid flow through porous media to examine the impact of matrix-filler interaction.

While reliability problems such as pump out and dry-out have been reported to occur for thermal greases after prolonged use (Viswanath et al., 2002), the reliability of gap pads and gap fillers has received less attention. The relatively large bondline and the inability of gap pads to flow and fill in the microscopic crevices at the interfaces contribute to the low thermal performance compared to greases, gels, and solders. Maguire et al. (2005) incorporated thermal gap pads into their case study

of TIMs in high power amplifier designs while Gwinn and Webb (2003) compared the performance of a variety of TIMs, including gap pads, using published data. The performance over time when subjected to stress was not evaluated in either of these studies. Viswanath et al. (2002) reported that typical failure mechanisms in thermal pads are increased thermal resistance due to inadequate pressure or loss of contact at one or more interfaces. The extent of degradation of TIMs in pad-form and its causes have yet to be fully described in the literature and were therefore examined in this study, along with an adhesive and gel.

Experimental studies of degradation of TIMs in packages are common in industry. In a series of tests including HAST, high temperature storage (150 °C), and temperature cycling (-55 to 125 °C), Islam et al. (2008) showed that adhesives outperformed greases and gels due to the excessive voiding, which decreased mechanical strength and thermal performance. In contrast to their perceived characteristic behavior, gels were still found to be susceptible to voiding, pump out, and other degradation issues. Li et al. (2008) performed qualification tests of TIMs in FC-PBGA (flip chip plastic ball grid array) configurations at both the component level and the system level under temperature cycling and elevated humidity. Their results showed that the thermal characteristics and mechanical integrity of the selected TIM can be evaluated using the same stress conditions used in package reliability qualification. Zheng et al. (2009) employed packaged TIMs to explain how hygroscopic expansion and TIM bondline deformation during reflow and moisture soaking at 85 °C/85% RH drives delamination.

Polymer and solder TIMs are susceptible to voiding and delamination, which are of particular concern when introduced into the package during assembly (Gektin, 2005; Hu et al., 2004). Delamination and voiding have similar effects on the thermal performance despite the fact that voids can occur deeper into the bulk of the TIM while delamination occurs at the interface. Voids and delamination near a hot spot can have a dramatic effect on the maximum chip temperature (Gektin, 2005). Voids are defects that can be a few millimeters to several hundred nanometers in length, so although they are often visible at the macro level, they can also occur at the micron or submicron levels. Voids form when air becomes trapped as the TIM flows during assembly and can result from insufficient volume or outgassing during curing (Gowda et al., 2004). During the manufacturing process, voids can form in the die attach bond layer, and grow and coalesce during thermal cycling and elevated temperature conditions (Fleischer et al., 2006). In comparing stencil printing to dispensing of adhesives, Mukadam et al. (2004) examined the effects of heat ramp rate and peak temperature and showed that the initial part of the cure profile up to the material gelling temperature largely determines void size distribution.

The similarities between TIMs (types 1 and 2) and die attach materials both in function and composition make degradation models of die attach materials attractive in explaining many forms of TIM degradation. Sundararajan et al. (1998) described the shear stress distribution in the die attach layer of a power electronic component during thermal cycling or power cycling to predict the life of the chip by die attach fatigue. Thermal fatigue of solder is one example where a large body of work exists on the reliability of materials used for other electronic applications besides TIMs

(Lall et al., 1997). Die attach failure has been well studied and Hu and Pecht (1993) summarized failure mechanisms and damage models in outlining a design approach based on physics of failure. Gektin et al. (1998) related dramatic improvement in underfilled flip chip reliability to reductions in solder joint strain, which followed a Coffin-Manson relationship.

Thermally conductive adhesive tapes have been studied by Lee (2007) and Evely et al. (2004) and Chu and Selvakumar (2009). Loss of adhesion due to creep can cause degradation and failure in thermal tapes. Evely et al. (2004) measured the effects of creep on pressure-sensitive adhesives and concluded that tape chemistry and construction as well as environmental factors determine joint reliability. Besides adhesive tapes, qualification or performance tests of other TIM types not considered in this research but described in the literature include phase change materials (Aoyagi et al., 2008; Bharatham et al., 2005), solders (Deppisch et al., 2006; Hua et al., 2006; Refai-Ahmed et al., 2007), graphite (Luo et al., 2002; Marotta et al., 2002), and carbon nanotubes (Fan et al., 2007).

Mechanical degradation of the TIM can have important consequences that impact system thermal performance. When silicone TIMs are used to bond a heat sink to a PCB (printed circuit board), the TIM layer absorbs much of the stress on the PCB caused by the CTE (coefficient of thermal expansion) mismatch between the PCB and heat sink which could otherwise lead to possible PCB damage (Zhang, 2009). Low shear modulus, needed to reduce the possibility of decoupling, can depend on crosslinking density, polymer molecular weight, and selective use of reinforcing

fillers. Decrease in bond strength is another consequence of TIM degradation (Viswanath et al., 2002).

In summary, despite significant developments in bulk thermal resistance models of particle laden TIMs that take into account surface chemistry as well as contact resistance models of solid surfaces that take into account mechanical deformation, predicting in-situ thermal performance is impractical for most TIMs. Understanding the impact of environmental stress conditions presents additional challenges. For instance, the role of contact interface effects such as delamination in contributing to thermal performance degradation has not been well studied. Relating the impact of the environment to individual parameters that determine interfacial thermal resistance in order to estimate overall degraded TIM thermal performance has not yet been performed. The lack of accurate degradation data has hampered development of physics-based degradation models. Furthermore, while considerable progress has been made in understanding how many types of TIMs degrade, there is a need to understand how TIMs in pad form degrade and the conditions for which degradation in performance occurs. While in many cases comparative TIM studies of thermal performance have included TIMs in pad form, they have not included degradation data. In view of the wide range of TIMs and application conditions, it is likely that future degradation models will not be broadly applicable; rather they will address how specific classes of TIMs degrade under specific application environments, surface combinations, and loading conditions.

Thermal Conductivity Measurement Techniques

Although many techniques are available to measure the thermal resistance or thermal conductivity of TIMs, often the results cannot be compared across different methods or testing conditions (Tzeng, 2000). In addition, the thermal contact resistance is often ignored or combined into the overall thermal resistance, leading to performance data that can be misleading to thermal designers. Steady-state techniques, such as the guarded heat flow method and the guarded comparative longitudinal heat flow method, are commonly used by TIM manufacturers. These methods involve a Fourier law-type of measurement in which temperature is measured across a heated test specimen after the instrument and specimen reach thermal equilibrium. However, the validity of the standards associated with these measurement methods, namely ASTM D5470 (2006) and ASTM E1530 (2006), has been questioned since reproducibility of vendor data is often difficult to achieve and the test conditions, such as the contact pressures and sample thicknesses, often do not correspond to typical in-use conditions (Lasance, 2003). Experiments examining the effects of surface characteristics on resistance measurements found that vendor data underestimated the real-life interface resistance by up to an order of magnitude (Lasance et al., 2006). Deficiencies in the ASTM standards for steady-state measurements have prompted many researchers to offer modifications or develop new test methods, many of which are capable of improved accuracy (Gwinn et al., 2002; Culham et al., 2002; Kearns, 2003; Stern et al., 2006). Gwinn et al. (2002) developed a TIM tester with the ability to switch out test blocks of different materials

and surface finishes, which can be useful in reliability evaluation. Improvements in steady-state methods have led to the availability of commercial testers suitable for thermal conductivity measurements with less than 5% error (Analysis Tech, 2009).

Transient methods offer some advantages over steady-state techniques in terms of measurement time and test sample flexibility (Lasance, 2003). The laser flash method, to be discussed in the following section, the hot disk method (He, 2005), and the modified hot wire method (Mathis, 1999) are examples of transient methods that have relatively fast measurement speeds and can be used to measure multiple TIM types, such as greases and adhesives. Bosch and Lasance (2000) and Lasance and Lacaze (1996) developed transient apparatuses to measure temperature-time curves, which when used in conjunction with numerical analysis allow thermal interface resistances to be determined more quickly than typical steady-state methods. Szekely et al. (2002) developed a technique based on the differential structure function that yields information on the heat flow path from the heat source to the heat sink using internal transient temperature response curves. The technique, which can be applied under typical TIM usage conditions, allows the thermal resistance of the TIM to be determined in packaged devices.

Use of thermal test vehicles has become an increasingly common method among end-users for evaluating TIM reliability. Thermal test vehicles typically consist of heating elements, temperature sensors, and dummy processors designed to replicate TIM usage conditions. They can approximate the stresses and strains in the TIM during environmental exposure more accurately than approaches that use material test specimens (Chen et al., 2008). However, thermal test vehicles can be

costly and time consuming to develop and may not be suitable if good absolute accuracy is required since thermal test vehicles require correlations to convert thermal resistance data to values that reflect in-situ performance (Jarrett et al., 2007). An accurate test methodology, such as a steady-state method, can be applied to calibrate test vehicles (Stern et al., 2006). In addition, using a test vehicle that is too specific to a single application may cause difficulty in extending the results to packages with different configurations and environmental conditions. On the other hand, some test vehicles are based on packages intended to represent multiple component-TIM combinations (Samson et al., 2005; Chiu et al., 2001).

Aside from thermal conductivity measurement, several experimental techniques have been employed to assess TIM degradation. These include using IR thermography (Gupta et al., 2006; Dias, 2003) for characterizing the integrity of thermal interfaces, differential scanning calorimetry to examine cure behavior and determine activation energies and endothermic peak temperatures (He, 2001), scanning electron microscopy to examine TIM bondlines and the interaction between filler particles and the polymer matrix, and digital radiography and tomography to detect voiding (Gowda et al., 2006). Scanning acoustic microscopy can detect physical features, such as cracks, voiding, non-coplanarity, and delamination, which have been shown to correlate with measured thermal resistance (Haque et al., 2000) and will be used in this study. This technique allows for nondestructive inspection and uses the interaction between focused sound waves with a sample immersed in a couplant such as water to generate images that can reveal differences in acoustic impedance. Gowda et al. (2005) and Chiu et al. (2002) demonstrated the use of

scanning acoustic microscopy to assess voiding effects leading to increased thermal resistance over time.

System-level effects such as warpage and the often complex interaction between the TIM and the package should be well understood in evaluating TIM reliability in realistic applications. Thus, TIM mechanical properties, including shear modulus (Wang, 2006; Lim and Valderrain, 2007) are needed to fully understand how the TIM behaves with contact pressure applied (Bharatham et al., 2006). Determining the bondline thickness accurately is a key experimental challenge that limits the ability to accurately needed to determine thermal resistance from the thermal conductivity (Smith and Culham, 2005; Galloway and Kanapurthi, 2008; Wunderle et al., 2008). It has considerable relevance to reliability evaluation because the test specimen as measured in a thermal conductivity tester may differ from that in an assembled configuration.

Because of the impact on the bondline thickness and the potential for voiding and delamination, warpage of the die and the package is a key factor affecting TIM thermal performance, particularly if operating conditions involve temperature cycling (Kearney et al., 2009). Several studies have sought to measure predict the degree of warpage and to understand the effects on TIM thermal resistance (Solbrekken et al., 2000; Han, 2003; Yang et al., 2009; Too et al., 2007; Li, 2003; Wei et al., 2008).

While the most recent revision to ASTM D5470 (Hanson, 2006) alleviated many issues regarding high contact pressures used in steady-state TIM thermal conductivity testing, concerns remain over how well these values represent in-use TIM thermal performance. In general, a thorough understanding of the conditions

used to obtain datasheet thermal conductivity values is critical in translating datasheet values to application-specific values.

Even with significant advances in the development of thermal conductivity techniques capable of high absolute accuracy, little work is available describing methodologies to evaluate TIM reliability using material test specimens. Presumably, evaluating TIM reliability using material test specimens would involve periodically removing test specimens from a test chamber and measuring the performance to generate a time-history profile of thermal performance. The ability for steady-state techniques to capture changes in TIM thermal performance has yet to be demonstrated in the literature. Steady-state instruments do not provide the high degree of control offered by environmental chambers. Samples must be removed from the chamber and periodically measured in the thermal conductivity measurement apparatus.

Laser Flash Method

This study focuses on the laser flash method, which measures thermal diffusivity, a transient property that describes a material's ability to conduct heat in comparison to its ability to store heat. Knowledge of thermal diffusivity provides a means to extract thermal conductivity, and the first thermal diffusivity measurements using a flash technique were described by Parker et al. (1961) in the 1960s. Various researchers have proposed refinements to more accurately describe the heat transfer occurring during measurement, including Cowan (1963), who modified the Parker model to account for heat loss in the test sample due to radiation, and Clark and

Taylor (1975), who used similar assumptions as Cowan but considered the heating part of the temperature rise curve. These methods differ from the Parker method (1961) in how the thermal diffusivity is calculated from a measured temperature rise curve. Sheikh et al. (2000) examined the effects of radial heating, which causes samples to conduct heat laterally due to nonuniform surface heating. Further efforts have improved the measurement technique to the point where the method is well established for material property measurements in many industries.

Some of the sources of error associated with the laser flash method will be examined in this study. A large body of work exists for describing sources of error of laser flash measurement, including work by Taylor (1975), Baba and Ono (2000), and Lee and Taylor (1978) among others, but their work did not address errors from the standpoint of TIM property measurement.

In this study, the thermal performance and reliability of thermal interface materials were examined using the laser flash method applied to three-layer sandwich structures in which the TIM is assembled in between two coupon or substrate layers. In the 1970s, Lee (1975) and Lee (1977) developed a methodology to measure the thermal diffusivity of multilayer structures. This approach has been applied by other researchers to the study of thermal greases (Gowda et al., 2005) and solders (Chiu et al., 2002). Campbell et al. (1999, 2000), Hasselman et al. (2000), and Kohli et al. (2001) characterized epoxy adhesives using laser flash measurements of three-layer composite samples.

Lee and Taylor (1978) showed that it is not practical to measure the thermal diffusivity of a thin highly conducting layer in between substrates of lower thermal

diffusivity. They did not provide criteria however for the acceptable the ratio between middle layer to outer layer thermal diffusivity, which is also absent from ASTM E1461, which describes laser flash measurements (2001). Lee (1977) presented solutions for two and three-layer composite structures, and identified layers as being resistive or capacitive. Capacitive layers have uniform temperature. Using the ratio of the heat diffusion times between layers to determine whether capacitive solutions or the more general resistance solutions should be applied, Lee (1977) presented a 3-layer resistive solution as well as a solution for 3-layer composite structures with capacitive first and third layers. However, Lee (1977) did not provide criteria for the general 3-layer resistive case despite warning that that the iterative algorithm should not be used on composite structures with large differences in the heat diffusion times, as small differences in 3-layer thermal diffusivity result in large differences in the calculated middle layer thermal diffusivity.

The rationale behind examining these issues is a better understanding of whether thermal diffusion time ratios could be used to determine when the laser flash method could be applied for a given 3-layer TIM composite test specimen. Such criteria can be used to determine what thicknesses need to be used when constructing 3-layer test specimens.

When used for TIM reliability evaluation, 3-layer measurements allow realistic stresses and strains to be captured during the course of a reliability test. Such a method would also be attractive due to the high degree of control possible for the environmental exposure, which could be implemented using an environmental chamber rather than inside the laser flash instrument. Many other features of the laser

flash method make it suitable for reliability evaluation. Measurements are relatively fast, the instrument does not contact the test specimen, and there is no need to log data using multiple thermocouple channels. In a survey of 17 thermal conductivity techniques, Graebner (1997) described the laser flash method as requiring “moderate” operator skill and “medium” cost (including instrumental and sample costs) relative to other techniques. Chiu et al. (2002) showed that voiding is detectable 3-layer composite structures. It has also been noted that the laser flash method is capable of measuring cracked specimens, and shows agreement within 5% of steady-state values (Shaw, 1969).

Smith et al. (2008) noted that the need for laser flash test samples to accommodate laser pulses limits their ability to be tested in a product-like test fixture. This does not diminish the value of the laser flash method toward quantifying some types of TIM thermal performance degradation, especially those not heavily affected by the rest of the package and contact surfaces. In the absence of a comprehensive study on of the laser flash method’s ability to detect degraded TIM structures, more work needs to be performed to confirm that laser flash method accurately captures the impact of TIM degradation and how test structures should be designed to hold test specimens in place during measurements.

Chapter 3: Reliability Tests

Theory of the Laser Flash Method

The first part of this study involved assessing the effects of temperature cycling and elevated temperature/humidity on TIM thermal performance, measured using the laser flash method.

Basic Operation

The laser flash method involves monitoring the temperature of the rear surface of a test sample after a burst of energy (supplied by a laser) heats the front surface of the sample and the resulting temperature rise propagates through the material. The temperature rise curve, usually measured by an infrared detector, yields the thermal diffusivity of the test sample as well as the specific heat when a reference measurement is also performed. The approach is summarized in Figure 3.1.

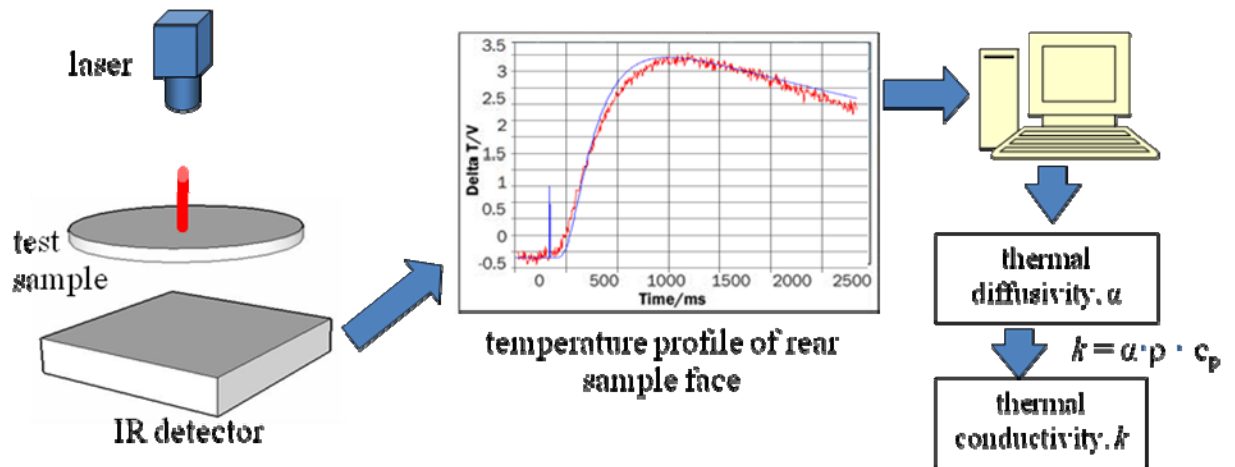


Figure 3.1: Illustration of the laser flash method.

When the thermal diffusivity and specific heat are known, the thermal conductivity can be calculated using the definition of the thermal diffusivity ($\alpha=k/\rho \cdot c_p$). In this study, the thermal diffusivity was determined using the Koski procedure (Koski, 1981), which requires time and temperature ratios of various points along the temperature rise curve (Parker et al., 1961).

Multilayer Analysis

The laser flash method can provide an indirect through-plane thermal conductivity measurement of a composite multilayer TIM test sample. For samples that require clamping using sample holder plates, the basic configuration is shown in Figure 3.2.

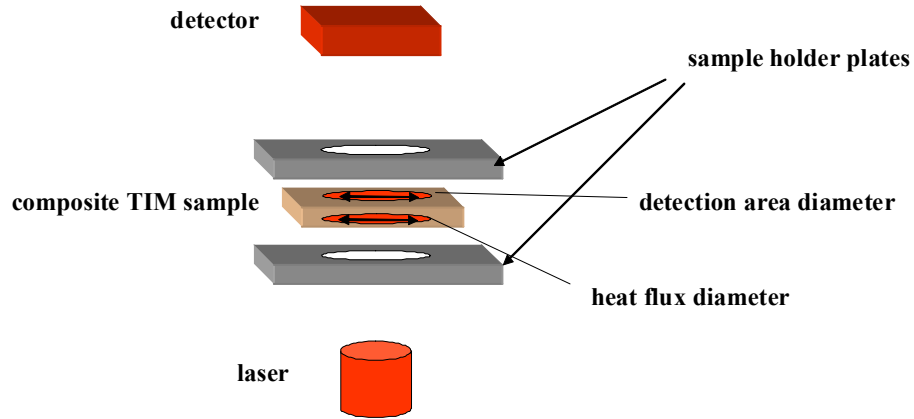


Figure 3.2: Configuration used for laser flash measurements of clamped 3-layer test samples.

The TIM thermal conductivity is derived from the thermal diffusivity measurement. For this study, an algorithm developed by H.J. Lee (1975) and T.Y.R. Lee (1977) was used to calculate the thermal conductivity across the TIM layer based on properties of the individual layers and the three-layer sample. Since contact component of the conductivity cannot be extracted from the three-layer case considered by Lee, the thermal conductivity calculated from the algorithm includes both bulk and interfacial contact contributions. Lee's formulation for layered composites relies on the following assumptions:

- 1-D heat flow
- No heat loss from the sample surfaces
- Heat is absorbed uniformly on one side of the sample
- Homogeneous layers
- Constant thermal properties over the temperature range

The half rise time of the temperature response of the composite sample was determined from the apparent diffusivity obtained from the measured data using the following relation described by Parker et al. (1961):

$$\alpha = \frac{1.38L^2}{\pi^2 \cdot t_{1/2}} \quad (3.1)$$

where $t_{1/2}$ = half rise time, L = thickness, and α = thermal diffusivity. The half rise time as well as the single layer properties were then used as inputs into the Lee algorithm. The k^{th} root of the characteristic equation, γ , must then be determined in order to solve for the inverse Laplace of the heat diffusion equation:

$$\cot(\eta_1\gamma)\cot(\eta_2\gamma) + H_{1/3}\eta_{3/1}\cot(\eta_2)\cot(\eta_2\gamma) + H_{2/3}\eta_{3/2}\cot(\eta_3\gamma)\cot(\eta_1\gamma) - 1 = 0 \quad (3.2)$$

where η_i is the square root of the heat diffusion time through layer i , η_{ij} is the ratio of η_i to η_j , and H is the volumetric specific heat. The back-side normalized temperature, V , of the composite sample was then calculated based on the algorithm inputs:

$$V = 1 + 2 \sum_{k=1}^{\infty} \frac{(\omega_1 X_1 + \omega_2 X_2 + \omega_3 X_3 + \omega_4 X_4) \cdot Q(\gamma_k, \eta_3, t)}{\omega_1 X_1 \cos(\omega_1 \gamma) + \omega_2 X_2 \cos(\omega_2 \gamma) + \omega_3 X_3 \cos(\omega_3 \gamma) + \omega_4 X_4 \cos(\omega_4 \gamma)} \quad (3.3)$$

where the X_i terms are functions of H , the ω terms are functions of η_{ij} , and Q is a function of the heat pulse. The diffusivity of the TIM layer was iterated until the normalized temperature using the three-layer composite solution at the half rise time converged to 0.5. The thermal conductivity can then be determined for the converged diffusivity value from the definition of thermal diffusivity. This procedure is summarized in Figure 3.3 and layers 1, 2, and 3 represent coupon 1, the TIM layer, and coupon 2, respectively.

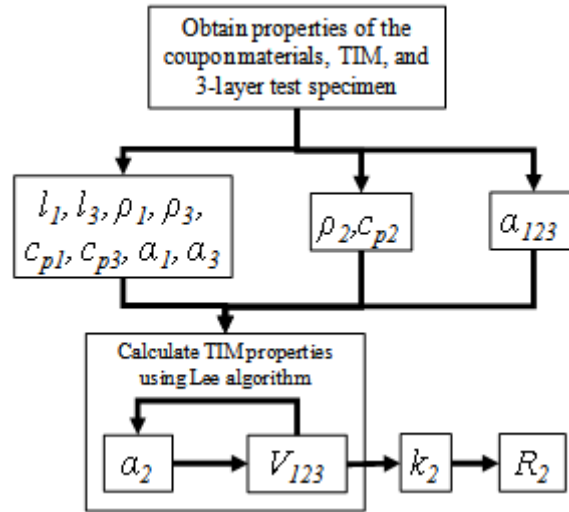


Figure 3.3: TIM thermal resistance measurement and calculation.

Experimental Approach

TIM samples were assembled to achieve a desired bondline thickness and then prepared for the laser flash measurements. A neodymium-glass (ND: glass) laser with a 1060 nm wavelength provided a 15J pulse during laser flash measurements. Baseline laser flash measurements were then performed prior to subjecting the samples to a defined environmental condition for a fixed period of time. Measurements were repeated periodically over the course of the environmental exposure. Scanning microscope images were taken of the samples after completing the environmental exposure. Ten samples of each type were measured to achieve statistical confidence in the assembly procedure, the laser flash data, and the three-layer calculations. This number included scanning acoustic microscope samples and room temperature samples used as a control group to assess room temperature effects.

Figure 3.4 provides an overview of the experimental procedure followed in this section.

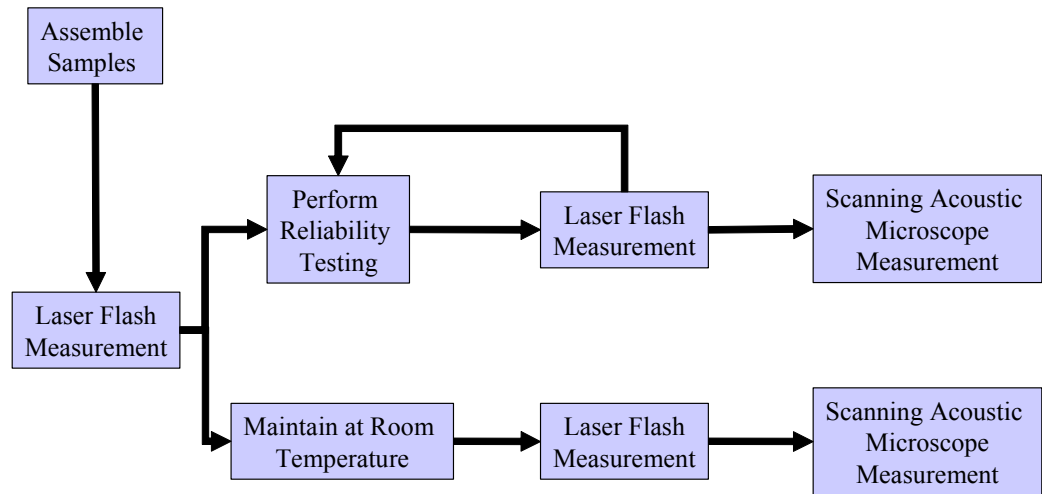


Figure 3.4: Overview of the experimental procedure.

Laser Flash Test Samples

TIM samples examined in this study were chosen from commercial offerings and represented a range of thermal interface materials. Specific samples within a TIM product line were selected based on the thickness constraints of the sample holder. All materials were suitable for so-called TIM 2 applications (heat spreader or thermal lid to heat sink) although the epoxy adhesive could also be used as a die attachment material (die to substrate). With the exception of the adhesive and gel, all samples were manufactured in pad form. The putty samples were silicone with either alumina or boron-nitride filler. Putties A and C, which were from the same manufacturer but differed in thermal conductivity, were tested with and without metal foil, which typically facilitates removal in in-use applications and also functions as a barrier layer between the TIM and the contacting surface. Gap filler is similar to putty but usually has an in-use compression level of 50% or lower. The gap pads had a thin layer of

pressure-sensitive adhesive (PSA) applied to promote adhesion at the interfaces, in addition to fiberglass reinforcement within the polymer matrix, as shown in Figure 3.5. The gap pads were from the same manufacturer, and Gap Pad B contained silicone while Gap Pad A was silicone-free. Measurements using electron dispersive microscopy indicated that the gap filler and gap pads contained aluminum oxide filler particles.

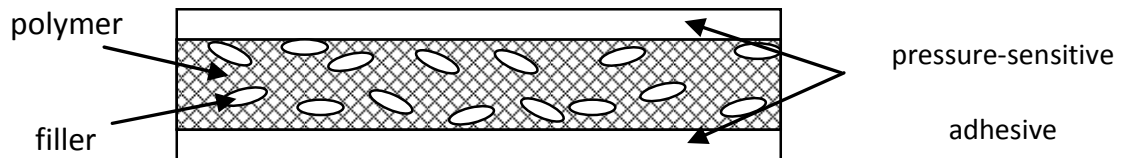


Figure 3.5: Illustration of TIM gap pad bondline.

The thermal gel and adhesive were diamond-filled, electrically insulating and thermally conductive silicone pastes. The gel was reworkable with an optional high temperature cure while the adhesive required high temperature curing. Table 3.1 summarizes the test samples examined in this study.

Table 3.1: TIM test samples.

Designation	Construction and Composition	Vendor k (W/m-K)	Temperature Cycling 1 (-40 to 125°C)	Temperature Cycling 2 (-55 to 125°C)	Elevated Temperature/Humidity
Putty A	alumina-filled silicone	11	yes	no	yes (w/ foil, no foil)
Putty B	boron nitride-filled silicone	3	no	yes	yes
Putty C	alumina-filled silicone	6	no	yes (w/ foil, no foil)	no
Adhesive	diamond-filled non-silicone paste	11.4	yes	yes	no
Gel	diamond-filled non-silicone paste	10	no	yes	yes
Gap Filler	alumina-filled silicone	2.8	yes	no	no
Gap Pad A	alumina-filled non-silicone	0.9	yes	no	yes
Gap Pad B	alumina-filled silicone	2.4	yes	no	no

Laser Flash Test Sample Holder

To simulate realistic loading conditions, laser flash measurements were performed on various TIMs assembled into three-layer sandwich structures, enabling the test samples to remain undisturbed between measurements performed periodically throughout the environmental exposure, as illustrated in Figure 3.6.

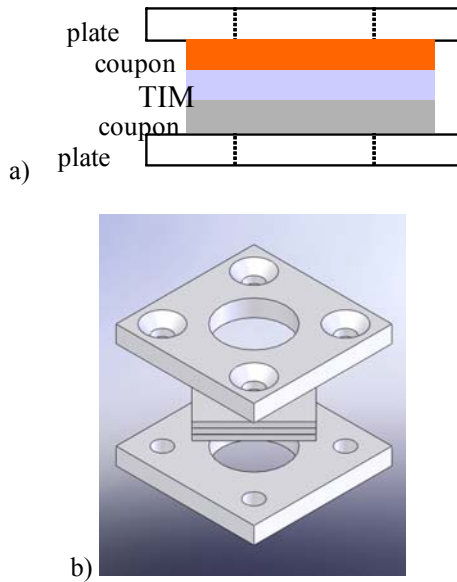


Figure 3.6: Illustration of clamped TIM : a) side view; b) isometric (exploded view).

The test specimens were three-layer sandwich samples consisting of the TIM sandwiched between two metal coupons. When assembled with the sample holder plates, some area of the test sample coupon (top or bottom) was in contact with the contacting clamping plate since the opening area was smaller than the coupon area, as shown in the exploded view in Figure 3.6. The sample holder plates restricted the area of the test sample illuminated by the laser, which was assumed to correspond to the entire area inside the opening of the plates. The center openings of the clamping plates (both top and bottom plates were identical in geometry) were 11.9 mm in diameter, which corresponded to the opening size of the manufacturer's sample holder used in single layer laser flash measurements, which expose over 90% of the test sample surface during laser flash measurements to approximate uniform heating of the sample surface.

The coupons used in the temperature cycling tests were 1-mm-thick squares with a side length of 16.4 mm; the coupons used in the elevated temperature/humidity test were 1-mm thick disks with a diameter of 12.7 mm. These sizes were greater than the typical 8 mm by 8 mm size typically used for single layer measurements in order to increase the area on which the force was applied when the samples were assembled. To set the initial bondline thickness and facilitate placement in the laser flash system, the layer stacks were held in place by aluminum plates. Figure 3.7 shows sample holder plates, which were fabricated out of aluminum and had four flat head screws clamping them together.

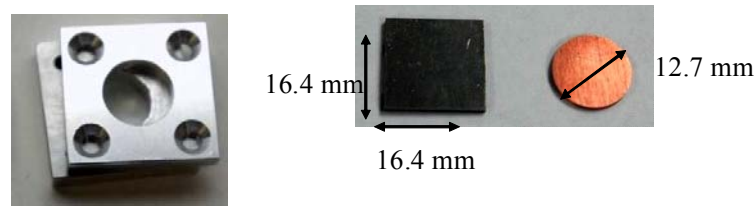


Figure 3.7: TIM sample holder plates with coupons.

The temperature cycling coupon materials, oxygen-free high conductivity (OFHC) copper and Alloy 42, were selected based on differences in their coefficients of thermal expansion (CTE) in order to increase the maximum shear stress. The configuration can be approximated as a bonded assembly of two dissimilar materials with a layer of adhesive subjected to a uniform temperature change. For the adhesive TIM, the maximum shear stress τ occurs at the edges and can be described as follows (Dasgupta, 1991):

$$\tau_{\max} = \frac{G\Delta T(\alpha_{CTE1} - \alpha_{CTE2}) \tanh(Al)}{LA} \quad (3.4)$$

$$A^2 = \frac{G}{L} \left(\frac{1-\nu_1}{E_1 A_1} + \frac{1-\nu_2}{E_2 A_2} \right) \quad (3.5)$$

where α_{CTE} is the CTE of the coupon, G is the shear modulus of the TIM, ΔT is the temperature difference, l is the TIM layer length, L is the TIM layer thickness, A is the cross-sectional area of the TIM layer, E is the Young's Modulus, and ν is Poisson's ratio. Alloy 42 was preferred over other low CTE materials, such as ceramic or silicon, as it is less brittle and less prone to cracking when loading is applied. Furthermore, Alloy 42 is less transparent than silicon in the infrared region of the spectrum and does not require a gold coating to reduce transmittance. The calculated maximum shear stress in a 0.25-mm-thick adhesive layer ($G = 1.5$ GPa) assuming a temperature cycle range of 160 °C was 9.2 MPa for the copper–Alloy 42 combination (with the same sample geometry used in laser flash measurements). This result was less than a 15% difference from 10.8 MPa, the calculated maximum shear stress for the copper-silicon combination. The elevated temperature/humidity test used copper coupons on the top and bottom. All sample coupons of a given material were fabricated from the same lot to prevent variations in surface roughness between samples from affecting the measurements.

Sample Preparation

The surfaces of the coupons were cleaned with isopropyl alcohol prior to assembling the sandwich structures. Graphite coating was applied to all test sample sandwiches to enhance the radiational absorptivity and emissivity prior to each sequence of laser flash runs. Five coats of graphite were applied in accordance with ASTM E1461 (2001) and the laser flash manufacturer's directions.

Although the laser flash measurement imposed restrictions on the sample geometry, applying contact force to the TIM allowed loading conditions to more closely match typical usage applications than those used in many bulk conductivity measurement tests. The thermal performance of gap pads and gap fillers, which generally require higher clamping forces for optimal performance compared to thermal greases, is highly dependent on the loading force (Maguire et al., 2005).

Many manufacturers control contact force when characterizing the thermal performance of their thermal interface materials per ASTM D5470, but the stresses in elastomeric materials change over time due to their viscoelastic nature. Since bondline thickness can be more accurately controlled than force, a nominal 25% compression was applied to the gap filler, putty, and gap pad samples during assembly. This thickness value was within the manufacturer's recommended compressed thickness values. The thickness was controlled manually by tightening the sample holder screws and measuring the thickness using a micrometer. Care was taken to ensure that tightening the screws to compress the TIM would result in a uniform thickness and not cause gaps that could have resulted in delamination during assembly. The bondline thicknesses of the as-prepared TIM specimens are summarized in Table 3.2 as mean values with standard deviations. Room temperature samples were assembled such that the bondline thicknesses matched those used in corresponding environmental exposure samples.

Table 3.2: TIM bondline thicknesses.

TIM	Initial Bondline Thickness (mm)		
	Temperature Cycling 1 (-40 to 125°C)	Temperature Cycling 2 (-55 to 125°C)	Elevated Temperature/ Humidity (85°C/85% RH)
Putty A (with foil)	1.1 ± 0.03	N/A	1.4 ± 0.03
Putty A (no foil)	N/A	N/A	1.4 ± 0.01
Putty B	N/A	1.4 ± 0.09	1.4 ± 0.01
Putty C (with foil)	N/A	1.4 ± 0.08	N/A
Putty C (no foil)	N/A	1.4 ± 0.04	N/A
Adhesive	0.3 ± 0.01	0.3 ± 0.02	N/A
Gel	N/A	0.1 ± 0.04	0.1 ± 0.01
Gap Filler	0.8 ± 0.04	N/A	N/A
Gap Pad A	0.6 ± 0.04	N/A	0.6 ± 0.01
Gap Pad B	0.5 ± 0.02	N/A	N/A

The bondline of epoxy adhesive samples, which were not held under pressure, was maintained using Kapton tape at the corners of the sample, chosen because of its good stability at high temperature. The amount of adhesive dispensed onto the coupon surfaces was controlled manually by the dispenser before the coupons were mated together. The adhesive samples were cured per the manufacturer’s instructions using a 60 °C prebake for 1 hr and a 150 °C bake for 0.5 hrs. For the adhesive samples, the top and bottom aluminum plates of the sample holder were used to mask the laser beam and radiation from the rear sample, and no clamping force was applied by tightening the screws. The gel samples, which were clamped, also used spacers of the same thickness.

Sample thicknesses of the gap pads and fillers were measured with a flat point micrometer, which had an accuracy of 25- μm , and values were averaged over 3 locations on the surface.

Reliability Test Procedure

The density of the TIM layer was determined by measuring the mass of the sample and the coupons and assuming that the TIM covered the entire face of the coupon (neglecting the material squeezed out when compressed). Furthermore, the vendor value of the TIM layer specific heat was used in the thermal resistance calculation for all samples except for the adhesive samples, which required DSC measurement to be performed. Vendor values of thermal diffusivity were determined from specific heat and vendor thermal conductivity values. Measured values for specific heat and thermal diffusivity were used for the coupon layers and assumed to be the same among all samples. The thermal diffusivity was determined to be 0.041 cm^2/s for Alloy 42 and 1.17 cm^2/s for copper. Thermo-mechanical analysis (TMA) yielded 3.2 $\text{ppm}/^\circ\text{C}$ and 14.7 $\text{ppm}/^\circ\text{C}$ for the Alloy 42 and copper coefficients of thermal expansion (CTE), respectively.

The Lee algorithm (1975, 1977) requires the specific heat values of the individual layers of the composite sample. Due to the difficulty in applying the graphite coating to single layer polymer TIMs, differential scanning calorimetry (DSC) was used for determining the specific heat in samples where vendor data was not provided. DSC is a thermoanalytical technique in which the difference in the amount of heat required to increase the temperature of a sample and reference are measured as a function of temperature. It is generally a more accurate technique for

measuring specific heat than the laser flash method as there is no variability in heat pulses between successive runs and no dependence on coating material or sample surface properties (Graebner, 1997).

All laser flash measurements were performed at room temperature, with five flashes per measurement, as recommended by the manufacturer. Although it can be shown that the value of the TIM layer thermal resistance is not dependent on which side faces the laser (Lee, 1975), all laser flash measurements were conducted with the copper side facing the laser beam to avoid variation due to the coupon surface finishes. A 50% optical filter, the highest transmittance available for this instrument, was used in the measurements to attenuate the beam power. For consistency, the method described by Cowan (1963) was used to determine the thermal diffusivity of all the samples.

Reliability Test Conditions

Since electronic hardware may experience temperature excursions due to the environment or daily operation in a variety of military, aerospace, and consumer applications, temperature cycling tests were used in this study to simulate the stresses experienced by TIMs during typical usage. In the absence of a standard method for environmental exposure of TIMs, the temperature range for the first temperature cycling test was chosen to be -40 to 125 °C, with one cycle lasting for 1 hr (10 °C per minute ramp rate, 15-min dwell at the low and high temperatures). This temperature profile was based on a measurement standard used for surface mount solder attachments (1995). The second temperature profile was -55 to 125°C, with one cycle lasting for 70 min (15-min dwell at the low and high extremes). Except for Putty B,

the selected test temperatures were within the normal operating temperature limits of the TIMs specified by their manufacturers.

To simulate the combination of elevated temperature and humidity encountered by electronic hardware, tests were also performed at 85 °C/85% RH. This stress condition, which allows for the effect of moisture on thermal performance to be examined, has been applied in other TIM studies and is commonly used in environmental testing of non-TIM electronic parts and components (Gowda et al., 2005; IPC, 1995).

Results

Nine samples of each TIM type were prepared for the first temperature cycling test while the second temperature cycling test and the elevated temperature/humidity test used 8 samples each. Laser flash measurements were taken prior to each test and nominally at increments of once every 250 cycles or every 250 hrs. Each thermal resistance value is given as a mean value and the standard deviation associated with each of the samples (1 value per sample is based on an average of 5 flashes).

Room Temperature Observations

Although examining the behavior of TIM samples subjected to temperature cycling and elevated temperature/humidity was the main objective of this study, separate trials were also performed to characterize the behavior of the samples over

time at room temperature to distinguish between room temperature and temperature cycling or elevated temperature/humidity effects.

Table 3.3 summarizes the changes in TIM layer thermal performance over time when stored at room temperature after being cured. Measurements were performed for three samples per type. The “time after assembly” refers to the time after the TIM was compressed between the sample holder plates and the screws were tightened.

Table 3.3: TIM layer thermal resistance at room temperature.

	Thermal resistance (mm²K/W)				
Time after assembly	Putty A (no foil)	Adhesive	Gap Filler	Gap Pad A	Gap Pad B
10 min	94 ± 7	133 ± 21	126 ± 18	223 ± 25	74 ± 5
1 hr	93 ± 7	116 ± 7	127 ± 15	220 ± 9	75 ± 7
1 day	93 ± 6	109 ± 12	126 ± 15	224 ± 20	72 ± 6
10 days	92 ± 7	97 ± 6	127 ± 13	220 ± 10	69 ± 7
30 days	91 ± 7	89 ± 5	123 ± 14	214 ± 21	61 ± 3
Change after 30 days	-3 (-3%)	-44 (-33%)	-3 (-2%)	-9 (-4%)	-13 (-17%)

After being subjected to a 1 hr prebake at 60°C and a 0.5 hr bake at 150°C, the epoxy adhesive showed a 33% reduction in resistance after storage for 30 days at room temperature (the largest change among the samples tested), reaching a thermal resistance of 89 mm²K/W. Material flow and other relaxation processes, as well as

handling (vibration/shock), could have improved the contact between the other TIMs and coupons after assembly. Storage of the samples over time could have led to a reduction in silicone content in the TIM layer by means of outgassing or extraction, which could have contributed to the observed resistance decreases at room temperature.

Temperature Cycling Test (-40 to 125 °C)

The results of the temperature cycling tests from -40 to 125 °C are summarized in Table 3.4. The resistance changes at the end of the temperature cycling tests (relative to the baseline resistance) are also provided.

Table 3.4: TIM layer thermal resistance under temperature cycling (-40 to 125 °C).

	Thermal resistance (mm ² K/W)				
	Putty A (no foil)	Adhesive	Gap Filler	Gap Pad A	Gap Pad B
Vendor	101	22	271	633	213
Baseline	80 ± 5	69 ± 7	125 ± 11	253 ± 42	69 ± 7
255 cycles	73 ± 5	61 ± 5	123 ± 12	267 ± 50	52 ± 9
510 cycles	73 ± 6	63 ± 5	124 ± 12	265 ± 51	52 ± 9
760 cycles	67 ± 5	67 ± 6	124 ± 11	269 ± 53	52 ± 9
Change after 760 cycles (-40 to 125°C)	-13 (-16%)	-2 (-3%)	-1 (-1%)	+16 (+6%)	-17 (-25%)
Change at end of test (room temp.)	-5 (-6%)	-5 (-8%)	-0.1 (0%)	+4 (+2%)	-19 (-27%)

As shown in Table 3.4, with the exception of Gap Pad A, a reduction in TIM thermal resistance was observed on average throughout the temperature cycling test, with the greatest changes usually occurring prior to the measurement at cycle 255. The observed thermal resistance reduction may have been caused by the release of silicone from the TIM onto the contacting surfaces. This effect, often referred to as silicone extraction, is known to affect silicone elastomeric pads and can contaminate nearby components (Bergquist, 2007), in some instances reducing the contact resistances by filling in the interstices. The Gap Pad A samples, which contained no silicone, showed a slight increase of $12 \text{ mm}^2\text{K/W}$ in resistance (5%), but this was within the uncertainty of the measurement. Higher levels of noise were observed in the temperature rise signals for the gap filler pads. A comparison with the room temperature study results in Table 3.4 indicates that factors independent of temperature cycling, but still temperature-related, may impact thermal performance. The elevated temperature of the cycling tests may have accelerated the processes occurring at room temperature.

The adhesive TIMs subjected to temperature cycling decreased in thermal resistance initially, but then gradually increased. Under room temperature, thermal resistance of the adhesive TIM continued to reduce throughout the observation period. Unlike the gap fillers and gap pads in this study, the adhesive was a dispensed epoxy material requiring a high temperature cure, so the resistance change could have been caused by additional crosslinking after the samples were subjected to the high temperature cure. Of all the materials tested, the adhesive baseline resistance was dramatically lower than the room temperature test values, starting with the 10-min

value. As the difference in average bondline thickness was less than a few percent between the two series of tests, this result may have been caused by differences in how the material was dispensed as well as the effects of storage, as some samples contained adhesive in containers that had been thawed and then refrozen. Under temperature cycling, interfacial effects precipitated by the thermal expansion mismatch between the TIM and the metal coupons may have countered the crosslinking effect observed under room temperature.

While few changes were evident in the appearance of the TIM samples after temperature cycling, Gap Pad A samples did show slight discoloration after 255 and 510 cycles, most likely due to crosslinking of the polymer matrix. The Putty A samples showed signs of pump out after 255 cycles. Figure 3.8 shows a sample after the first thermal performance measurement. The “before” image shown is for a different sample assembled in the same manner, and is representative of all Putty A samples prior to temperature cycling exposure.

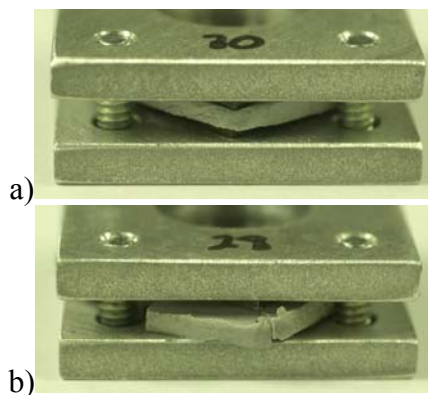


Figure 3.8: Pump-out in the Putty A samples:

a) before temperature cycling; b) after 255 temperature cycles.

This pump out was likely caused by the repeated expansion and contraction of the TIM relative to the sample holder structure during temperature cycling. Due to the concern over pump-out, the thickness of this TIM type was measured prior to each intermediate thermal performance measurement and not assumed constant, as were the other samples. The thickness of the TIM layer was found to decrease an average of 0.1 mm as measured during each periodic thermal performance measurement. The screws were not tightened further after assembly. The excess material that was pumped out was removed to allow the TIM sample to fit in the sample holder during the laser flash measurement. Despite the pump-out seen after only the first thermal performance measurement in the Putty A samples, the thermal resistance of the putty experienced a reduction in part due to the decrease in thickness. Since the three-layer sandwich was not held at a fixed bondline thickness, the compression and shear at the putty-to-coupon interface may have improved wetting between the surfaces, further enhancing the thermal performance.

Widely used in industry to detect defects and failures in ICs, scanning acoustic microscopy (SAM) was used in this study to detect voids, delamination, and morphological changes that might explain changes in the thermal characteristics of the TIMs. This method can be useful given that the uncertainty in the calculated values, based on laser flash measurements, may not allow small changes in the thermal resistance to be resolved with statistical confidence. Furthermore, because of the nature of the laser flash measurement, in which thermal wave propagation through a sample material causes a temperature rise, the laser flash measurement may not capture all occurrences of delamination or voiding, particularly if the delamination

regions are located near the edges of the area illuminated by the laser beam incident on the sample.

Since the application of SAM requires that specimens be immersed in a liquid, SAM images were taken of a separate group of test samples that were assembled in the same manner as those used in environmental exposure tests. This step prevented direct comparison of before- and after-temperature cycling images, but prevented the influence of absorbed moisture from affecting the thermal diffusivity measurements.

All measurements used a 75 MHz transducer, and images were taken in C-scan mode. Only the area within the round opening of the aluminum sample holders that was used for laser flash measurements was acoustically visible as the aluminum attenuated the acoustic signal outside of the opening. A pulse echo beam was used, as this was suitable for the material combinations examined in the measurement.

The SAM measurements revealed delamination near the edges of the viewable area occurring at the TIM-copper coupon interfaces in nearly all of the Gap Pad A samples. A representative image is shown in Figure 3.9. SAM images of a non-temperature-cycled sample aged at room temperature and assembled at the same time as the temperature-cycled one are shown for comparison in Figures 3.9 and 3.10.

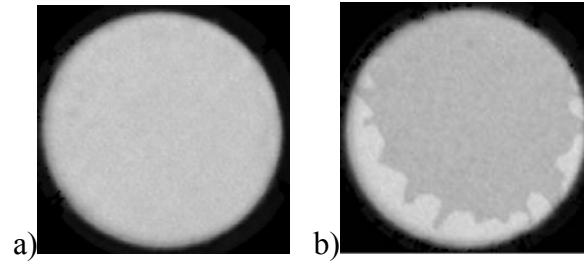


Figure 3.9: Scanning acoustic microscope image:

- a) Non-temperature-cycled Gap Pad A sample;
- b) Temperature-cycled Gap Pad A sample (after 760 cycles).

Cracking of the TIM layer in the temperature-cycled putty samples was visible at the TIM-Alloy 42 coupon interface, as shown in Figure 3.10. The dark spots were attributed to scratches on the graphite coating.

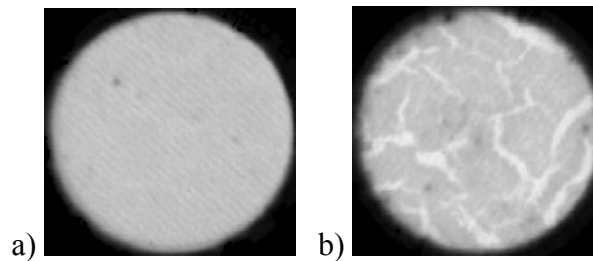


Figure 3.10: Scanning acoustic microscope image:

- a) non-temperature-cycled Putty A sample;
- b) temperature-cycled Putty A sample (after 760 cycles).

Regions of non-uniform TIM coverage were visible in all of the SAM images of the temperature-cycled adhesive samples. This non-uniformity may have resulted from how the adhesive was dispensed onto the coupons, as well as from additional crosslinking of the epoxy adhesive during temperature cycling. SAM measurements

did not reveal any loss of contact at the TIM-coupon interfaces for the Gap Pad B and gap filler samples.

Temperature Cycling Test (-55 to 125 °C)

The results of temperature cycling from -55 to 125 °C performed on a second group of test samples are shown in Table 3.5. The error bars show the standard deviation associated with each of the samples (1 value per sample is based on an average of 5 flashes).

Table 3.5: Calculated TIM thermal resistance under temperature cycling (-55 to 125 °C).

	Thermal Resistance (mm ² K/W)				
	Putty C (no foil)	Putty C (w/ foil)	Putty B	Adhesive	Gel
Vendor	227	232	450	26	12
Baseline	208 ± 30	282 ± 69	361 ± 25	129 ± 16	36 ± 20
246 cycles	196 ± 33	318 ± 89	499 ± 22	116 ± 8	16 ± 22
493 cycles	188 ± 33	284 ± 133	598 ± 18	114 ± 10	18 ± 21
765 cycles	200 ± 35	275 ± 234	731 ± 19	103 ± 11	19 ± 6
1009 cycles	181 ± 35	265 ± 188	726 ± 17	102 ± 12	19 ± 19
1295 cycles	175 ± 33	275 ± 210	745 ± 19	100 ± 12	19 ± 19
1538 cycles	174 ± 32	249 ± 240	740 ± 24	103 ± 12	20 ± 19
1789 cycles	178 ± 35	253 ± 212	709 ± 22	106 ± 13	21 ± 19
2098 cycles	174 ± 31	234 ± 274	664 ± 20	98 ± 13	21 ± 17
Change after 2098 cycles (-55 to 125°C)	-34 (-16%)	-48 (-17%)	+303 (+84%)	-31 (-24%)	-15 (-42%)
Change at end of test (room temp.)	+1 (+0.3%)	-42 (-12%)	+76 (+24%)	-5 (-4%)	-18 (-54%)

With the exception of Putty B, which degraded by over 50% in thermal performance after the first 765 cycles, the thermal resistance did not increase appreciably for any of the specimens up to 2098 cycles. The observed improvement in thermal performance of Putty C may have been caused by silicone extraction, as seen in the other temperature cycling test. A comparison of the thermal resistance values throughout temperature cycling with the values from room temperature

samples indicated that the changes in thermal resistance throughout the temperature cycling tests can be partly attributed to non-temperature-related effects. Putty C showed some signs of pump-out throughout the test, but not at the levels seen in Putty A in the other temperature cycling test. SAM images of adhesive samples showed regions of non-uniform coverage and lack of coverage.

Analysis of Putty B Thermal Performance Degradation

Because SAM measurements performed after temperature cycling exposure did not reveal any features at the TIM-coupon interfaces that could have contributed to thermal performance changes in Putty B, the thermal performance degradation was likely caused by changes in the bulk of the material.

To test the effect of elevated temperature, the thermal performance was measured nominally every 200 hrs in additional tests conducted at 125 °C. Eight samples were subjected to elevated temperature while 2 samples were held at room temperature. The results shown in Table 3.6 indicate that the samples at elevated temperature on average experienced a 14-percent decrease in effective thermal conductivity after 1016 hrs, a decrease that was not at the level seen in the temperature cycling tests after 246 cycles.

Table 3.6: Calculated Putty B thermal conductivity based on laser flash measurements.

	Effective TIM Thermal Conductivity (W/m-K)	
	125°C	Room temperature
Baseline	3.5 ± 0.4	3.4 – 3.6
194 hours	3.2 ± 0.3	3.4 – 3.6
386 hours	3.0 ± 0.4	3.4 – 3.6
596 hours	2.9 ± 0.2	3.4 – 3.5
802 hours	2.9 ± 0.2	3.2 – 3.5
1016 hours	3.0 ± 0.2	3.2 – 3.6
% change after 1016 hours	-14	+2

As Table 6 shows, thermal decomposition of the TIM due to elevated temperature was unlikely to be the primary cause for Putty B degradation. This finding was reasonable since silicone decomposition, which can result from a thermal decomposition reaction in which the silicone chain is shortened and a cyclic compound is formed (Dal, 2004; Clarson and Semlyen, 1993), should occur above 180 °C, well above the maximum temperature of the temperature cycling tests, making this effect alone an unlikely explanation for the observed behavior of Putty B.

The impact of temperature cycling on bulk performance was studied by examining the effect of the glass transition temperature (T_g) on the thermal performance of the TIM. The glass transition temperature, T_g , represents the temperature at which amorphous solids transition from the rubbery to the glassy state.

The T_g of Putty B was measured using a dynamic thermal mechanical analyzer (DTMA) and was performed on a TA Instruments RSA III in dynamic, strain-controlled, temperature ramp mode. The measurement followed the ASTM E1640-04 Test standard (2004) and used a 5% strain level, a 1-Hz frequency, and a 1 °C/min ramp rate. Using the temperature at which a change occurs in the slope of the storage modulus with temperature, as shown in Figure 3.11, the test yielded a T_g of -55 °C, which was a reasonable value since the presence of filler particles in the silicone can increase the T_g above that of pure silicone, which is -120 °C (Materials, 2008), and Putty B was composed of 45% boron nitride (BN) and 55% silicone.

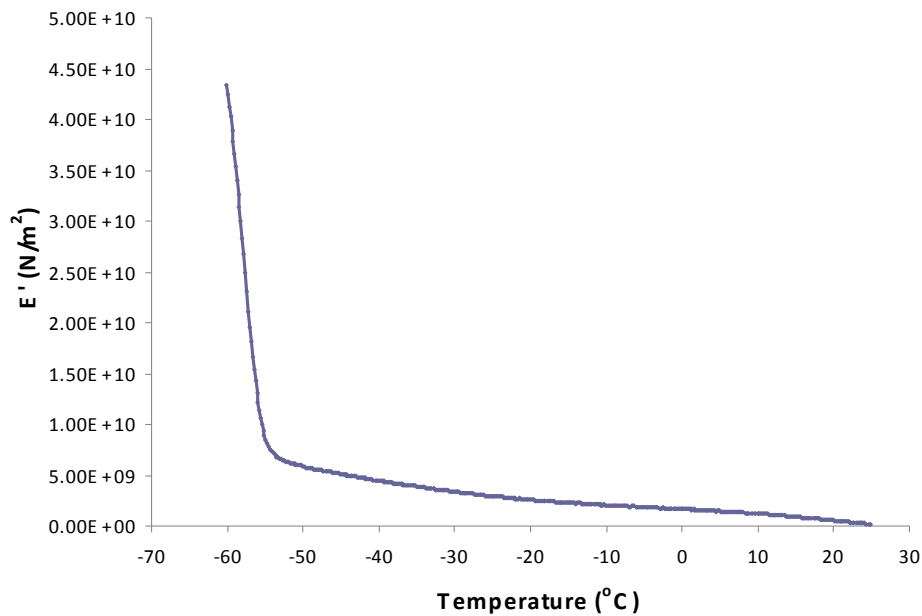


Figure 3.11: Putty B storage modulus as a function of temperature.

Repeated temperature excursions near the T_g in Putty B may have caused repeated changes from a hard, brittle state to a soft, rubbery state, leading to degradation over time. Repeated thermal expansion and contraction, combined with

the CTE mismatch of the coupons, may have contributed to additional degradation. It is important to note that since the minimum temperature during the temperature cycling test (-55 °C) was below the minimum operating temperature (-45 °C) recommended by the manufacturer, this behavior may not pose a problem in a typical application.

Elevated Temperature/Humidity Results

For the elevated temperature/humidity test, the round 12.7 mm diameter metal coupons were used rather than the 16.4 mm square coupons. This change was found to result in higher baseline thermal resistance values and a closer match to vendor data. The results of the elevated temperature/humidity test conducted at 85 °C/85% RH on a third group of test samples are shown in Table 7. For the elevated temperature/humidity tests, all samples with the exception of the Gap Pad A samples showed an overall resistance decrease at the end of the test compared to the baseline measurement. The greatest differences between the foil and non-foil were found early in the test. After 553 hrs, these differences became smaller because the foil most likely deformed to the contours of the surface. The improvement in performance was most likely caused by the improved wetting at the contact interfaces due to the presence of silicone, as was the case for temperature cycling. The Gap Pad A samples, which were silicone-free, experienced on average a 4% increase in thermal resistance while other samples experienced up to a 40% reduction in thermal resistance. The best performing samples were the thermal gels, due to their high bulk thermal conductivity and thin bondline. Room temperature Gap Pad A and gel samples remained relatively constant in thermal resistance on average, like the

corresponding elevated temperature/humidity samples, as shown in Table 3.7. For the gel, crosslinking at room temperature may have contributed to a reduction in thermal resistance in the room temperature samples. For both the Putty A and gel samples, the greatest overall thermal resistance change occurred after initial exposure (between the baseline and the measurement at 265 hours), which may have been largely due to thermal expansion. SAM measurements did not reveal features at the interface that would have led to changes in thermal performance for the room temperature and elevated temperature/humidity conditions.

Table 3.7: Calculated TIM thermal resistance under 85 °C/85%RH.

	Thermal Resistance (mm²K/W)				
	Putty A (no foil)	Putty A (w/ foil)	Putty B	Gap Pad A	Gel
Vendor	125	127	467	656	11
Baseline	163 ± 10	229 ± 48	479 ±31	431 ± 76	41 ± 10
265 hours	147 ± 8	158 ± 15	435 ±14	437 ± 71	28 ± 8
553 hours	147 ± 9	162 ± 12	444 ±17	435 ± 66	27 ± 8
813 hours	146 ± 9	160 ± 11	443 ±11	438 ± 71	26 ± 7
1063 hours	142 ± 8	156 ± 13	374 ±18	428 ± 72	26 ± 8
1310 hours	136 ± 7	154 ± 10	404 ±16	426 ± 65	26 ± 7
1621 hours	141 ± 7	153 ± 14	409 ±23	440 ± 75	26 ± 7
1909 hours	144 ± 8	160 ± 12	407 ±20	441 ± 73	26 ± 7
2173 hours	149 ± 11	172 ± 45	406 ±19	450 ± 72	25 ± 7
Change after 2173 hours (85°C/85%RH)	-14 (-9%)	-57 (-25%)	-73 (-15%)	+19 (+4%)	-16 (-40%)
Change at end of test (room temp.)	-8 (-5%)	-98 (-36%)	-72 (-14%)	+19 (+5%)	-14 (-34%)

While laser flash data were used to detect changes in TIM thermal performance, the measured TIM thermal resistance values in temperature cycling tests were generally lower in magnitude than those calculated using vendor thermal conductivity values throughout the environmental exposure, with the exception of the adhesive and some putty samples. This may have been caused by differences in contact pressure, which could have affected both contact and bulk resistances, or non-uniform surface heating of the test samples during the laser flash measurement. Heating of the sample holder clamping plates during the laser flash measurement may explain much of the lack of agreement in thermal resistance values from temperature cycling tests, which used the larger square coupons, and elevated temperature/humidity tests, which used round coupons that more closely matched the laser flash sample holder openings. The larger coupons allowed more heat to be conducted into the aluminum sample holder plates due to the higher area in direct contact with the plates. This effect would have increased the apparent 3-layer thermal diffusivity based on the measured temperature rise curve, causing experimental TIM thermal conductivity values to be higher than actual values for the temperature cycling tests. Measured changes in thermal conductivity over time would also have been higher than actual values. Using finite element models that simulated heating of the sample holder plates (to be described in Chapter 4), the actual change in thermal resistance for the putty B samples, which showed the highest levels of degradation, was estimated to be up to approximately 33% lower than the measured thermal resistance changes reported in Table 3.5 as a result of sample holder plate heating.

Simulations indicate that samples which showed little change in thermal resistance due to environmental exposure would still have showed little change even with this effect. In addition to these effects, variability in thermal resistance values for some temperature cycling and elevated temperature/humidity test specimens can be partly attributed to variability in the bondline thickness of the assembled TIM specimens.

Chapter 4: Validation of Laser Flash Results from Reliability Tests

Modeling Approach

To study potential issues arising from use of the laser flash method on clamped TIM specimens and to explain reliability test measurements presented Chapter 3, finite element (FE) models were constructed and simulations were performed. More specifically, thermal finite element model simulations of the laser flash test measurement assessed the impact of the sample holder on the calculated TIM thermal conductivity while structural simulations examined mechanical loading on TIM test specimens.

Thermal Simulations

In Chapter 3, laser flash measurements of 3-layer test specimens clamped between two sample holder plates yielded TIM thermal conductivity values much higher than those reported in vendor datasheets. It was surmised that nonuniform surface heating, leading to radial conduction in the test specimen and heating of the sample holder plates, was responsible for this discrepancy, but this effect was not investigated and is therefore explored in this study. When the test coupons are much larger than the opening in the top sample holder plate, only the open area of the sample is directly irradiated. Because the surface heating is now localized in the center of the test specimen surface, lateral heat spreading occurs, and the temperature

waves propagate both radially (in plane) and through the thickness of the three-layer specimen. This is a deviation from ideal laser flash measurements, where the entire area on one side of the test specimen is irradiated, effectively producing one-dimensional conduction through the 3-layer test specimen.

The approach used in the FEA simulation of the laser flash measurement involved first assuming a value for thermal conductivity of the TIM layer and applying a transient heat flux to the test specimen to approximate the pulse from the laser that irradiates the test specimen. The half-rise times obtained from the temperature rise curve of the simulated 3-layer test sample resulted in thermal diffusivity values, from which TIM thermal conductivity could be determined using the Lee method. Since this value may differ from the initial value of thermal conductivity assumed in the model, the value must be iterated. This procedure is summarized in Figure 4.1. The finite element model was generated assuming no heat conduction to the sample holder plate and screws, no radiative heat losses from the test specimen, and isotropic, homogeneous material properties.

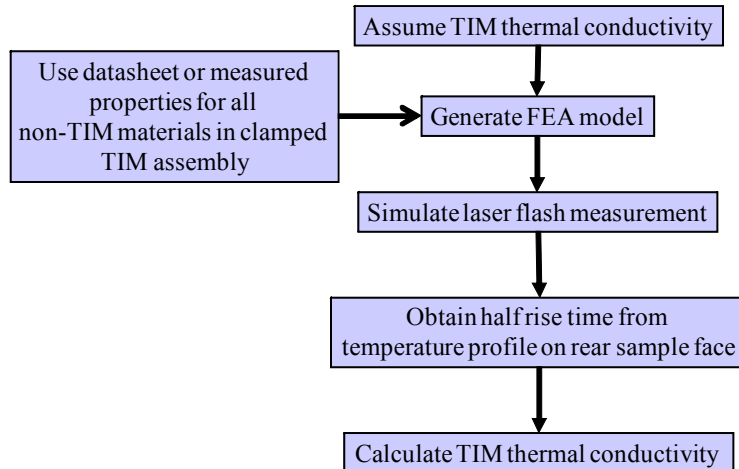


Figure 4.1: Overview of TIM thermal conductivity calculation procedure.

For this study, the heat flux was imposed on an area corresponding to the area of the sample holder opening (laser-side) and the heat flux was assumed to be uniform over the area of coverage, while the area visible to the detector corresponded to the area of the sample holder opening (detector-side).

Structural Simulations

TIMs experience compression in typical applications due to screws or clips that help ensure good thermal contact between the heat spreader and the heat sink. The laser flash method requires one surface to be exposed to the laser and the other surface to be in view of an IR detector. For the three-layer test specimens, openings on the top and bottom of the sample holder plates, required for laser flash measurements, prevented force from being applied uniformly over the top and bottom surfaces of the three-layer TIM sandwich. The purpose of the structural finite element analysis in this study was to assess the effect of any deformation experienced by the

TIM layer, as a result of the opening in the sample holder plates that clamp the TIM. The results would help determine how well the TIM laser flash test fixtures approximate typical TIM application loading conditions, which are assumed to result in a uniform bondline thickness.

TIMs in this study were assumed to exhibit linear viscoelastic behavior. The generalized Maxwell model approximates linear viscoelastic behavior as a series of springs and dashpots in parallel (Ferry, 1980). Mechanical material properties can be represented using the kernel function of generalized Maxwell elements expressed in terms of the Prony series as follows (Ferry, 1980; ANSYS, 2009):

$$G = G_{\infty} + \sum_{i=1}^{n_G} G_i \exp\left(-\frac{t}{\tau_{time}}\right) \quad (4.1)$$

where G is the elastic shear modulus and τ is the relaxation time for each Prony component. The viscoelastic material properties were determined using Prony series fits with 5 terms. Assuming the material was isotropic, shear modulus (G) was determined from elongation modulus (E) data (ANSYS, 2009), using $\nu = 0.49$, the isotropic material assumption, and the following relation:

$$G = \frac{E}{2(1 + \nu)} = \frac{E}{2.98} \quad (4.2)$$

To measure the material properties of the TIM layer used in the finite element models, stress relaxation tests were conducted using dynamic mechanical analysis (DMA). Input properties for the sample holder plates and coupons were based on reference handbook values. Simulations were performed with and without the openings in the sample holder plates used for laser flash measurements, keeping all other parameters constant to examine the impact of the opening on TIM deformation.

Some mechanisms for degradation, such as delamination, occur or originate at the interface between the TIM and the contacting structure, rather than the bulk of the TIM. Accurately simulating thermomechanical stresses and strains in the test structure, including the interactions between the surfaces and the TIM, is important in simulating conditions that give rise to degradation in TIM thermal performance. Manufacturing relating conditions and CTE mismatch induced by warpage can lead to surface non-planarity in the application environment. The initial TIM bondline could be considered to be relatively flat since flatness tolerances on contacting components are on the order of 0.002 inch per inch of travel for microprocessor applications (Dean, 1998).

Experimental Results

Laser flash measurements on multiple TIM samples were carried out using square and round test coupons, as summarized in Table 4.1. Vendor values of thermal resistance were based on TIM thermal conductivity datasheet values using assembled thickness values of the test specimens. Laser flash data generally yielded moderately lower thermal resistances than those based on vendor datasheet values, but for clamped square specimens, which used samples much larger than the opening, the differences were up to a factor of 3. Differences with vendor values and discrepancies among laser flash measurements performed on the same TIM suggested that test coupons in combination with the sample holders may be contributing to error.

Table 4.1: Comparison of laser flash measurements with vendor values:

a) square test coupons; b) round test coupons.

a)

	Thermal Resistance (mm²K/W)				
	Putty A (no foil)	Adhesive	Gap Filler	Gap Pad A	Gap Pad B
Vendor	101	22	271	633	213
Measured	80 ± 5	69 ± 7	125 ± 11	253 ± 42	69 ± 7

b)

	Thermal Resistance (mm²K/W)				
	Putty A (no foil)	Putty A (w/ foil)	Putty B	Gap Pad A	Gel
Vendor	125	127	467	656	11
Measured	163 ± 10	229 ± 48	479 ± 31	431 ± 76	41 ± 10

To evaluate the impact of radial heating and sample holder plate heating effects, five round samples of varying radii and five square samples of varying side length of Gap Pad A were measured at a compression level of between 5-10%. While these measurements showed that a square TIM specimen larger than the opening can increase the calculated TIM thermal conductivity, the round specimens did not show this trend, and in some cases, a higher radius led to a lower calculated TIM layer thermal conductivity. These results are summarized in Figure 4.2. It was also seen that with increasing sample area, the signal also decreased and for samples with larger radii or side lengths, the temperature profiles had lower signals to noise ratios, indicating that these data points may not be suitable for establishing a trend. As shown in Figure 4.3, which shows measured TIM thermal conductivity values for various sample sizes using aluminum or Lexan sample holder plates, Gap pad A

TIMs did not show a clear increase in measured TIM thermal conductivity with increasing sample area, as would be expected from radial heating assumptions and previous measurements. For measurements on the same TIM (Gap Filler), as shown in Figure 4.3, use of aluminum holder plates led to higher measured TIM thermal conductivity values than those obtained using Lexan plates. The increase in measured TIM thermal conductivity with increasing area (slope) was higher in tests conducted using aluminum holder plates than those conducted using Lexan plates. These trends indicate that the sample holder material plays a dominant role in increasing the measured TIM thermal conductivity and that radial conduction effects may be small in comparison.

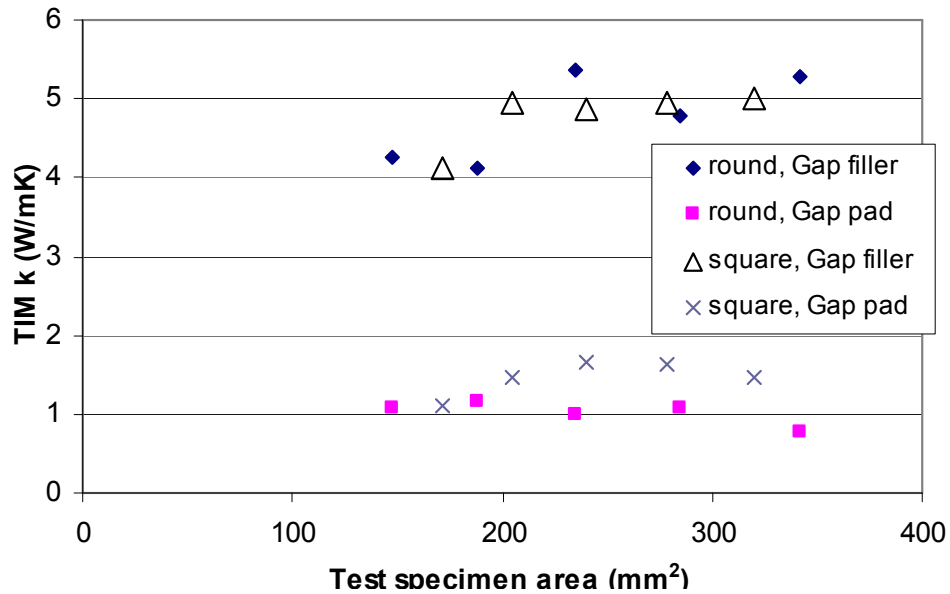


Figure 4.2: Effect of area on TIM thermal conductivity based on the laser flash measurements.

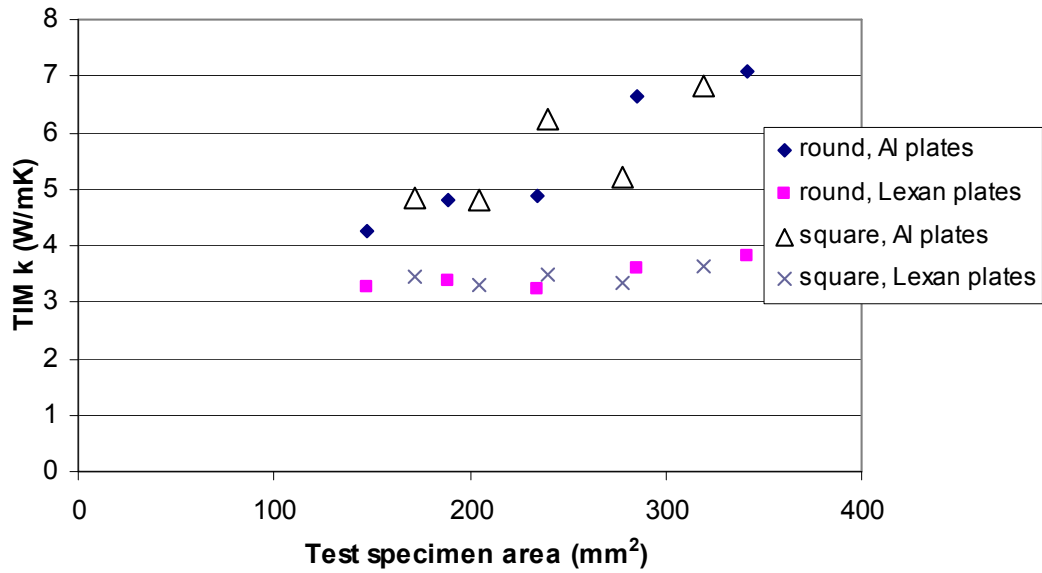


Figure 4.3: Effect of area on TIM thermal conductivity based on the laser flash measurements of Gap Filler.

Tests in which both Lexan and aluminum were used in combination for sample holder plates during the same measurements yielded data used to distinguish between the relative contributions of each plate in increasing the measured TIM thermal conductivity values, as summarized in Table 4.2. Heat flow into the top and bottom sample holder plates appears to have contributed equally to the increase in apparent measured TIM thermal conductivity, suggesting that heating of both sample holder plates led to increased measured TIM thermal conductivity values.

Table 4.2: TIM thermal conductivity based on laser flash measurements with aluminum and Lexan sample holder plates.

Test specimen area (mm²)	Bottom plate (toward laser)	Top plate (toward detector)	Measured TIM thermal conductivity (W/m-K)
342 (round)	Al	Al	7.1
342 (round)	Lexan	Al	4.9
342 (round)	Al	Lexan	4.7
342 (round)	Lexan	Lexan	3.8
320 (square)	Al	Al	6.8
320 (square)	Lexan	Al	5.2
320 (square)	Al	Lexan	5.1
320 (square)	Lexan	Lexan	3.6

Modeling Results

The thermal finite element models generated in this section were used to simulate the three layer test specimen and the sample holder plates used to clamp the 3-layer test specimen. The screws holding the sample holder plates together were neglected.

Thermal Simulations

To examine why experimental laser flash results depended on the sample holder plate material and explain how sample holder plate heating affected laser flash data used to determine TIM thermal conductivity values, transient thermal finite element models were generated of the assembled TIM structures using aluminum or Lexan as the sample holder plate materials. Simulations were also performed for a configuration with no sample holder plates. The pulse from the laser was

approximated as a 15 J transient heat flux with a triangular profile lasting 0.3 ms. Other than the laser irradiation, the entire structure was assumed to be insulated, allowing for no convective or radiative cooling to the surrounding ambient. A typical finite element mesh (which contained around 60,000 nodes) is shown in Figure 4.4.

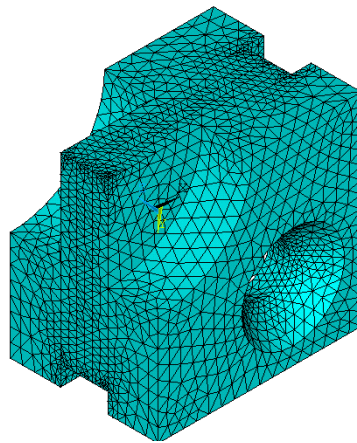


Figure 4.4: Thermal finite element mesh.

Assuming no thermal contact resistance between the 3-layer TIM specimen (using properties of the Gap Filler) and the sample holder plates, the temperature profiles of the rear coupon face, inside the opening on the sample holder plate, were averaged. The circular openings of both sample holder plates were 5.9 mm in radius. The temperature profiles are shown in Figure 4.5 with distinct curves for aluminum, Lexan and no holder plates.

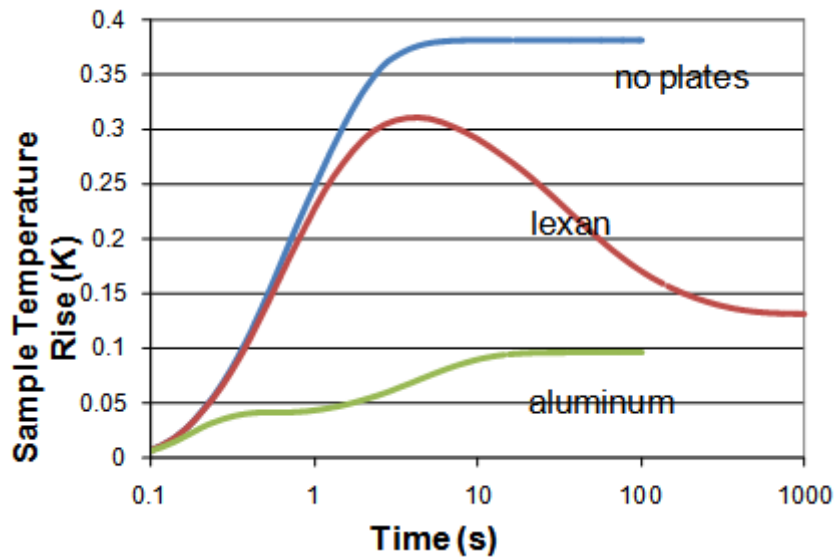


Figure 4.5: Temperature rise profiles from laser flash simulations.

Examining these curves, it is possible to conclude that absorption of heat by the aluminum and Lexan sample holder plates led to a slower initial temperature rise than would have been experienced by the sample in the absence of these plates. While initially the rate of temperature increase was highest in the no-plate case, as shown in Figure 4.5, the temperature reached the maximum value (within 90%) after 4-5 seconds due to the time for heat to flow through the 3-layer sample. The half-rise time for the “no plates” case was within 0.01 to 1.3 seconds, the range predicted by Parker’s equation based on treating the 3-layer composite structure as being composed of all TIM or all coupon material. The heat flux at a location along the opening edge of the top plate is shown in Figure 4.6.

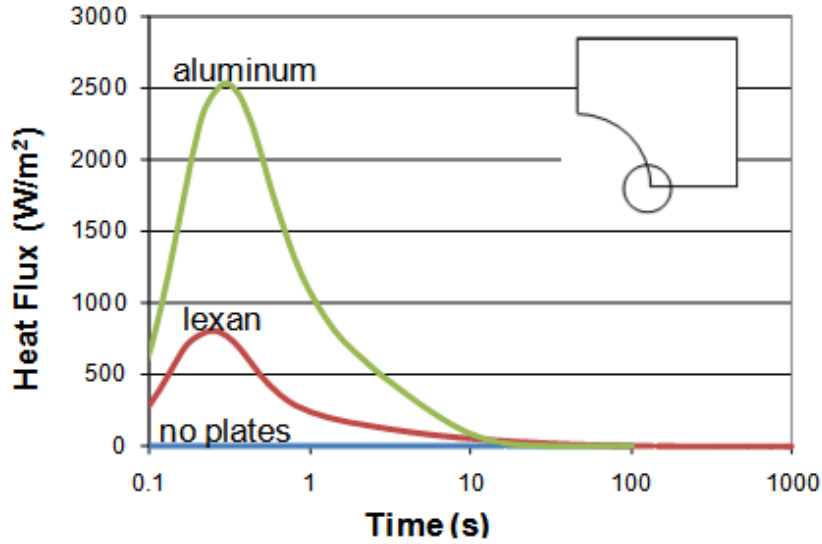


Figure 4.6: Local heat flux profiles on top clamping plate (coupon side) from laser flash simulations.

Heat flowed initially into the aluminum holder plates from the test sample, due to the high plate thermal diffusivity, and after the aluminum plates became heated, thermal equilibrium was achieved by having the heat flux from the 3-layer sample into the plates reach a maximum and then decrease over time, causing the sample temperature to continue to rise gradually. For Lexan, heat flowed into the plates initially but at a slower rate than for aluminum, and after the sample temperature reached a maximum point, the plates continued to draw heat away slowly because of the low Lexan thermal diffusivity until the 3-layer sample and plates reached a thermal equilibrium condition.

Figure 4.7 shows nodal temperature profiles at multiple locations through the thickness of the assembly test structure (3-layer Gap Filler sample with Lexan plates). The nodal temperatures shown are located at the side of the assembly as illustrated in the schematic in Figure 4.7 (top view), where in the side view “T1” is closest to the

side with the applied heat flux and “T7” is on the opposite side of the test structure on the rear plate. The irradiated side of the coupon experienced the highest temperature rise, which peaked around the time of the applied heat flux. The bottom Lexan plate in contact with the irradiated coupon heated up initially then decreased before being heated up by the test sample while the top Lexan plate heated up more slowly after the temperature wave propagated through the 3-layer test sample.

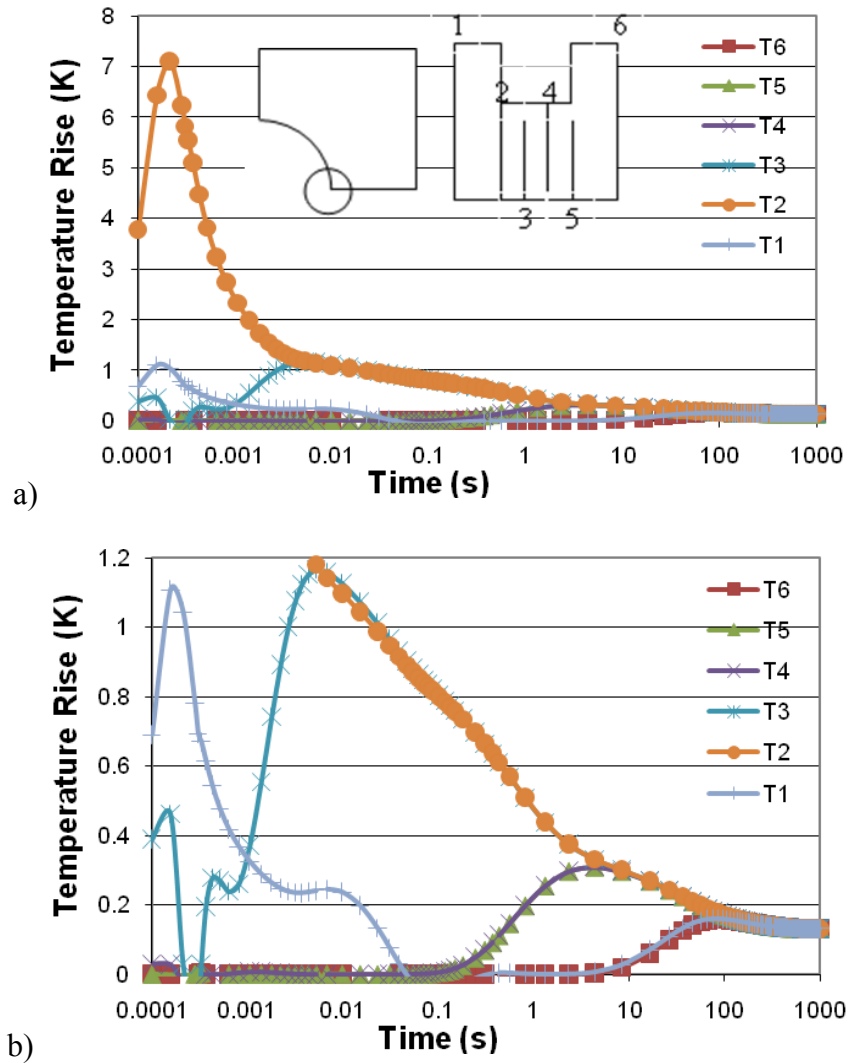


Figure 4.7: Local temperature rise profiles throughout assembled test structure from laser flash simulations: a) y-axis scale from 0 to 8 K; b) y-axis scale from 0 to 1.2 K.

Since the entire simulated structure was insulated (except for the initial laser pulse), the final temperature was above the initial temperature. The temperature rise of the entire assembly at the steady-state condition (when the temperature no longer changed with time) depended on the specific heat capacity values, with the lower specific heat values corresponding to the higher steady-state temperatures. Using an energy balance and treating the 3-layer sample and plates as a single system with no heat loss, the steady-state temperature rises from the simulation were calculated to be 0.32, 0.12, and 0.09 K, for no plates, Lexan, and aluminum, respectively by summing the heat capacity contributions from all materials and assuming lumped capacitance. These values were within 15% of the steady-state values from the FE simulation, which were 0.38, 0.13, and 0.09 K, respectively.

Using the thermal properties of the gap filler, which had a datasheet thermal conductivity value of 2.8 W/m-K, simulations were performed with round and square test specimens. No thermal contact resistance was assumed between the TIM test sample and sample holder plates. Half-rise time values were based on the early part of the temperature rise profile, which resulted primarily from heating of the test specimen, rather than the sample holder plates. Due to the suppression of the sample temperature rise by the holding plates, the increase in TIM thermal conductivity was higher in the simulations with larger test specimens, which lead to a larger area being in contact with the sample holder plates, and higher in the simulations with aluminum plates compared to those with Lexan plates. The discrepancy between measured and simulated results in tests using the aluminum

plate may have been largely due to the no contact resistance assumption. Measurements with Lexan plates, however, showed a different trend, higher measured values than simulated values, and this may have resulted from the actual TIM thermal conductivity being higher than the datasheet value used for the input value in the model. In addition, the Lexan plate samples may not have had the same plate-to-sample contact resistance as the aluminum plate samples during laser flash measurements. These results are summarized in Table 4.3.

Table 4.3: Calculated TIM thermal conductivity based on simulation of Gap Filler assuming no contact resistance between the TIM test sample and sample holder plates.

Test specimen area (mm²)	Plate material	Measured TIM thermal conductivity (W/m-K)	FEA TIM thermal conductivity (W/m-K)
147 (round)	Al	4.2	9.8
147 (round)	Lexan	3.2	2.9
147 (round)	None	N/A	2.7
320 (square)	Al	6.8	11.0
320 (square)	Lexan	3.6	3.2
320 (square)	None	N/A	2.8

Adding the same level of simulated plate-to-sample contact resistance (0.2 or 0.5 W/m-K layer with a 0.5 mm thickness) had a greater impact on TIM thermal conductivity values for the aluminum plate samples than for the Lexan plate samples, as shown in Table 4.4. Since the aluminum plates were conductive, additional contact resistance significantly reduced the calculated TIM thermal conductivities due to

sample holder plate heating (10.7 to 3.7 W/m-K by adding 0.5 W/m-K effective contact layers with 0.5 mm thickness) whereas this did not greatly impact the Lexan plates, which were already relatively insulating.

Table 4.4: Calculated TIM thermal conductivity based on simulation of Gap Filler using 320 mm² square samples varying contact resistance between the TIM test sample and sample holder plates.

Contact layer thermal conductivity (W/m-K)	Plate material	FEA TIM thermal conductivity (W/m-K)
0.2	Al	3.2
0.5	Al	3.7
167	Al	10.7
0.2	Lexan	3.1
0.5	Lexan	3.2
2	Lexan	3.0

The mesh density of the thermal finite element models was determined to be sufficient based on a mesh sensitivity study carried out of gap filler (square sample) with a 1 mm bondline thickness and Lexan holder plates using two other meshes, where the finest mesh (which contained 456,000 nodes) yielded a TIM thermal conductivity value of 3.3 W/m-K, which was within 3% of the value resulting from the model with a mesh density close to those used to obtain the other results. Calculations of TIM thermal conductivity based on simulated temperature profiles thus indicated that sample holder plate heating increased TIM thermal conductivity values, matching the apparent trend found in laser flash measurements performed

with aluminum sample holder plates. This result was because the laser flash method assumes that for thin test samples uniformly heated on one side, the half-rise time (time to reach one-half the maximum value) associated with the temperature rise on the opposite side, is inversely related to the thermal diffusivity, as described by equation 2. Clamping the TIM specimens altered their temperature history considerably from the ideal laser flash test specimen conditions, which allow for heat flow through the 3-layer specimen only. This resulted in lower slopes and more complex temperature rise profiles, and the equivalent half rise times for clamped samples were highly dependent on the magnitude of the first local maximum temperature (first inflection point in the temperature profile). The half rise time was calculated using the first inflection point since the laser flash instrument likely used the early part of the temperature rise profile to calculate thermal diffusivity. This reference point was lower for configurations with a greater sample holder plate heating effects. For samples with aluminum plates, using the second inflection point in the temperature rise profile would have resulted in TIM thermal conductivity values that were lower than those based on the first inflection point: 1.2 W/m-K rather than 11.0 W/m-K for the square samples and 5.4 W/m-K rather than 9.8 W/m-K for the round samples. Since lower half rise times resulted in higher thermal diffusivities, the TIM thermal conductivity values based on three-layer thermal diffusivity values were higher for samples experiencing a greater sample holder plate heating effect. This has important consequences for reliability evaluation since measured changes over time are experimentally determined as measured differences

in TIM thermal conductivity at different times, which would also be higher than actual changes in TIM thermal conductivity over time.

Even though sample holder plate heating should be avoided, using a plate design that reduces these effects may be difficult in some circumstances; for instance, when environmental conditions in a given reliability test and structural considerations also drive the plate material design and selection. Correcting for this effect requires performing a series of simulations to establish the relationship between input TIM thermal conductivity in the FE model, which corresponds to the actual value in a realistic case, and output TIM thermal conductivity from the FE model, which would be affected by sample holder plate heating. At least one accurate TIM thermal conductivity measurement, obtained from a datasheet, an accurate alternative test method, or laser flash data obtained using a low conductivity sample holder plate material could be used as the input TIM thermal conductivity in the FE model. The contact resistance between the test specimen and each plate can then be varied until agreement is achieved between the TIM thermal conductivity calculated from the finite element model and the value used in the model (assumed to be accurate). Using this contact resistance value for a given TIM and loading condition, the input TIM thermal conductivity values can then be varied to obtain the relationship between the actual and calculated TIM thermal conductivity values. This fitting approach assumes that the contact resistance between the test specimen and each plate does not change over time. For example, in measurements of Putty B using aluminum plates, the plots shown in Figure 4.8, which show results with a 0.5 mm-thick effective contact resistance layer between the 3-layer test sample and each sample holder plate,

indicated that the slope of the curve determines how to correct for measured TIM thermal conductivity changes.

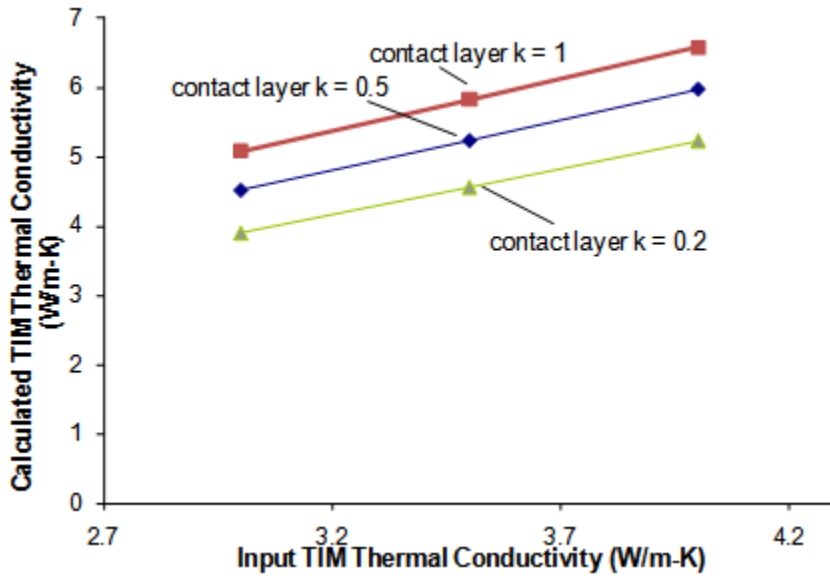


Figure 4.8: Output TIM thermal conductivity based on FEA simulation as a function of input TIM thermal conductivity.

Generally, the lower the contact resistance between the 3-layer laser flash test specimen and sample holder plates, the lower the magnitude of the increase due to sample holder plate heating and the lower the slope (change in measured TIM thermal conductivity as a function of actual TIM thermal conductivity). This trend can be seen in Figure 4.8. Therefore, on Putty B samples that showed a 1.8 W/m-K change after 2098 temperature cycles using aluminum sample holder plates, the actual change was up to approximately 1.2 W/m-K, a difference of 33 percent.

In the tests conducted and described in Chapter 3, the screws holding the plates together restricted some movement of the plates, which were still free to move closer together over the course of the environmental exposure. Because of this aspect

of the sample holder design, the contact resistance between the test sample and the clamping plates would have been likely to increase if the TIM layer experienced stress relaxation, which would have decreased the TIM bondline thickness over time. For any measured thermal performance degradation over time, the actual amount of degradation would have been lower than if the contact resistance remained constant since the measured value at the later time would have been closer to the actual value than the initial measurement. Similarly, for measured thermal performance improvement over time, the actual amount of improvement would have been higher than if the contact resistance remained constant due to a decreasing bondline thickness over time.

As a result of stress relaxation in the TIM layer, the correction procedure described here would then yield an upper limit in thermal performance change in cases of measured degradation with sample holder plate heating effects present due to the possibility that later measurements were conducted with increasing contact resistance between the sample and the plates. Overall, changes in the contact resistance between the test sample and the clamping plates over time limits the effectiveness of this correction procedure and underscores the importance of avoiding sample holder plate heating by designing the sample holder plates accordingly. Some amount of stress relaxation may have occurred in the Putty B samples given the change in room temperature performance, but whether the total change in thermal performance due to temperature cycling was caused by this effect is unclear.

The overall impact of sample holder plate heating can be reduced by using a low contact pressure and a thermally insulating material for the sample holder sample

holder plates with low thermal diffusivity and specific heat. TIM test coupons should only be slightly larger than the openings of the sample holder plates, minimizing the contact area between the holder plates and the test specimen such that the laser pulse area nearly covers the entire test specimen on one side during the laser flash measurement. If a high conductivity material like metal is needed for the sample holder sample holder plates, a thin insulating layer could be added at the interface between the test coupons and the sample holder plates. Other sample holder plate shapes, such as a ring, may be possible as long as there is little contact between the plates and the test specimen.

Structural Simulations

Structural finite element models simulated test samples as assembled for laser flash measurements, in which the three layer samples were clamped using either Lexan or aluminum sample holder plates. Putty B and Gap Pad A were selected as representative TIMs to be modeled, and copper and alloy 42 were used as the coupons in the 3-layer sandwich. To obtain the TIM shear modulus profiles, stress relaxation tests were performed using dynamic mechanical analysis (DMA) in strain-controlled transient mode at room temperature. DMA test specimens were 4 mm by 4 mm in area, and the initial thicknesses of the Putty B and Gap Pad A specimens were 1 mm and 0.55 mm, respectively, matching the initial thicknesses in the simulated laser flash test structures.

The Prony series coefficients were generated in ANSYS based on the measured shear modulus profiles, and the resulting values were used to determine TIM material property inputs in the FEA model. In the finite element models, screws

were neglected, surface roughness was not considered between the TIM and the coupons, and clamping of the 3-layer test specimens was simulated as a fixed constant displacement in the z-direction (through-plane) applied to the conical region at the top of one of the sample holder plates where the screw head would contact the sample holder plate. The bottom surface of the bottom sample holder plate (side opposite the applied force) was fixed. A free mesh was used with approximately 110,000 nodes and 80,000 elements. Solid187 (10-noded tetrahedral structural solid) elements were used in the model and 2-axis sample symmetry (horizontal, vertical) was assumed. Sample meshes used for some Putty B simulations are shown in Figure 4.9, where “solid” refers to geometries considered in simulation that included plates with no openings.

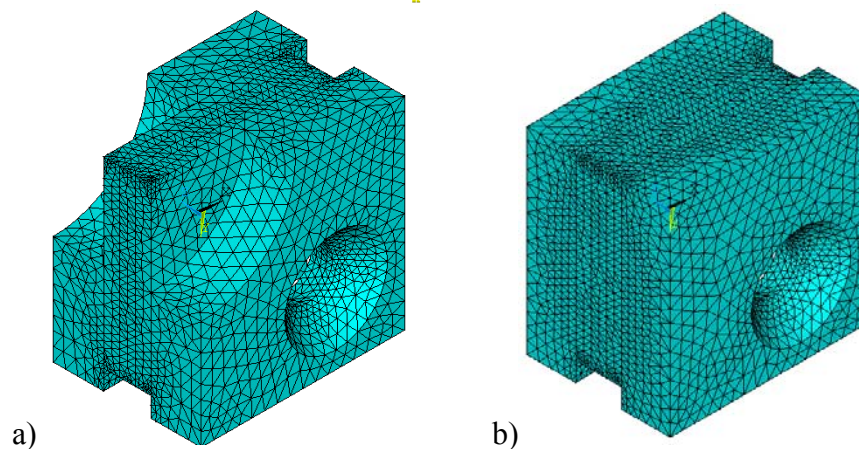


Figure 4.9: Structural finite element mesh (5.9 mm opening, 16.4 mm/side square test specimen): a) open; b) solid.

Through-plane (z-direction) displacement in the top surface (the side with the applied force) of the TIM layer, which approximates the total deformation of the TIM due to compression, was used to quantify changes in the bondline thickness. Force

was applied to the top surface of the top sample holder plate, and the bottom of the bottom plate was held fixed, causing the TIM layer to be compressed primarily from the top. The variation in the z-displacement was calculated as the difference between the maximum and minimum displacement at a steady-state condition (final time). For Putty B, clamped at a 25% compression level using Lexan plates with an opening radius of 5.9 mm, the z-displacement variation in the TIM was approximately 1.5×10^{-7} m, which was larger than the variation achieved with solid plates, 8×10^{-8} m, and was within 0.1% of the uncompressed bondline thickness. The z-displacement nodal contour plots of the TIM layer at the final time, shown in Figure 4.10, indicate that the highest deflection was located near the outer edges of the test specimen, where the plates were in contact with the coupons.

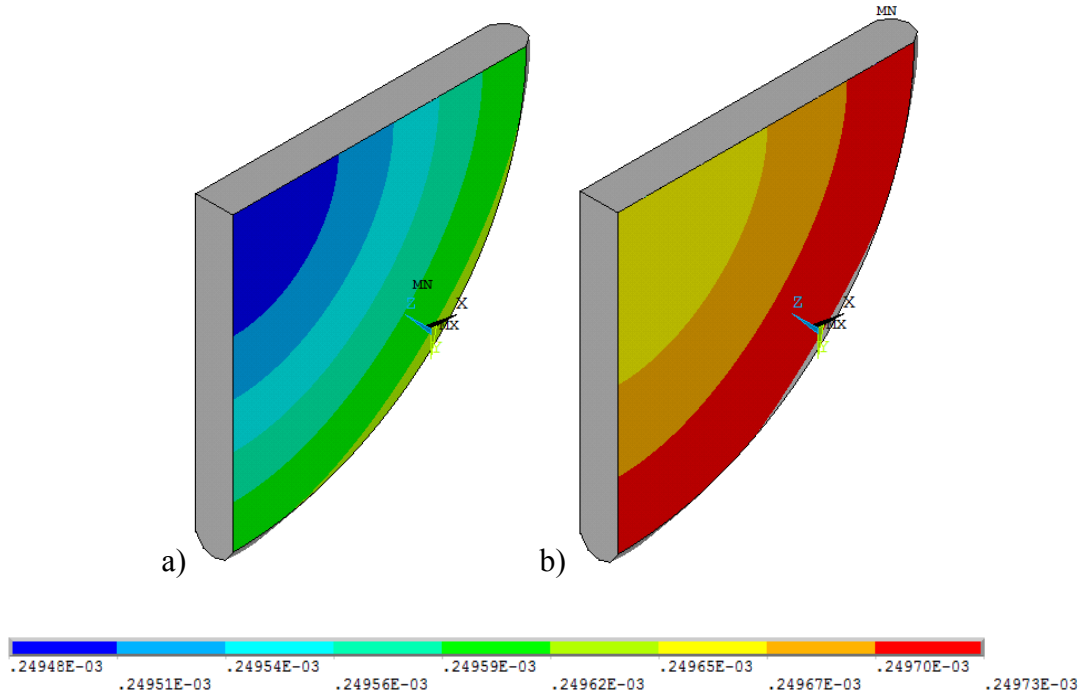


Figure 4.10: Z-displacement (m) of Putty B at a 25% TIM compression level: a) open; b) solid.

Gap Pad A simulations also showed the highest deflection near the outer edges of the test specimen. At the same compression level, the variation in the z-displacement of Gap Pad A (2.4×10^{-6} m for the solid case and 4.2×10^{-6} m for the open case, which was nearly 0.8% of the initial bondline thickness) was higher than for Putty B but still small relative to the initial thickness, and the differences between the results with and without the openings were slightly larger, but still smaller than the experimental accuracy of a typical bondline thickness measurement (1×10^{-6} m). Simulations for both Putty B and Gap Pad A were carried out until 500 seconds since the stress relaxation data showed that the elongation modulus of Putty B leveled off after that time. Simulations carried out until 1000 seconds indicated that 500 seconds was well

within the steady-state range. The mesh density was determined to be sufficient based on a mesh sensitivity study carried out using two other meshes. The finest mesh (with 444,000 nodes and 310,000 elements) for the Gap Pad A simulation for the solid case at 25% compression level yielded a z-displacement variation of 3.7×10^{-6} m, which was within 11% of the result obtained using the other mesh.

Nodal contour plots of the z-displacement showed similar distributions in the TIM z-displacement at higher compression levels for both materials, and the displacement variation increased with increasing compression level. Assembly configurations for the open and solid cases matched each other well (within 1×10^{-6} m for Putty B, and 1×10^{-5} m for Gap Pad A) at multiple TIM compression levels from 10% to 75% when comparing variation in TIM z-displacement, as summarized in Table 4.5.

Table 4.5: Steady-state TIM z-displacement.

TIM	% Compression (TIM layer)	Through-plane displacement variation of TIM layer (m)	
		Open	Solid
Putty B	10	5.20E-08	3.00E-08
Putty B	25	1.50E-07	8.00E-08
Putty B	50	2.60E-07	1.50E-07
Putty B	75	4.70E-07	2.90E-07
Gap Pad A	10	1.85E-06	1.20E-06
Gap Pad A	25	4.20E-06	2.44E-06
Gap Pad A	50	9.34E-06	6.10E-06

Varying the size of the openings in the sample holder plates caused the TIM layer to deform more uniformly in thickness with decreasing opening size for simulations of Gap Pad A at a 25% compression level. The z-displacement variation at a radius of 8.1 mm was around a factor of 10 higher compared to results using an opening radius of 5.9 mm. With aluminum holder plates at a 25% compression level, the variation in z-displacement with a 5.9 mm opening was around 60% lower than with Lexan plates. Simulations with thinner Lexan plates, however, resulted in plate deflection, causing the overall compression level of the TIM layer to be much lower than the applied displacement. In experiments, this could lead to a test structure that deviates significantly from a typical loading condition and pose problems during assembly of the test specimen. Results varying the plate opening size, material, and thickness are summarized in Table 4.6.

Table 4.6: Steady-state TIM s-displacement of Gap Pad A.

Plate Material	Radius of Plate Opening (mm)	Plate Thickness (mm)	Through-plane displacement variation of TIM layer (m)	
			Open Plates	Solid Plates
Lexan	5.9	3.18	4.20E-06	2.44E-06
Lexan	2	3.18	2.98E-06	2.44E-06
Lexan	4	3.18	3.67E-06	2.44E-06
Lexan	8	3.18	3.30E-05	3.20E-05
Aluminum	5.9	3.18	2.41E-06	2.40E-07
Lexan	5.9	0.80	1.85E-06	1.20E-06

Given these trends, a configuration with a large opening and coupon area, low stiffness plates, and a high stiffness TIM layer would be expected to result in the most nonuniform deformation in the TIM. For a Gap Pad A sample compressed at 50% of the initial thickness and clamped using Lexan plates with an 8 mm radius opening, the variation in displacement of the TIM layer was found to be 3.3×10^{-5} m, still within 6 % of the uncompressed bondline thickness. Even in this extreme case, the TIM remained relatively uniform in thickness, indicating that TIM specimens of similar dimensions, geometries, and moduli would also be suitable for laser flash measurements, assembled in clamped 3-layer structures. These results indicate that laser flash test structures can approximate typical TIM loading conditions that produce uniform bondline thicknesses.

Comparison of Laser Flash Data with Steady-State Data

Steady-state thermal conductivity measurements were performed to validate the capability of laser flash measurements to accurately measure TIM thermal resistance (magnitude) and to accurately capture TIM thermal conductivity changes over time. Generally, steady-state measurements are a more commonly accepted method of evaluating TIM thermal performance than the laser flash method.

Steady-State Tester Design

The steady-state tester design was intended to use test specimens that approximates TIM specimens as assembled in laser flash test structures. Heat was applied using a Kapton film heater attached to a copper block and the temperature

difference across the TIM specimen was measured using thermocouples embedded in aluminum blocks, which were in contact with the test specimen on both sides. Each thermocouple was fed in through the side, midway through the thickness, with the bead located at the center of each aluminum block. An active heat sink was used to cool the top of the tester. Thermal insulation in contact with the heater on the bottom was a woven ceramic layer. Thermal grease was used to improve the thermal contact between solid surfaces. Figure 4.11 shows the steady-state tester.

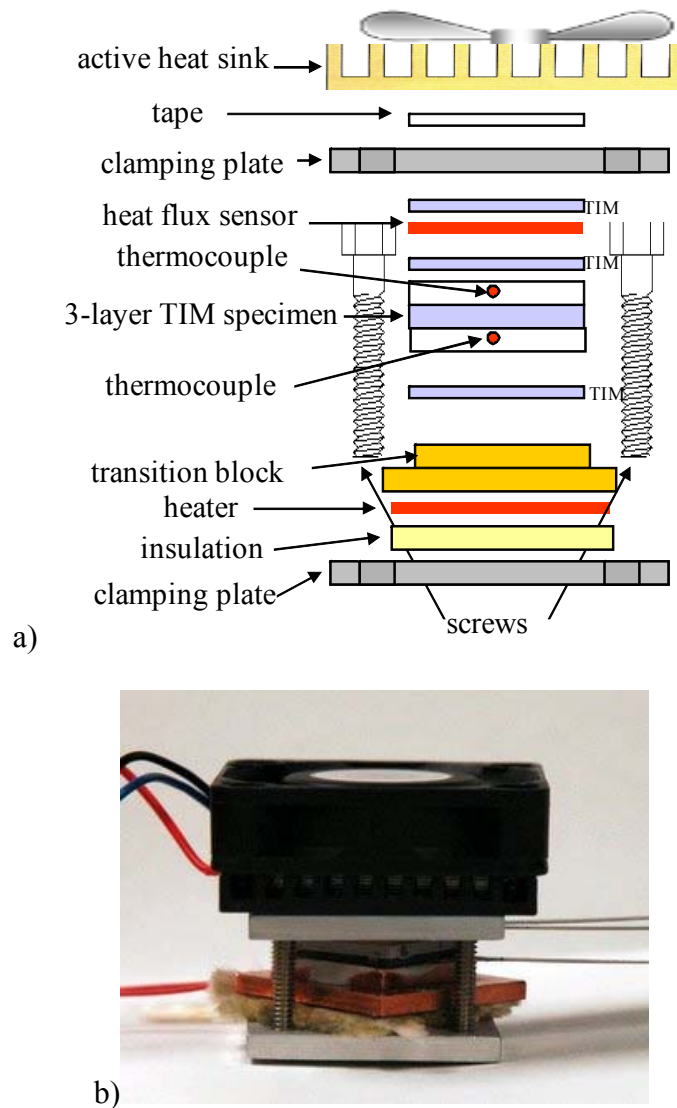


Figure 4.11: Steady-state thermal resistance test vehicle: a) TIM tester schematic; b) assembled TIM tester.

The temperature was measured after approximately 15 minutes, after the heater reached a steady-state condition. The bondline thickness was measured after temperature measurements were performed and the tester was disassembled due to the difficulty of performing an in-situ thickness measurement. The applied power was approximately 6.5 W and the square test specimens were 16.4 mm in side length.

Time-Dependent Steady-State Measurements of Gel Samples

Gel samples were cured at 80 °C for 1 hour. Samples were then held at room temperature and the effective thermal conductivity of two samples were measured over time using the laser flash method and two additional samples measured using a steady-state technique. Over the course of 13 days, the thermal conductivity of the samples increased due to crosslinking in the polymer, but the overall change in thermal conductivity of the steady-state samples was about 50% lower on average than that of the laser flash samples, as shown in Figure 4.12. Variability in sample assembly and preparation and sample holder plate heating may have contributed to discrepancies between laser flash and steady-state data in the initial measurement since agreement in the thermal conductivity values after 13 days was within 0.1 W/m-K on average.

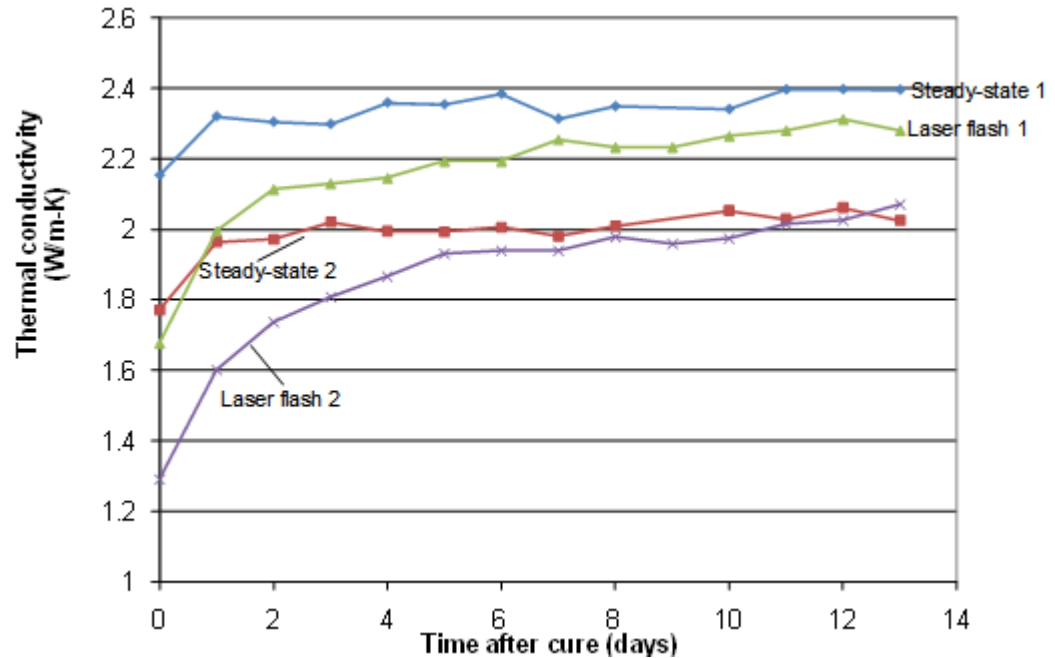


Figure 4.12: Measured gel thermal conductivity after high temperature cure.

Absolute Steady-State Thermal Conductivity Comparison

Comparisons of multiple TIMs generally showed good agreement in absolute thermal conductivity values (within x %) with laser flash measurements and vendor data. Laser flash tests used 8 mm diameter round copper coupons on both sides of each test specimen with Lexan samples holder plates. All measurements were performed at a room ambient temperature and are summarized in Table 4.7. In instances where the laser flash values differed considerably from vendor values, such as the gel and Putty A, the steady-state values showed better agreement with laser flash values. This may have been largely due to differences in contact pressure and time in the high temperature cure.

Table 4.7: Comparison between experimental TIM thermal conductivity values with datasheet values.

	Effective TIM thermal conductivity (W/m-K)				
	Putty A (no foil)	Putty A (w/ foil)	Putty B	Gap pad A	Gel
Vendor	11	11	3	0.9	10
Measured laser flash	7.6	3.2	2.6	1.0	1.8
Measured steady-state	8.3 – 10.5	4.6 – 5.2	3.2 – 3.3	0.8 – 1.0	1.3 – 1.7

Steady-State Measurement Uncertainty Analysis

The thermocouples used in the steady-state tester were Type T with 0.5 °C error and the heat flux sensors had a 10% error. The root-mean-squared (rms) error associated with the steady-state measurements considered error in the heat flux, temperature measurement, and thickness values. Inability to perfectly center the heat flux sensors and thermocouples on the test specimen and to evenly tighten the screws may have contributed to heat flow non-uniformity. Using the method described by Kline and McClintock (1953), the overall TIM thermal conductivity uncertainty was determined to be on the order of 20%.

Laser Flash Uncertainty Analysis and Convergence Study

The overall experimental accuracy of the laser flash TIM thermal conductivity values, which depends on the error of each input in the Lee algorithm, can be affected

by the design of the samples and the coupons, which comprise the 3-layer test specimen. Since the thermal resistance values are derived, errors can propagate through both the laser flash measurement and the thermal resistance calculation. Lee (1977) cautioned against using the laser flash method to measure the thermal diffusivity of a thin highly conductive material deposited on a low conductivity substrate. For thermal interface materials, this could be a concern when applying the laser flash method to a thin high conductivity TIM, such as grease, gel or solder, assembled in between thicker lower conductivity substrates or coupon layers. In the Lee method (1977) used in the TIM thermal conductivity calculation, the k^{th} root of the characteristic equation, γ , must be determined in order to solve for the normalized temperature, V , as shown in equations 3.2 and 3.3. The solution for γ , however, is highly sensitive to the thermal diffusion time ratios between the top or bottom layer and the middle layer of a three-layer test specimen. Lee used thermal diffusion time ratios as criteria to determine when a given layer in a multilayer sample is capacitive—that is, when the temperature is uniform throughout the layer. Some 3-layer configurations can yield high root mean squared (RMS) error in the calculated TIM thermal conductivity values obtained from the Lee algorithm or not result in a converged solution at all. As a result, the selection of the material, bondline thickness, coupon material, and coupon thickness can affect the accuracy of calculated TIM thermal conductivity values, and the ability of the Lee method to arrive at a converged solution. As an illustration, varying the 3-layer thermal diffusivity and keeping all other inputs to the Lee algorithm constant effectively allows the TIM thermal conductivity to be varied. For a copper-Gap Pad A-Alloy 42

composite test specimen, small changes in the η ratios lead to increasingly larger changes in the calculated TIM thermal conductivity values as the η ratios increase, and above around 190 W/m-K, the Lee algorithm does not result in a converged solution for a step size of 1×10^{-6} , as shown in Figure 4.13.

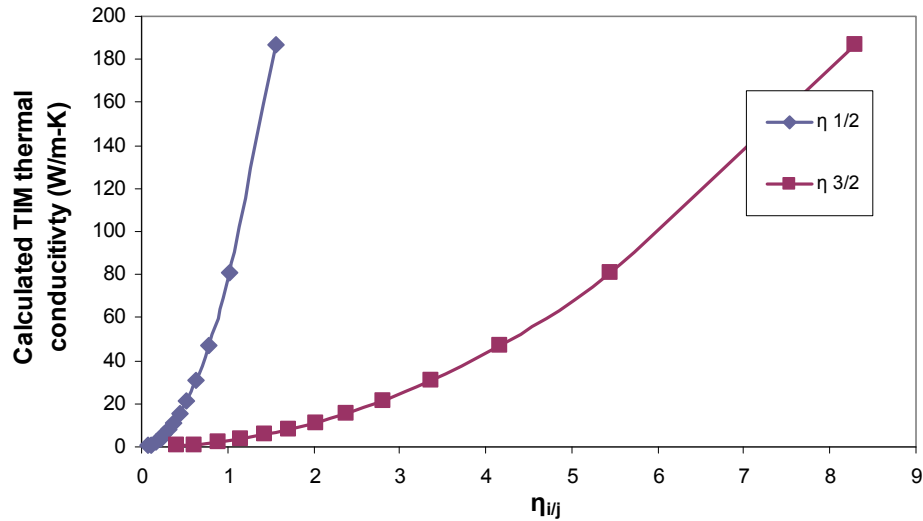


Figure 4.13: Calculated TIM thermal conductivity as a function of thermal diffusion time ratios of 3-layer copper-Gap Pad A-alloy 42 test specimen.

For measured samples in this study, this effect led to varying levels of RMS error, calculated using the method described by Kline and McClintock (1953) and Moffat (1988).

RMS error in calculated TIM thermal conductivity values reached 37% for the gel, which was the thinnest material with the highest in conductivity in the group when assembled with 1 mm copper and alloy 42 coupons, as shown in Table 4.8. By varying assumed hypothetical values of the 3-layer thermal diffusivity and using all the same inputs used in measurements, the calculated maximum $\eta_{\text{coupon}/\text{TIM}}$ values (the

maximum values beyond which the Lee method produced nonconverged solutions for TIM thermal conductivity) was determined for each of the two coupon-TIM combinations per samples as summarized in Table 4.8. The maximum value for each η ratio pair varied from less than 4 to over 26, and values that led to converged solutions for one material did not result in converged solutions for others. While configurations with low η ratios may be more suitable for applying Lee algorithm, the results suggest that acceptable η ratios may be material dependent and that η ratios alone may not be sufficient for use as definitive criteria to determine suitability of applying the Lee algorithm for all TIM types.

Table 4.8: Comparison of laser flash measurements with vendor values.

	Gap Filler	Putty B	Gel	Adhesive	Gap Pad A
Experimental TIM thermal conductivity \pm rms error (W/m-K)	6.5 \pm 0.9	3.9 \pm 0.4	6.7 \pm 2.5	2.1 \pm 0.7	2.1 \pm 0.3
Experimental rms error (%)	14	10	37	34	16
Experimental $\eta_{1/2}$	0.2	0.1	1.5	0.3	0.2
Experimental $\eta_{3/2}$	1.0	0.5	8.2	1.7	0.9
Calculated maximum $\eta_{1/2}$	0.9	0.7	4.9	1.6	2.7
Calculated maximum $\eta_{3/2}$	4.7	3.5	26.4	8.3	14.6

The thermal diffusivity of the three-layer sandwich was assumed to be the same for the determination of each sensitivity term, leading to a conservative error estimate, since changes in the inputs would lead to a change in the three-layer thermal diffusivity. As an example, for the Gap Filler samples, the uncertainty expressed in terms of thermal resistance was determined to be on the order of 25% based on an uncertainty of 31 mm²K/W using representative values for Gap Filler with a 123 mm²K/W thermal resistance. Table 4.9 summarizes the contributions from each input value. The largest contributors to the uncertainty of the TIM layer resistance value appear to be the single layer density values and the three-layer thermal diffusivity. The uncertainty value is high compared to that of Gowda et al. (2006), who reported an uncertainty of less than 5% in their laser flash thermal resistance values, as well as those of ASTM D5470-based testers, which can have thermal resistance uncertainty of less than 5% (Gwinn et al., 2002).

Table 4.9: Uncertainty analysis overview of Gap Filler laser flash measurements.

	Thickness			Density			Specific Heat			Thermal Diffusivity			Overall
	1	2	3	1	2	3	1	2	3	1	3	1+2+3	
Layer	1	2	3	1	2	3	1	2	3	1	3	1+2+3	1+2+3
Error (%)	2.5	3.1	2.5	3.7	3.7	3.7	7	7	7	5	5	5	25
ΔR (mm²K/W)	6.8	7.7	1.8	17.7	13.2	12.3	3.4	3.05	2.8	<0.1	3.5	13.0	31.0

Chapter 5: Conclusions and Recommendations

Conclusions

TIM degradation can affect the ability of electronic devices to perform reliably. Since interfacial thermal resistance from the chip to the heat sink is becoming a significant fraction of the total junction-to-ambient thermal resistance in many applications, understanding the causes of degradation can help prevent thermally-induced malfunctions or failure. Although advances have been made experimentally and in understanding the conditions leading to degradation for some TIMs, there is a need for improved experimental techniques to obtain accurate degradation data. The primary goal of the proposed research was to examine degradation for select polymer TIMs and in validating laser flash data obtained from reliability tests, address a few of the outstanding issues associated with applying the laser flash method to TIM reliability characterization.

TIM Reliability Study

With the exception of Gap Pad A and Putty B, the selected environmental conditions examined in this study were not found to degrade the thermal performance of the TIMs under test. Silicones, which represent many of the TIMs examined in this study, are known for their inherent stability due to their high dissociation bond energies which allowed them to remain stable over the course of the environmental

exposure tests. Little change or a reduction in thermal resistance was observed throughout temperature cycling tests conducted on filled polymer TIMs using two temperature profiles (-40 to 125 °C for 760 cycles and -55 to 125 °C for 2098 cycles) that conformed to the manufacturer's recommended operating temperatures with one exception. Gap Pad A experienced a 6 percent overall thermal resistance increase and appeared to show delamination occurring at the TIM-copper coupon interfaces. Temperature cycling also led to thermal expansion of some putty samples and the formation of cracks that were visible in SAM images. Silicone extraction, which can reduce thermal contact resistance by filling in gaps and asperities, may have caused thermal performance to improve slightly over time for some gap filler and putty samples.

Crosslinking most likely contributed to improvement in thermal performance of the epoxy adhesive and gel over time. Bulk changes in Putty B led to over a 50% decrease in thermal performance at the more extreme temperature cycling profile (-55 to 125 °C) after 765 cycles, indicating that silicone elastomer TIMs are susceptible to thermal performance degradation if subjected to temperature cycling conditions with temperatures near the glass transition temperature. The repeated changes in the material (from a glassy to rubbery state) over time caused the material to lose integrity. Elevated temperature/humidity tests (85°C/85% RH) performed up to 2173 hours did not lead to a substantial increase (greater than 10%) in thermal resistance for the samples in this study.

Laser Flash Method Study

The laser flash method has been well studied and has been applied to TIM thermal characterization. Measurements for some thermal interface materials, however, presents additional challenges beyond the thermal diffusivity measurement if the goal is to capture changes in thermal performance over time while simultaneously maintaining clamping to simulate a typical application loading condition.

Potential errors in conducting laser flash measurements of TIM specimens assembled in 3-layer sandwich structures and clamped using sample holder plates were examined. It was found that sample holder plates can distribute loading over clamped 3-layer sandwich structures, resulting in relatively uniform bondline thicknesses (usually within 1% variation in the initial thickness for typical TIM compression levels) that approximate as-assembled TIMs in many typical applications. However, heat from the laser pulse can flow into the plates during the laser flash measurement, which can increase the calculated TIM thermal conductivity values obtained from thermal diffusivity data. To avoid this problem, low conductivity materials should be used for the sample holder plates and test specimens should be sized to match the opening of the sample holder plates. In addition, since higher thermal diffusion time ratios between the TIM layer and the coupon layer appeared to lead to high overall error and problems with nonconvergence in TIM thermal conductivity calculations, thin, conductive coupon layers (<1 mm) should be used when laser flash measurements are performed on thin, high conductivity TIMs, such as gels or solder.

Contributions

The primary contributions from this study were as follows:

- 1) Explained for the first time physical processes leading to thermal performance degradation in putty and gap pad TIMs.

While this study confirmed that TIMs in pad form, which remain relatively unexplored in the literature, perform reliably under the temperature cycling and elevated temperature/humidity conditions (which match commonly used accelerated stress test conditions used for SMT components) and durations tested, this study led to the first instance of degradation reported in the literature for TIMs in pad form, which are generally considered to be among the most reliable TIMs on the market. For these TIMs that exhibited degraded performance, the change in thermal resistance was attributed to physical changes in the bulk of the TIM or the contact interface. The temperature cycling test results suggest that silicone-free pads may be more susceptible to delamination than silicone ones under the conditions tested. Furthermore, exceeding the recommended operating temperature at the low extreme may result in problems due to repeated changes near the T_g , which can have consequences for uprating of TIMs. Demonstrating good stability of gels under the environmental conditions considered is also of practical significance because many of the best thermally performing conventional TIMs on the market, greases and solders, often exhibit poor reliability under high temperature or temperature cycling conditions.

2) Concluded that sample holder plate heating, an effect previously unreported in the literature, can lead to error (up to a factor of 3 increase for test conditions in this study) in experimentally determined laser flash thermal conductivity values.

This study examined the interaction between the laser flash sample holder and the TIM test sample, which has not been explored in the literature since most previous laser flash studies of TIMs examined bonded or cured specimens, which don't require clamping. This is important because the sample holder can affect the temperature profiles obtained in a laser flash measurement used to determine thermal conductivity. Furthermore, structural differences between the sample holder clamping plate with typical TIM application conditions may limit the usefulness of laser flash TIM degradation data, however accurate it may be. Identification of sample holder plate heating as a problem was a key finding since this issue can lead to considerable error in the calculated TIM thermal conductivity values but has not yet been described in the literature. Tradeoffs arise since the ability to withstand the conditions in the reliability test may factor in heavily to the selection of the material of the sample holder plates. This study also sheds light on the limitations and potential sources of error of the laser flash method. For TIM users and manufacturers, this can be useful for product selection, material development, surface engineering, and assembly process development.

3) Developed a method based on FEA and experiments to correct laser flash data for sample holder heating effects.

A semi-empirical methodology was proposed to reduce the increase in TIM thermal conductivity values resulting from these effects. While it was demonstrated that sample holder plate heating can exaggerate measured changes over the course of a reliability test based on laser flash data, these effects can be corrected using a combination of finite element simulation results and at least one accurate thermal conductivity value of a non-degraded test specimen. This procedure assumes that the contact resistance between the 3-layer test sample and the clamping plates remains constant over time.

4) Verified that clamped test specimens, despite the presence of openings on the top and bottom of the sample holder plates needed for laser flash measurements, have uniform bondline thicknesses (variation within 10% of the total thickness), thus approximating realistic TIM mechanical loading conditions.

An investigation into how well the laser flash test structures mechanically simulate realistic TIM loading conditions confirmed initial expectations that clamped test specimens have uniform bondline thicknesses, which was an important finding since typical applications result in uniform bondline thicknesses (Dean and Gettings, 1998). This result also suggested that tradeoffs between reducing sample holder heating and achieving a uniform bondline thickness, which can affect the sample holder plate thickness and opening size, may not be difficult to overcome.

It was also found that the potential for a nonconverged solution in the TIM thermal conductivity calculation can complicate the selection of suitable materials for the coupon layer and the TIM for highly conductive TIMs with a low bondline thickness. If metals such as copper are used as the coupons materials (with

thicknesses similar to those used for the tests in this study), the laser flash method would be more suitable for TIMs in pad form rather than dispensed TIMs, which can also have high error due to the difficulty in measuring the bondline thickness.

Taken together, the findings from this study combined with existing knowledge in the literature clarify how the laser flash method, given its strengths and weaknesses with respect to currently available techniques, would be useful in realistic product development environments. The outcomes also include guidelines on how to apply the laser flash method to obtaining thermal performance data of clamped test specimens, which has not been previously described in the literature. This affects the design of the coupons, clamping plates, and suitable TIMs and thicknesses. While precautions must be taken to avoid sample holder plate heating and error due to thermal diffusivity differences in the 3-layer test sample, the laser flash method can accommodate a wide range of TIM-coupon material combinations, surface roughnesses, and specimen sizes that match common die sizes in TIM applications. In addition, as a technique for reliability evaluation, the laser flash method may be an attractive alternative to steady-state ASTM D5470-based approaches (2006) due to the non-contact nature of the measurement, which allows the TIM specimens to remain undisturbed after being removed from an environmental chamber to be measured in a laser flash instrument. This makes it particularly useful for detecting contact interface effects, such as delamination, which other techniques may not capture. Overall, the laser flash method has value as a technique that uses material test specimens (rather than the actual package), yet can capture important aspects that govern degradation, such as a realistic CTE and T_g properties of the TIM and

contacting surfaces and surface characteristics. In the product development cycle, the laser flash method could be of value early on in the TIM selection process as a means of screening out TIMs based on their degradation behavior. A more detailed evaluation, as needed for product qualification, could then involve use of thermal test vehicles. Despite the potential for high error in TIM thermal conductivity data compared to ASTM D5470 (2006) data, the laser flash method may hold promise as a tool to evaluate end of life TIM thermal performance, particularly for TIMs in pad form. In general, experimental progress in improving the laser flash method and other TIM thermal conductivity measurement techniques should facilitate developments in TIM degradation models, which could be validated using accurate degradation data.

Recommendations for Future Work

Future work should focus on two main areas: improving the laser flash test sample holder design and validating the laser flash data using alternative thermal conductivity measurement techniques.

One aspect of the laser flash sample holder design not explored in-depth in this study was how the plates were held in relation to the 3-layer test specimen. The screws, when tightened, provided an upper limit to how much the 3-layer can expand in thickness, but the TIM can relax (decrease in thickness) throughout the environmental exposure test. In a typical TIM 1 application, the gap distance for the TIM layer should be essentially fixed (barring any warpage), and in a TIM 2 application, there may be a stop, preventing movement below a certain gap distance. Examination of typical TIM applications conditions would be needed to fully explore

this issue. In a typical application with a fixed gap distance, stress relaxation in the TIM could lead to lower bondline thicknesses or create additional contact resistance at the top TIM-substrate interface. One consequence is that laser flash TIM specimens using the current design may experience lower stresses and strains than in realistic applications, resulting in lower levels of TIM degradation than in the actual application. In addition, the impact of using larger square sample areas should be better understood to ensure that the laser flash test specimens properly capture warpage effects encountered in typical applications. Not addressing this potential concern would also lead to lower levels of measured TIM degradation than in the actual application.

Future additional validation studies should include comparisons of laser flash data to data obtained using other techniques, including thermal test vehicles. While the steady-state data presented in this study were used to validate the ability of a laser flash method-based approach to capturing bulk changes over time, the ability to capture the effects of degradation caused by physical processes originating at the contact interface should also be verified and may better reflect realistic TIM applications. The thermal test vehicle would be a simplified approximation of a realistic application of a TIM and consist of a nonfunctional chip package, TIM, and heat sink. Among currently available thermal conductivity measurement techniques, thermal test vehicles are believed to approximate actual TIM applications well thermomechanically. Comparison studies could clarify which types of degradation are detectable using the laser flash method and which ones would present difficulties.

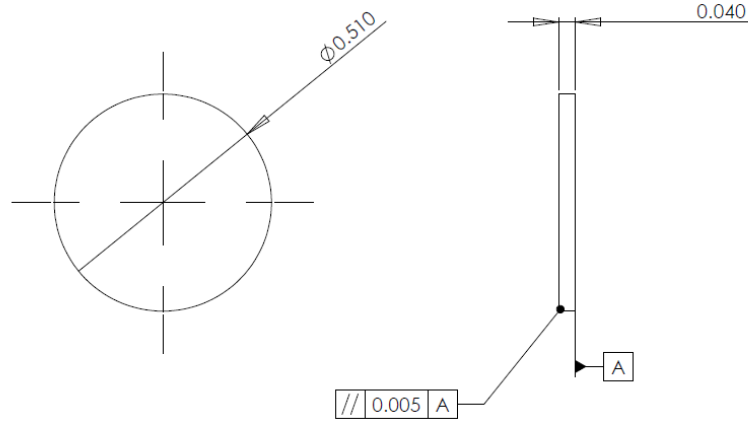
Appendix

Drawings A-D: Laser flash TIM sample holder (clamping plates and coupons).

Drawings E-H: Steady-state TIM tester (clamping plates, thermocouple blocks, and transition block)

NOTES:

1. MATERIAL IS OFHC COPPER
2. ALL COUPON PIECES MUST COME FROM THE SAME LOT FOR A GIVEN MATERIAL



PROPRIETARY AND CONFIDENTIAL
 THE INFORMATION CONTAINED IN THIS DRAWING IS THE SOLE PROPERTY OF ©INSECT COMPANY NAME HERE. ANY REPRODUCTION IN PART OR AS A WHOLE WITHOUT THE WRITTEN PERMISSION OF ©INSECT COMPANY NAME HERE IS PROHIBITED.

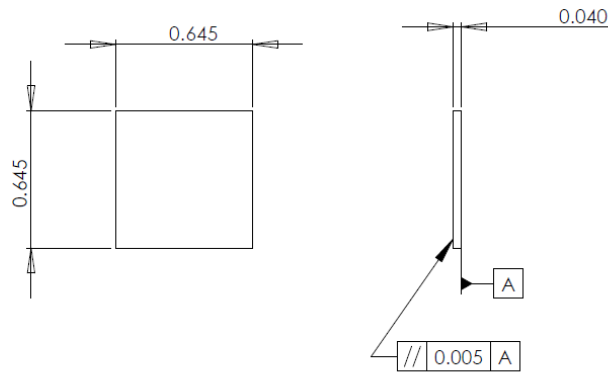
		UNLESS OTHERWISE SPECIFIED:	NAME	DATE	VINH KHUU
		DIMENSIONS ARE IN INCHES	DRAWN	KHUU	12/20/07
		TOLERANCES:	CHECKED		
		FRACTIONALS	ENG APPR.		
		ANGULAR: MACH ± 0.01	MFG APPR.		
		TWO PLACE DECIMAL ± 0.01	G.A.		
		THREE PLACE DECIMAL ± 0.005	COMMENTS:		
		INTERPRET GEOMETRIC TOLERANCING PER:			
		MATERIAL			
		SEE NOTE 1			
NEXT ASSY	USED ON	FINISH			
APPLICATION		DO NOT SCALE DRAWING			

TITLE:		SIZE	DWG. NO.	REV
COUPON TIM HOLDER		A	LF-2007-04-01	A
SCALE: 4:1	WEIGHT:	SHEET 1 OF 1		

5 4 3 2 1

NOTES:

1. MATERIAL IS OFHC COPPER OR MACOR CERAMIC
2. ALL COUPON PIECES MUST COME FROM THE SAME LOT FOR A GIVEN MATERIAL



PROPRIETARY AND CONFIDENTIAL
 THE INFORMATION CONTAINED IN THIS DRAWING IS THE SOLE PROPERTY OF ©CALICE. ANY REPRODUCTION IN PART OR AS A WHOLE WITHOUT THE WRITTEN PERMISSION OF ©CALICE IS PROHIBITED.

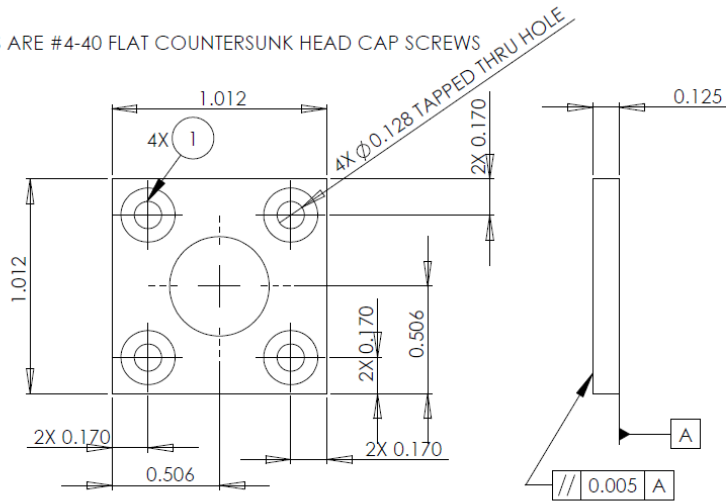
		UNLESS OTHERWISE SPECIFIED:	NAME	DATE	VINH KHUU
		DIMENSIONS ARE IN INCHES	DRAWN	KHUU	8/17/06
		TOLERANCES:	CHECKED		
		FRACTIONALS	ENG APPR.		
		ANGULAR: MACH ± 0.010	MFG APPR.		
		TWO PLACE DECIMAL ± 0.010	G.A.		
		THREE PLACE DECIMAL ± 0.005	COMMENTS:		
		INTERPRET GEOMETRIC TOLERANCING PER:			
		MATERIAL			
		SEE NOTE 1			
NEXT ASSY	USED ON	FINISH			
APPLICATION		DO NOT SCALE DRAWING			

TITLE:		SIZE	DWG. NO.	REV
COUPON TIM HOLDER		A	LF-2006-01-03	A
SCALE: 2:1	WEIGHT:	SHEET 1 OF 1		

5 4 3 2 1

NOTES:

1. SCREWS ARE #4-40 FLAT COUNTERSUNK HEAD CAP SCREWS



PROPRIETARY AND CONFIDENTIAL
THE INFORMATION CONTAINED IN THIS DRAWING IS THE SOLE PROPERTY OF CALICE. ANY REPRODUCTION IN PART OR AS A WHOLE WITHOUT THE WRITTEN PERMISSION OF CALICE IS PROHIBITED.

		UNLESS OTHERWISE SPECIFIED:	NAME	DATE	VINH KHUU	
		DIMENSIONS ARE IN INCHES	DRAWN	KHUU	8/1/06	TITLE:
		TOLERANCES:	CHECKED			BOTTOM PLATE TIM HOLDER
		FRACTIONALS:	ENG APPR.			
		ANGULAR: MACH ± BEID ±	MFG APPR.			
		TWO PLACE DECIMAL ± 0.010	G.A.			SIZE
		THREE PLACE DECIMAL ± 0.005	COMMENTS:			DWG. NO.
		INTERPRET GEOMETRIC TOLERANCING PER:				LF-2006-01-02
		MATERIAL				REV
		Al 6061-T6				B
		FINISH				SCALE: 2:1
NEXT ASSY	USED ON	APPLICATION				WEIGHT:
		DO NOT SCALE DRAWING				SHEET 1 OF 1

5

4

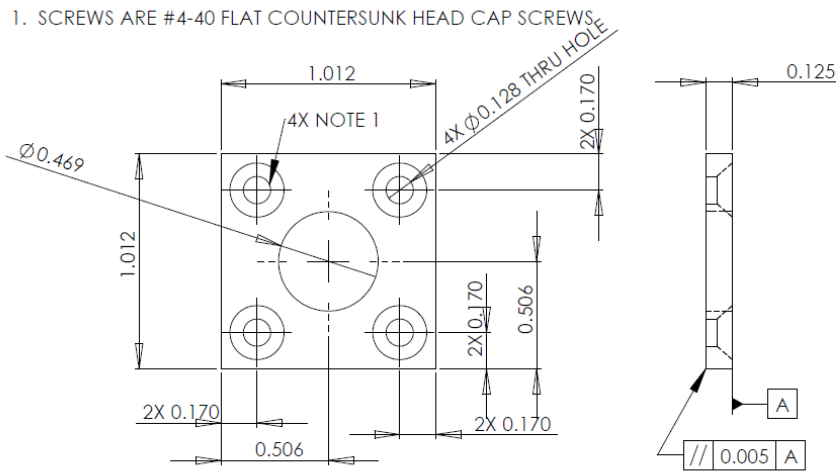
3

2

1

NOTES:

1. SCREWS ARE #4-40 FLAT COUNTERSUNK HEAD CAP SCREWS



PROPRIETARY AND CONFIDENTIAL
THE INFORMATION CONTAINED IN THIS DRAWING IS THE SOLE PROPERTY OF CALICE. ANY REPRODUCTION IN PART OR AS A WHOLE WITHOUT THE WRITTEN PERMISSION OF CALICE IS PROHIBITED.

		UNLESS OTHERWISE SPECIFIED:	NAME	DATE	VINH KHUU	
		DIMENSIONS ARE IN INCHES	DRAWN	KHUU	12/2007	TITLE:
		TOLERANCES:	CHECKED			TOP PLATE TIM HOLDER
		FRACTIONALS:	ENG APPR.			
		ANGULAR: MACH ± BEID ±	MFG APPR.			
		TWO PLACE DECIMAL ± 0.010	G.A.			SIZE
		THREE PLACE DECIMAL ± 0.005	COMMENTS:			DWG. NO.
		INTERPRET GEOMETRIC TOLERANCING PER:				LF-2006-01-01
		MATERIAL				REV
		Al 6061-T6				B
		FINISH				SCALE: 2:1
NEXT ASSY	USED ON	APPLICATION				WEIGHT:
		DO NOT SCALE DRAWING				SHEET 1 OF 1

5

4

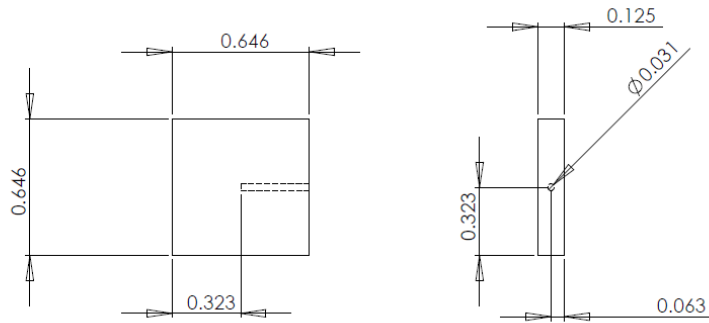
3

2

1

NOTES:

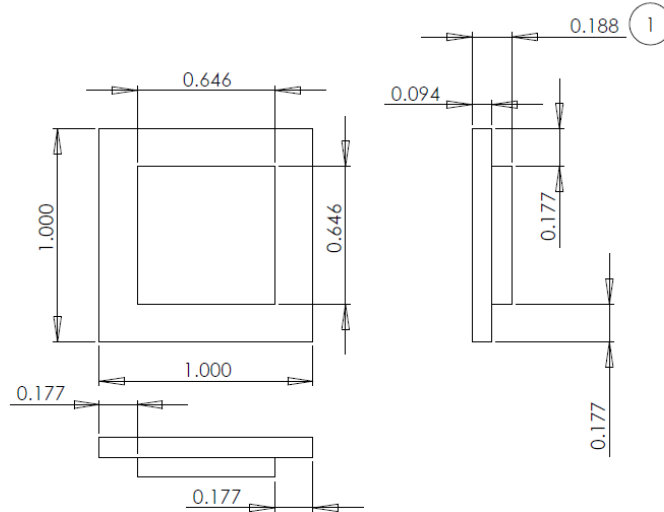
1. MATERIAL IS ALUMINUM 6061-T6
2. ALL PIECES MUST COME FROM THE SAME LOT FOR A GIVEN MATERIAL



<p>PROPRIETARY AND CONFIDENTIAL THE INFORMATION CONTAINED IN THIS DRAWING IS THE SOLE PROPERTY OF <INSERT COMPANY NAME HERE>. ANY REPRODUCTION IN PART OR AS A WHOLE WITHOUT THE WRITTEN PERMISSION OF <INSERT COMPANY NAME HERE> IS PROHIBITED.</p>		UNLESS OTHERWISE SPECIFIED:		NAME	DATE	VINH KHUU	
		DIMENSIONS ARE IN INCHES	DRAWN	KHUU	05/20/09	TITLE:	
		TOLERANCES:	CHECKED				THERMOCOUPLE BLOCK
		FRACTIONALS	ENG APPR.				
		ANGULAR: MACH ± 0.01	MFG APPR.				
	TWO PLACE DECIMAL ± 0.005	G.A.				SIZE DWG. NO.	
	THREE PLACE DECIMAL ± 0.0005	INTERPRET GEOMETRIC TOLERANCING PER:	COMMENTS:			A LF-2009-01-04	
		MATERIAL				REV	
		FINISH				A	
	NEXT ASSY	USED ON				SCALE: 4:1	
	APPLICATION	DO NOT SCALE DRAWING				WEIGHT:	
						SHEET 1 OF 1	

NOTES:

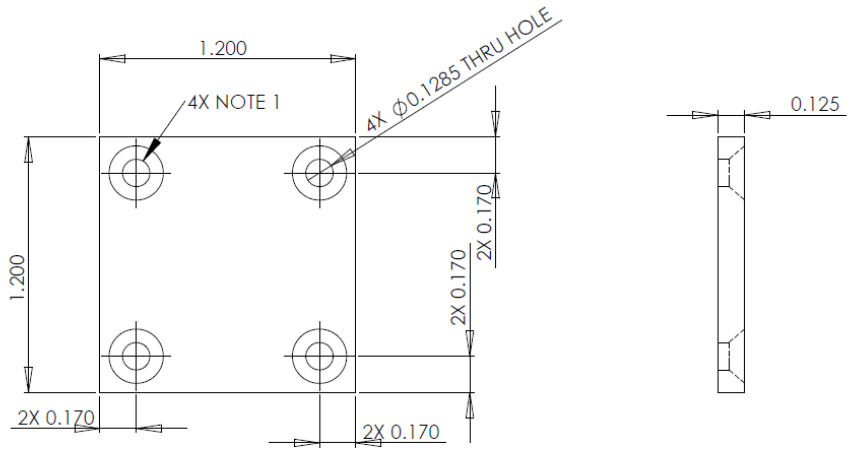
1. USE CLOSEST STOCK SIZE (3/16 INCH THICKNESS)



<p>PROPRIETARY AND CONFIDENTIAL THE INFORMATION CONTAINED IN THIS DRAWING IS THE SOLE PROPERTY OF <INSERT COMPANY NAME HERE>. ANY REPRODUCTION IN PART OR AS A WHOLE WITHOUT THE WRITTEN PERMISSION OF <INSERT COMPANY NAME HERE> IS PROHIBITED.</p>		UNLESS OTHERWISE SPECIFIED:		NAME	DATE	VINH KHUU	
		DIMENSIONS ARE IN INCHES	DRAWN	KHUU	4/14/08	TITLE:	
		TOLERANCES:	CHECKED				BOTTOM TRANSITION BLOCK
		FRACTIONALS	ENG APPR.				
		ANGULAR: MACH ± 0.01	MFG APPR.				
	TWO PLACE DECIMAL ± 0.010	INTERPRET GEOMETRIC TOLERANCING PER:	G.A.			SIZE DWG. NO.	
	THREE PLACE DECIMAL ± 0.0005	MATERIAL	COMMENTS:			A SS-2008-01-01	
		FINISH				REV	
	NEXT ASSY	USED ON				SCALE: 2:1	
	APPLICATION	DO NOT SCALE DRAWING				WEIGHT:	
						SHEET 1 OF 1	

NOTES:

1. SCREWS ARE #4-40 FLAT COUNTERSUNK HEAD CAP SCREWS

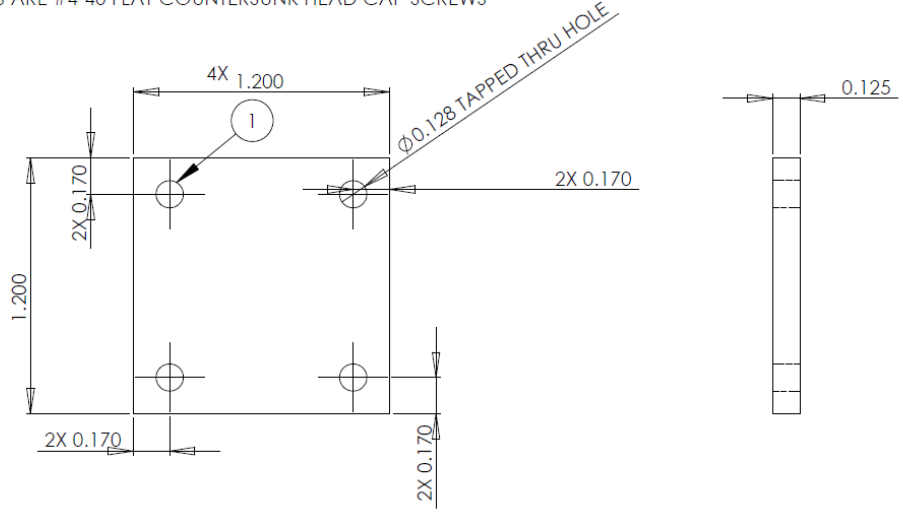


PROPRIETARY AND CONFIDENTIAL
 THE INFORMATION CONTAINED IN THIS DRAWING IS THE SOLE PROPERTY OF [INSERT COMPANY NAME HERE]. ANY REPRODUCTION IN PART OR AS A WHOLE WITHOUT THE WRITTEN PERMISSION OF [INSERT COMPANY NAME HERE] IS PROHIBITED.

		UNLESS OTHERWISE SPECIFIED:	NAME	DATE	VINH KHUU
		DIMENSIONS ARE IN INCHES	DRAWN	KHUU	4/16/08
		TOLERANCES:	CHECKED		TITLE:
		FRACTIONALS			TOP PLATE
		ANGULAR: MACH ± BEND ±	BIG APPR.		STEADY STATE HOLDER
		TWO PLACE DECIMAL ± 0.010	MFG APPR.		
		THREE PLACE DECIMAL ± 0.005			
		INTERPRET GEOMETRIC TOLERANCING PER:	Q.A.		
		MATERIAL	COMMENTS:		
		Al 6061-T6			
NEXT ASSY	USED ON	FINISH			
APPLICATION:		DO NOT SCALE DRAWING			
5	4	3	2	1	

NOTES:

1. SCREWS ARE #4-40 FLAT COUNTERSUNK HEAD CAP SCREWS



PROPRIETARY AND CONFIDENTIAL
 THE INFORMATION CONTAINED IN THIS DRAWING IS THE SOLE PROPERTY OF [INSERT COMPANY NAME HERE]. ANY REPRODUCTION IN PART OR AS A WHOLE WITHOUT THE WRITTEN PERMISSION OF [INSERT COMPANY NAME HERE] IS PROHIBITED.

		UNLESS OTHERWISE SPECIFIED:	NAME	DATE	VINH KHUU
		DIMENSIONS ARE IN INCHES	DRAWN	KHUU	4/16/08
		TOLERANCES:	CHECKED		TITLE:
		FRACTIONALS			BOTTOM PLATE
		ANGULAR: MACH ± BEND ±	BIG APPR.		STEADY STATE HOLDER
		TWO PLACE DECIMAL ± 0.010	MFG APPR.		
		THREE PLACE DECIMAL ± 0.005			
		INTERPRET GEOMETRIC TOLERANCING PER:	Q.A.		
		MATERIAL	COMMENTS:		
		Al 6061-T6			
NEXT ASSY	USED ON	FINISH			
APPLICATION:		DO NOT SCALE DRAWING			
5	4	3	2	1	

Bibliography

Abadi, P. S. S., Leong, C, Chung, D. D. L., "Factors That Govern the Performance of Thermal Interface Materials," *Journal of Electronic Materials*, Vol. 38, Issue 1, pp. 175-192, 2009.

Analysis Tech, Inc., Wakefield, Massachusetts, <http://www.analysisstech.com/>, retrieved August 30, 2009.

Aoyagi, Y., "Antioxidant-Based Phase-Change Thermal Interface Materials with High Thermal Stability." *Journal of Electronic Material*, 2008, Vol. 37, No. 4, pp. 448-461, 2008.

Application Note 056: Note on Gap Pad Silicone Extraction. The Bergquist Company,

Baba, T., Ono, A., "Improvement of the Laser Flash Method to Reduce Uncertainty in Thermal Diffusivity Measurements," *Meas. Sci. Technol.*, Vol. 12., pp. 2046-2057, 2001.

Bharatham, L., Fong, W.S., Leong, C.J., Chiu, C-P., "A Study of Application Pressure on Thermal Interface Material Performance and Reliability on FCBGA Package," *International Conference on Electronic Materials and Packaging*, (EMAP 2006), pp. 1-7, 11-14 Dec. 2006.

Bharatham, L., Fong, W. S., Torresola, J., Koang, C.-C., "Qualification of Phase Change Thermal Interface Material for Wave Solder Heat Sink on FCBGA Package," *Proceedings of 7th Electronic Packaging Technology Conference (EPTC 2005)*, Vol. 2, pp. 6, 7-9 Dec. 2005.

Bosch, E.G.T., and C.J.M. Lasance, "Accurate Measurement of Interface Thermal Resistance by Means of a Transient Method," *Proc. SEMITHERM XVI*, San Jose, CA, pp. 167-173, 2000.

Brunschwiler, T., Kloter, U., Linderman, R.J., Rothuizen, H., Michel, B., "Hierarchically Nested Channels for Fast Squeezing Interfaces With Reduced Thermal Resistance," *IEEE Transactions on Components and Packaging Technologies*, Vol.30, No.2, pp. 226-234, June 2007.

Campbell, R. C., Smith, S.E., and Dietz, R.L. "Laser Flash Diffusivity Measurements of Filled Adhesive Effective Thermal Conductivity and Contact Resistance Using Multilayer Methods," *Thermal Conductivity 25*, pp. 191-202, 2000.

Campbell, R.C., Smith, S.E., and Dietz, R.L., "Measurements of Adhesive Bondline Effective Thermal Conductivity and Thermal Resistance Using the Laser Flash Method", *Proceedings of SEMITHERM XV*, pp. 83-97, 1999.

Chen, C.I., Ni, C.Y., Pan, H.Y., Chang, C.M., Liu, D.S., “Practical Evaluation for Long-term Stability of Thermal Interface Material,” *Experimental Techniques*, Vol. 33, no. 1, pp. 28-32, 2009.

Chiu, C.-P., Chandran, B., Mello, M., Kelley, K., “An Accelerated Reliability Test Method to Predict Thermal Grease Pump-Out in Flip-Chip Applications,” *Proceedings of 51th Electronic Components & Technology Conference*, Orlando, FL, pp. 91-97, May/June 2001.

Chiu, C.-P., Maveety, J.G., and Tran, Q.A., “Characterization of Solder Interfaces Using Laser Flash Metrology,” *Microelectronics Reliability*, Vol. 42, Iss. 1, pp. 93-100, January 2002.

Chu, H., Selvakumar, A., “Performance Characterization of Pressure Sensitive Adhesive Thermal Interface Materials,” *Semiconductor Thermal Measurement and Management Symposium, 2009. SEMI-THERM 2009. 25th Annual IEEE*, pp. 299-303, 15-19 March 2009.

Clark, L. M. and Taylor, R. E., “Radiation Loss in the Flash Method for Thermal Diffusivity.” *Journal of Applied Physics*, Vol. 46, Issue 2, 1975, pp. 714-719.

Clarson, S.J., and Semlyen, J.A., “Depolymerization, Degradation and Thermal Properties,” in *Siloxane Polymers*, PTR Prentice Hall, Englewood Cliffs, New Jersey, 1993.

Cowan, R. D., “Pulse Method of Measuring Thermal Diffusivity at High Temperatures,” *Journal of Applied Physics*, Vol. 34, Iss. 4, Part 1, pp. 926 – 927, 1963.

Culham, J., Teerstra, O., Savija, I., Yovanovich, M., “Design, Assembly and Commissioning of a Test Apparatus for Characterizing Thermal Interface Materials,” *Proceedings IITHERM 2002*, San Diego, California, USA, pp. 128-134, May 30-June 1, 2002.

Cunnington, G., R., “Thermal Conductance of Filled Aluminum and Magnesium Joints in a Vacuum Environment,” *ASME Winter Annual Meeting*, New York, 1964.

Dal, S. “Degradation Mechanisms of Siloxane-Based Thermal Interface Materials Under Reliability Stress Conditions,” *2004 IEEE International Reliability Physics Symposium Proceedings*, Phoenix AZ, pp. 537-542, 25-29 April 2004.

Dani, A., Matayabas, J., and Koning, P., “Thermal Interface Material Technology Advancements and Challenges: An Overview,” *ASME Conf. Proc. 2005*, 511, 2005.

- Dasgupta, A., "Thermomechanical Analysis and Design," *Handbook of Electronic Package Design*, Ed. Michael Pecht, M., Marcel Dekker, Inc., 1991.
- Dean, N.F. and Gettings, A.L., "Experimental Testing of Thermal Interface Materials on Non-Planar Surfaces", *Proceedings of SEMITHERM XIII*, San Diego, CA, 1998, pp. 88-94.
- Deppisch, C., Fitzgerald, T., Raman, A., Hua, F., Zhang, C., Liu, P., Miller, M., "The Material Optimization and Reliability Characterization of an Indium-solder Thermal Interface Material for CPU Packaging," *JOM*, Vol. 58, No. 6, pp. 67-74, June 2006.
- Dias, R., "Investigation of Interfaces with Analytical Tools," *Device and Materials Reliability, IEEE Transactions on*, Vol. 3, No. 4, pp. 179-183, Dec. 2003.
- Emerson, J., Rightley, M., Galloway, J., Huber, D., Rae, D., Cotts, E. "Minimizing the Bondline Thermal Resistance in Thermal Interface Materials Without Affecting Reliability," *International Workshop on Thermal Investigation on ICs and Systems*, Belgirate Lake Maggiore, Italy, pp. 106-111, 27-30 Sep 2005.
- Eveloy, V., Rodgers, P. and Pecht, M., "Reliability of Pressure-Sensitive Adhesive Tapes for Heat Sink Attachment in Air-Cooled Electronic Assemblies," *IEEE Transactions on Device and Materials Reliability*, Vol. 4, No. 4, pp. 650-657, 2004.
- Ferry, J.D., *Viscoelastic Properties of Polymers*, 3rd. ed., Wiley, New York, 1980.
- Fleischer, A. S., Chang, L-H., Johnson, B.C., "The Effect of Die Attach Voiding on the Thermal Resistance of Chip Level Packages," *Microelectronics and Reliability*, Vol. 46, Iss. 5-6, pp. 794-804, May-June 2006.
- Galloway, J., Kanuparthi, S., "BLT Control and Its Impact on FCBGAs Thermal Performance," *Thermal and Thermomechanical Phenomena in Electronic Systems, 2008. ITherm 2008. 11th Intersociety Conference on*, pp.388-394, 28-31 May 2008.
- Gektin, V., "Thermal Management of Voids and Delamination in TIMs," *Proceedings of IPACK2005*, San Francisco, CA, July, 2005.
- Gektin, V., Bar-Cohen, A., Witzman, S., "Coffin-Manson Based Fatigue Analysis of Underfilled DCAs," *Components, Packaging, and Manufacturing Technology, Part A, IEEE Transactions on*, Vol. 21, No. 4, pp. 577-584, Dec 1998.
- Goel, N., Bhattacharya, A., Cervantes, J.A., Mongia, R.K., Machiroutu, S.V., Lin, H., Huang, Y., Fan, K., Denq, B., Liu, C., Lin, C., Tien, C., Pan, J., "Technical Review of Characterization Methods for Thermal Interface Materials (TIM)," *Electronics Packaging Technology Conference, 2008. EPTC 2008. 10th*, pp. 1461-1471, 9-12 Dec. 2008.

- Gomatam, R., and Sancaktar, E., "Fatigue and Failure Behavior of Silver-Filled Electronically-Conductive Adhesive Joints Subjected to Elevated Temperatures," *Journal of Adhesion Science and Technology*, Vol. 18, No. 15-16, pp. 1833-1848, 2004.
- Gowda, A., Esler, D., Paisner, S., Tonapi, S., Nagarkar, K., "Reliability Testing of Silicone-Based Thermal Grease," *Proceedings of SEMITHERM XXI*, San Jose, California, pp. 64-71, March 2005.
- Gowda, A., Esler, D., Tonapi, S., Nagarkar, K., Srihari, K., "Voids in Thermal Interface Material Layers and Their Effect on Thermal Performance," *Electronics Packaging Technology Conference, 2004. EPTC 2004. Proceedings of 6th*, pp. 41-46, 8-10 Dec. 2004
- Gowda, A., Esler, D., Tonapi, S., Zhong, A., Srihari, K., Schattenmann, F., "Micron and Submicron-Scale Characterization of Interfaces in Thermal Interface Material Systems," *Journal of Electronic Packaging*, Vol. 128, Iss. 2, pp. 130-136, June 2006.
- Gowda, A., Zhong, A., Esler, D., David, J., Tonapi S., Srihari, K., Schattenmann, F., "Design of a High Reliability and Low Thermal Resistance Interface Material for Microelectronics," *Electronics Packaging Technology, 2003 5th Conference (EPTC 2003)*, pp. 557-562, 10-12 Dec. 2003.
- Gowda, A., Zhong, A., Esler, D., David, J., Tonapi, S.S., Schattenmann, F., and Srihari, K., "In-Situ Performance of Silicone Thermal Interface Materials: Influence of Filler Characteristics," *Proceedings of Polytronic 2003*, Switzerland, pp. 177-182, October 2003.
- Graebner, J., "Measuring Thermal Conductivity and Diffusivity," *Thermal Measurements in Electronics Cooling*, Ed. Azar, K., Boca Raton, FL: CRC Press LLC, 1997.
- Gupta, A., Liu, Y., Zamora, N., Paddock, T., "Thermal Imaging for Detecting Thermal Interface Issues in Assembly and Reliability Stressing," *Thermal and Thermomechanical Phenomena in Electronics Systems, 2006. ITherm '06. The Tenth Intersociety Conference on*, pp. 942-945, May 30 2006-June 2 2006.
- Gwinn, J., Saini, M., Webb, R., "Apparatus for Accurate Measurement of Interface Resistance of High Performance Thermal Interface Materials," *Proceedings ITherm 2002*, pp. 644-650.
- Gwinn, J.P., Webb, R.L., "Performance and Testing of Thermal Interface Materials," *Microelectronics Journal*, Vol. 34, No. 3, pp. 215-222, March 2003.

- Han, B., "Optical Measurement of Flip-chip Package Warpage and its Effect on Thermal Interfaces," *Electronics Cooling*, http://electronics-cooling.com/articles/2003/2003_february_a1.php, February 2003.
- Hanson, K., "ASTM D 5470 TIM Material Testing," *Semiconductor Thermal Measurement and Management Symposium, 2006 IEEE Twenty-Second Annual IEEE*, pp. 50-53, 14-16 March 2006.
- Haque, S., Lu, G-Q., Goings, J., Sigmund, J., "Characterization of Interfacial Thermal Resistance by Acoustic Micrography Imaging," *Microelectronics Reliability*, Vol. 40, No. 3, pp. 465-476, March 17, 2000.
- Hasselman, D. P. H., "Interfacial Thermal Resistance and Temperature Dependence of Three Adhesives for Electronic Packaging", *IEEE Trans. Components and Packaging Tech.*, Vol. 23, No. 4, pp. 633-637, 2000.
- He, Yi, "Rapid Thermal Conductivity Measurement with a Hot Disk Sensor: Part 1. Theoretical Considerations," *Thermochimica Acta*, Vol. 436, Iss. 1-2, pp. 122-1291, October 2005.
- He, Yi, "Rapid Thermal Conductivity Measurement with a Hot Disk Sensor: Part 2. Characterization of Thermal Greases," *Thermochimica Acta*, Vol. 436, Iss. 1-2, pp. 130-134, 1 October 2005.
- He, Yi, "DSC and DMTA Studies of a Thermal Interface Material for Packaging High Speed Microprocessors," *Thermochimica Acta*, Vol. 392-393, pp. 13-21, 15 September 2002.
- Hua, F., Deppisch, C., Fitzgerald, T., "Indium as Thermal Interface Material for High Power Devices," *Advancing Microelectronics*, Vol. 33, No. 5, pp. 30-32, September/October 2006.
- Hu, J., M. Pecht and A. Dasgupta, "Design of Reliable Die Attach," *International J. Microcircuits and Electronic Packaging*, Vol. 16, pp. 1-21, 1993.
- Hu, X., Jiang, L., Goodson, K.E., "Thermal Characterization of Eutectic Alloy Thermal Interface Materials with Void-like Inclusions," *Semiconductor Thermal Measurement and Management Symposium, 2004. Twentieth Annual IEEE*, pp. 98-103, 9-11 Mar 2004.
- Islam, N., Lee, S. W., Jimarez, M., Lee, J.Y., Galloway, J., "TIM Degradation in Flip Chip Packages," *Thermal and Thermomechanical Phenomena in Electronic Systems, 2008. ITherm 2008. 11th Intersociety Conference on*, pp. 259-265, 28-31 May 2008.

- Jarrett, R.N., Merritt, C.K., Ross, J.P., Hisert, J., "Comparison of Test Methods for High Performance Thermal Interface Materials," *Semiconductor Thermal Measurement and Management Symposium, 2007. SEMI-THERM 2007. Twenty Third Annual IEEE*, pp. 83-86, 18-22 March 2007.
- Jung, H. H., Sai, A., Pecavar, S., and Jones, J., "Influence of Package-Sink Interface Materials on Die Performance and Reliability," *ASME Conf. Proc. InterPACK2003*, 2003.
- Kearney, A., Li, L., Sanford, S., "Interaction Between TIM1 and TIM2 for Mechanical Robustness of Integrated Heat Spreader," *Semiconductor Thermal Measurement and Management Symposium, 2009. SEMI-THERM 2009. 25th Annual IEEE*, pp. 293-298, 15-19 March 2009.
- Kearns, D., "Improving Accuracy and Flexibility of ASTM D 5470 for High Performance Thermal Interface Materials," *Semiconductor Thermal Measurement and Management Symposium, 2003. Nineteenth Annual IEEE*, pp. 129-133, 11-13 March 2003.
- Kline, S. J., McClintock, F.A., "Describing Uncertainties in Single-Sample Experiments," *Mech. Eng.*, pp. 3, January 1953.
- Kohli, P., Sobczak, M, Bowin, J., Matthews, M., "Advanced Thermal Interface Materials for Enhanced Flip Chip BGA," *Proceedings - Electronic Components and Technology Conference*, pp. 564-570, 2001.
- Koski, J. A., "Improved Data-Reduction Methods for Laser Pulse-Diffusivity Determination with the Use of Minicomputers," *Intern. Joint Conf. on Thermophys. Properties*, Gaithersburg, Md., pp 94-103, 15 June 1981.
- Lall, P., Pecht, M.G., Hakim. E.B., *Influence of Temperature on Microelectronics and System Reliability*, Boca Raton: CRC Press, 1997.
- Lasance, C., "The Urgent Need for Widely Accepted Test Methods for Thermal Interface Materials," *Proceedings of SEMITHERM XIX*, San Jose, pp. 123-128, March 2003.
- Lasance, C., Lacaze, C., "A Transient Method for the Accurate Measurement of Interface Thermal Resistance," *Proc. SEMITHERM XII*, Austin, TX, pp.43-45, 1996.
- Lasance, C., Murray, T., Saums, D., Rencz, M., "Challenges in Thermal Interface Material Testing," *Proceedings of the 22nd IEEE Semi-therm Symposium*, Dallas, TX, USA, pp. 42-49, 2006.
- Lee, H.J., Purdue University Ph.D. Thesis, "Thermal Diffusivity in Layered and Dispersed Composites," University Microfilms International, 1975.

Lee, T.R., Purdue University Ph.D. Thesis, "Thermal Diffusivity of Dispersed and Layered Composites," University Microfilms International, 1977.

Lee, T.Y.R., and Taylor, R.E., "Thermal Diffusivity of Dispersed Materials," *J. Heat Transfer*, Vol. 100, pp. 720-724, Nov. 1978.

Lee, Y. J., "Thermally Conductive Adhesive Tapes: A Critical Evaluation and Comparison," *Advanced Packaging*, May 2007.

Li, L., Nagar, M., Jie, X., "Effect of Thermal Interface Materials on Manufacturing and Reliability of Flip Chip PBGA and SiP Packages," *Electronic Components and Technology Conference, 2008. ECTC 2008. 58th*, pp. 973-978, 27-30 May 2008.

Li, Yuan, "Accurate Predictions of Flip Chip BGA Warpage," *Electronic Components and Technology Conference, 2003. Proceedings. 53rd*, pp. 549-553, May 27-30, 2003.

Lim, T., Velderrain, M., "Calculated Shear Stress Produced by Silicone and Epoxy Thermal Interface Materials (TIMs) During Thermal Cycling," *Electronics Packaging Technology Conference, 2007. EPTC 2007. 9th*, pp. 914-916, 10-12 Dec. 2007.

Linderman, R., Brunschwiler, T., Smith, B., Michel, B., "High-Performance Thermal Interface Technology Overview," *Thermal Investigation of ICs and Systems, 2007. THERMINIC 2007. 13th International Workshop on*, pp.129-134, 17-19 Sept. 2007.

Liu, J., Michel, B., Rencz, M., Tantolin, C., Sarno, C., Miessner, R., Schuett, K.-V., Tang, X., Demoustier, S., Ziaei, A., "Recent Progress of Thermal Interface Material Research - an Overview," *Thermal Investigation of ICs and Systems, 2008. THERMINIC 2008. 14th International Workshop on*, pp.156-162, 24-26 Sept. 2008.

Luo, X., Chugh, R., Biller, B. C., Hoi, Y. M., Chung, D.D.L., "Electronic Applications of Flexible Graphite," *Journal of Electronic Materials*, Vol. 31, No. 5, pp. 535-544, 1 May 2002.

Luo, X., Xu, Y., and Chung, D. D. L. "Thermal Stability of Thermal Interface Pastes, Evaluated by Thermal Contact Conductance Measurement," *J. Electron. Packag.*, Vol. 123, pp. 309-311, 2001.

Madhusudana, C.V., *Thermal Contact Conductance*, Springer, New York, 1995.

Maguire, L, Behnia, M. and Morrison, G., "Systematic Evaluation of Thermal Interface Materials—A Case Study in High Power Amplifier Design," *Microelectronics Reliability*, Vol. 45, pp. 711-725, 2005.

Marotta, E.E.; LaFontant, S.; McClafferty, D.; Mazzuca, S., "The Effect of Interface Pressure on Thermal Joint Conductance for Flexible Graphite Materials: Analytical and Experimental Study," *Thermal and Thermomechanical Phenomena in Electronic Systems, 2002. IThERM 2002. The Eighth Intersociety Conference on*, pp. 663-670, 2002.

Matayabas, J.C., and LeBonheur, V., "Silicone Gel Thermal Interface Materials for High Heat Dissipation and Thermo-Mechanical Stress Management for Good Reliability Performance," *Proceedings of I-Pack 2005*, San Francisco, CA, pp. 1863-1873, July 17-22.

Mathis, N., "New Instrument for Thermal Management," *Design, Proc. Int. Symp. On Packaging Systems*, San Diego, CA, 1999.

Moffat, R., "Describing the Uncertainties in Experimental Results," *Experimental Thermal and Fluid Science*. Vol. 1, pp. 3-17, Jan. 1988.

Mukadam, M.; Schake, J.; Borgesen, P.; Srihari, K., "Effects of Assembly Process Variables on Voiding at a Thermal Interface," *Thermal and Thermomechanical Phenomena in Electronic Systems, 2004. IThERM '04. The Ninth Intersociety Conference on*, Vol. 1, pp. 58-62, 1-4 June 2004.

Nakayama, W., and Bergles, A., "Thermal Interfacing Techniques for Electronic Equipment-A Perspective," *Journal of Electronic Packaging*, Vol. 125, pp. 192-199, 2003.

Nnebe, I. M. and Feger, C., "Drainage-Induced Dry-Out of Thermal Greases," *Advanced Packaging, IEEE Transactions on*, Vol. 31, Iss. 3, pp. 512-518, Aug. 2008.

Parker, W., Jenkins, R., Butler, C., and Abbott, G., "Flash Method of Determining Thermal Diffusivity, Heat Capacity, and Thermal Conductivity," *Journal of Applied Physics*, Vol. 32, No. 9, pp. 1679-1684, Sept. 1961.

Prabhakumar, A., Zhong, A., Tonapi, S., Sherman, D., Cole, H., Schattenmann, F., Srihari, K., "Comparison of the Adhesion Strength of Epoxy and Silicone Based Thermal Interface Materials," *Electronic Components and Technology Conference, 2003. Proceedings. 53rd*, pp. 1809-1814, May 27-30, 2003.

Prasher, R., "Surface Chemistry and Characteristics Based Model for Thermal Contact Resistance of Fluidic Interstitial Thermal Interface Materials," *Journal of Heat Transfer*, Vol. 123, 2001.

Prasher, R. "Thermal Interface Materials: Historical Perspective, Status, and Future Directions," *Proceedings of the IEEE*, Vol. 94, Iss. 8, pp. 1571-1586, Aug. 2006.

- Prasher, R., Matayabas, J., "Thermal Contact Resistance of Cured Gel Polymeric Thermal Interface Material," *IEEE Transactions on Components and Packaging Technology*, Vol. 27, No. 4, pp. 702-709, 2004.
- Prasher, R., Shipley, J., Prstic, S., Koning, P., and Wang, J-L, "Thermal Resistance of Particle Laden Polymeric Thermal Interface Materials," *Journal of Heat Transfer*, Vol. 125, December 2003.
- Refai-Ahmed, G., He, Z., Hejan, E., Vincent, R., Rude, T., Van Heerden, D., "Comparison of Thermal Performance of Current High-End Thermal Interface Materials", *INTERPACK 2007*, Vancouver BC, Canada, July 8-12.
- Rodgers, P., Evely, V., Pecht, M., "Limits of Air-Cooling: Status and Challenges," *IEEE Twenty First Annual - Semiconductor Thermal Measurement and Management Symposium*, pp. 116-124, March 15-17, 2005.
- Rodgers, P., Evely, V., Rahim, E., Morgan, D., "Thermal Performance and Reliability of Thermal Interface Materials: A Review," *Proceedings of EuroSIME 2006*, Milan, Italy, April 23-26, 2006.
- Samson, E. C., Machiroutu, S. V., Chang, J. Y., Santos, I., Hermerding, J., Dani, A., Prasher, R., Song, D.W., "Interface Material Selection and a Thermal Management Technique in Second-Generation Platforms Built on Intel Centrino Mobile Technology," *Intel Technology Journal*, Vol. 9, Iss. 1, Feb. 17, 2005.
- Sarvar, F., Whalley, D.C., Conway, P.P., "Thermal Interface Materials - A Review of the State of the Art," *Electronics System Integration Technology Conference, 2006. Ist*, Vol. 2, pp. 1292-1302, Sept. 2006.
- Savija, I., Culham, J.R. Yovanovich, M.M., "Effective Thermophysical Properties of Thermal Interface Materials: Part I, Definitions and Models," *InterPACK2003-35088, International Electronic Packaging Technical Conference and Exhibit*, Maui, Hawaii, July 6-11, 2003.
- Shaw, D., Goldsmith, L. A., Little, A., "Suitability of the Flash Method for Measuring the Thermal Diffusivity of Cracked Specimens," *Journal of Physics D: Applied Physics*, Vol. 2, Iss. 4, pp. 597-604, 1969.
- Sheikh, M.A, Taylor, S.C., Hayhurst, D.R., and Taylor, R., "Measurement of Thermal Diffusivity of Isotropic Materials Using a Laser Flash Method and its Validation by Finite Element Analysis," *J. Phys. D: Appl. Phys.*, Vol. 33, pp. 1536-1550, 2000.
- Sikka, K.K., Toy, H.T., Edwards, D.L., Iruvanti, S., Ingalls, E.M. and DeHaven, P.W., "Gap-reduced Thermal Paste Package Design for Cooling Single Flip-Chip Electronic Modules," *Proc. IEEE Inter Soc. Conf. Thermal Phenom.*, 2002, pp. 651-657.

Sim, L.C., Ramanan, S.R., Ismail, H., Seetharamu, K.N., Goh, T.J., "Thermal Characterization of Al₂O₃ and ZnO Reinforced Silicone Rubber as Thermal Pads for Heat Dissipation Purposes," *Thermochimica Acta*, Vol. 430, Iss. 1-2, pp. 155-165, June 2005.

Singhal, V., Siegmund, T., Garimella, S.V., "Optimization of Thermal Interface Materials for Electronics Cooling Applications," *Components and Packaging Technologies, IEEE Transactions on*, Vol. 27, No. 2, pp. 244-252, June 2004.

Smith, B., Brunschwiler, T., Michel, B., "Comparison of Transient and Static Test Methods for Chip-to-sink Thermal Interface Characterization," *Microelectronics Journal*, in press, 2008.

Smith, R.A., Culharn, R.J., "In-situ Thickness Method of Measuring Thermo-Physical Properties of Polymer-like Thermal Interface Materials," *Semiconductor Thermal Measurement and Management Symposium, 2005 IEEE Twenty First Annual IEEE*, pp. 53-63, 15-17 March 2005.

Solbrekken, G.L., Chiu, C.P., Byers, B., Reichebbaicher, D., "The Development of a Tool to Predict Package Level Thermal Interface Material Performance," *Thermal and Thermomechanical Phenomena in Electronic Systems, 2000. IThERM 2000. The Seventh Intersociety Conference on*, Vol. 1, pp. 54, 2000.

Somasundaram, S., Tay, A., Kandasamy, R., "Evaluation of Thermal Resistance of TIMs in Functional Packages Using a Thermal Transient Method," *Electronics Packaging Technology Conference, 2008. EPTC 2008. 10th*, 9-12 Dec. 2008, pp. 1479-1485.

Stern, M.B., Gektin, V., Pecavar, S., Kearns, D., Chen, T., "Evaluation of High Performance Thermal Greases for CPU Package Cooling Applications," *Semiconductor Thermal Measurement and Management Symposium, 2005 IEEE Twenty First Annual IEEE*, pp. 39-43, 15-17 March 2005.

Stern, M.B., Jhoty, G., Kearns, D., Ong, B., "Measurements of Mechanical Coupling of Non-Curing High Performance Thermal Interface Materials," *Semiconductor Thermal Measurement and Management Symposium, 2006 IEEE Twenty-Second Annual IEEE*, pp. 37-41, 14-16 March 2006.

Stern, M.B., Kearns, D., Gektin, V., Jhoty, G., "A Methodology for Thermal Evaluation of Strongly Bonded Packaging Materials," *Thermal and Thermomechanical Phenomena in Electronics Systems, 2006. IThERM '06. The Tenth Intersociety Conference on*, pp. 505-511, May 30 2006-June 2 2006.

Sundararajan, R., McCluskey, P., Azarm, S., "Semi-Analytic Model for Thermal Fatigue Failure of Die Attach in Power Electronic Building Blocks," *High*

Temperature Electronics Conference, 1998. HITEC. 1998 Fourth International, pp. 94-102, 14-18 Jun 1998.

Szekely, V., Ress, S., Poppe, A., Torok, S., Magyari, D., Benedek, Z., Torki, K., Courtois, B., and Rencz, M., "New Approaches in the Transient Thermal Measurements," *Microelectron. J.*, Vol. 31, Iss. 9-10, 2000, pp. 727-734.

Taylor, R. E., "Critical Evaluation of Flash Method for Measuring Thermal Diffusivity," *Revue Int. Hautes Temp. Refract.*, Vol. 12, pp. 141-5, 1975.

Test Method D5470-06, "Standard Test Method for Thermal Transmission Properties of Thin, Thermally Conductive Solid Electrical Insulation Materials," American Society for Testing and Materials, *Annual Book of ASTM Standards*, Vol. 10.02, 2006.

Test Method E1461-01, "Standard Test Method for Thermal Diffusivity of Solids by the Flash Method," American Society for Testing and Materials, *Annual Book of ASTM Standards*, Vol. 14.02, 2001.

Test Method E1530-06, "Standard Test Method for Evaluating the Resistance to Thermal Transmission of Materials by the Guarded Heat Flow Meter Technique," American Society for Testing and Materials, *Annual Book of ASTM Standards*, Vol. 14.02, 2006.

Too, S. S., Hayward, J., Master, R., Tan, T. S., Keok, K. H. "Effects of Organic Package Warpage on Microprocessor Thermal Performance," *Electronic Components and Technology Conference, 2007. ECTC '07. Proceedings. 57th*, pp. 748-754, May 29 2007-June 1 2007.

Tummala, R.R., Rymaszewski, E. J., *Microelectronics Packaging Handbook*. New York, N.Y.: Van Nostrand Reinhold, 1989.

Tzeng, J.J.-W., Weber, T.W., Krassowski, D.W., "Technical Review on Thermal Conductivity Measurement Techniques for Thin Thermal Interfaces," *Semiconductor Thermal Measurement and Management Symposium, 2000. Sixteenth Annual IEEE*, pp.174-181, 2000.

Viswanath, R., Wakharkar, V., Watwe, A., Lebonheur, V., "Thermal Performance Challenges from Silicon to Systems," *Intel Technology Journal*. Vol. Issue 2, May 16, 2002.

Yovanovich, M.M., "Four Decades of Research on Thermal Contact, Gap, and Joint Resistance in Microelectronics," *Components and Packaging Technologies, IEEE Transactions on*, Vol. 28, Iss. 2, pp. 182-206, June 2005.

Wang, J., "Shear Modulus Measurement for Thermal Interface Materials in Flip Chip Packages," *Components and Packaging Technologies, IEEE Transactions on*, Vol. 29, No. 3, pp. 610-617, Sept. 2006.

Wei, X., Marston, K., Sikka, K., "Thermal Modeling for Warpage Effects in Organic Packages," *Thermal and Thermomechanical Phenomena in Electronic Systems, 2008. ITherm 2008. 11th Intersociety Conference on*, pp. 310-314, 28-31 May 2008.

Wunderle, B., Kleff, J., Mrossko, R., Abo Ras, M., May, D., Schacht, R., Oppermann, H., Keller, J., Michel, B., "In-situ Measurement of Various Thin Bond-line-thickness Thermal Interface Materials with Correlation to Structural Features," *Thermal Investigation of ICs and Systems, 2008. THERMINIC 2008. 14th International Workshop on*, pp. 112-117, 24-26 Sept. 2008.

Yang, Y., Zhang Z., Touzelbaev, M., "Impact of Temperature-Dependent Die Warpage on TIM1 Thermal Resistance in Field Conditions," *Semiconductor Thermal Measurement and Management Symposium, 2009. SEMI-THERM 2009. 25th Annual IEEE*, pp. 285-292, 15-19 March 2009.

Zhang, H., "Thermal-Mechanical Decoupling by a Thermal Interface Material," <http://www.arlon-std.com>, Retrieved 8/20/09.

Zheng, J., Jadhav, V., Wakil, J., Coffin, J., Iruvanti, S., Langlois, R., Yarmchuk, E., Gaynes, M., Liu, H., Sikka, K., Brofman, P., "Delamination Mechanisms of Thermal Interface Materials in Organic Packages During Reflow and Moisture Soaking," *Electronic Components and Technology Conference, 2009. ECTC 2009. 59th*, pp. 469-474, 26-29 May 2009.

Zhou, P. and Goodson, K. E., "Modeling and Measurement of Pressure-Dependent Junction-Spreader Thermal Resistance for Integrated Circuits," *Proc. ASME Int. Mechanical Engineering Congr. And Exposition*, pp. 51-67, 2001.

Zou, W., Coffin, J., Arvelo, A., "Reliability Analysis on Epoxy Based Thermal Interface Subjected to Moisture Environment," *Thermal and Thermomechanical Phenomena in Electronics Systems, 2006. ITherm '06. The Tenth Intersociety Conference on*, pp. 1082-1087, May 30 2006-June 2 2006.